AD_____

Award Number: DAMD17-03-1-0479

TITLE: The Impact of Exercise on the Vulnerability of Dopamine Neurons to Cell Death in Animal Models of Parkinson's Disease

PRINCIPAL INVESTIGATOR: Michael J. Zigmond, Ph.D.
Amanda Smith, Ph.D.
Anthony Liou, Ph.D.

CONTRACTING ORGANIZATION: University of Pittsburgh
Pittsburgh, PA 15260

REPORT DATE: July 2008

TYPE OF REPORT: Final

PREPARED FOR: U.S. Army Medical Research and Materiel Command
Fort Detrick, Maryland 21702-5012

REPORT DOCUMENTATION PAGE

Form Approved
OMB No. 0704-0188

1. REPORT DATE *(DD-MM-YYYY)*	**2. REPORT TYPE**	**3. DATES COVERED** *(From - To)*
01-07-2008	Final	16 Jun 2003 – 15 Jun 2008

4. TITLE AND SUBTITLE

The Impact of Exercise on the Vulnerability of Dopamine Neurons to Cell Death in Animal Models of Parkinson's Disease

5a. CONTRACT NUMBER

5b. GRANT NUMBER
DAMD17-03-1-0479

5c. PROGRAM ELEMENT NUMBER

6. AUTHOR(S)

Michael J. Zigmond, Ph.D.; Amanda Smith, Ph.D. and
Anthony Liou, Ph.D.
E-Mail: zigmond@pitt.edu

5d. PROJECT NUMBER

5e. TASK NUMBER

5f. WORK UNIT NUMBER

7. PERFORMING ORGANIZATION NAME(S) AND ADDRESS(ES)

University of Pittsburgh
Pittsburgh, PA 15260

8. PERFORMING ORGANIZATION REPORT NUMBER

9. SPONSORING / MONITORING AGENCY NAME(S) AND ADDRESS(ES)
U.S. Army Medical Research and Materiel Command
Fort Detrick, Maryland 21702-5012

10. SPONSOR/MONITOR'S ACRONYM(S)

11. SPONSOR/MONITOR'S REPORT NUMBER(S)

12. DISTRIBUTION / AVAILABILITY STATEMENT
Approved for Public Release; Distribution Unlimited

13. SUPPLEMENTARY NOTES – Original contains colored plates: ALL DTIC reproductions will be in black and white.

14. ABSTRACT

Parkinson's disease results in part from the loss of dopamine neurons. We hypothesize that exercise reduces the vulnerability of dopamine neurons to neurotoxin exposure, which is modulated by stress. We have outlined experiments to test this hypothesis in rats treated with one of several neurotoxins, beginning with 6-hydroxydopamine. Over the past year, we increased the size and training of our research team and made a number of observations of direct relevance to our hypothesis. We also have received permission to expand our original Statement of Work to include critical studies on the mechanism of the actions of exercise, using both in vivo and in vitro approaches. Our focus continues to be on the effects of stress and exercise on the vulnerability of DA neurons, and the role played in these phenomena by trophic factors and intracellular signaling cascades.

15. SUBJECT TERMS
Basal ganglia, dopamine, ERK, exercise, MAPK, neuroprotection, Parkinson's disease, preconditioning, LRRK2

16. SECURITY CLASSIFICATION OF:			**17. LIMITATION OF ABSTRACT**	**18. NUMBER OF PAGES**	**19a. NAME OF RESPONSIBLE PERSON**
a. REPORT	**b. ABSTRACT**	**c. THIS PAGE**			USAMRMC
U	U	U	UU	80	**19b. TELEPHONE NUMBER** *(include area code)*

Table of Contents

Introduction

Parkinson's disease (PD) results in part from the progressive loss of dopamine (DA) neurons projecting from substantia nigra (SN) to striatum. Although the cause of this neurodegenerative process is unknown, one candidate is oxidative stress. This is likely to result from exposure to environmental toxins, perhaps coupled with one or more risk factors, which results in an increased vulnerability. Such increased vulnerability could include genetic predisposition, emotional or physical stress, traumatic brain injury, or exposure to certain recreational drugs. Our hypotheses regarding these matters are under continual refinement as we and others collect and publish additional data. Currently, we are guided by the following conceptualization (see also Figure 1 and accompanying legend):

> *Exercise reduces the neurological consequences that would otherwise develop in some individuals as a result of toxin exposure. This results in part from an exercise-induced increase in neurotrophic factors (NTFs) acting thought intracellular cascades, such as those involving the kinases ERK and Akt. This NTF/kinase axis produces its ameliorating effects in several complimentary ways, including (a) reducing the vulnerability of DA neurons to the toxin, (b) increasing the functional capacity of residual DA neurons, and (c) facilitating the transfer of some functions previously attributable to DA neurons to other projections, including those utilizing serotonin. These effects of exercise are promoted by low levels of stress (which exercise itself may elicit), but are inhibited by high levels of stress.*

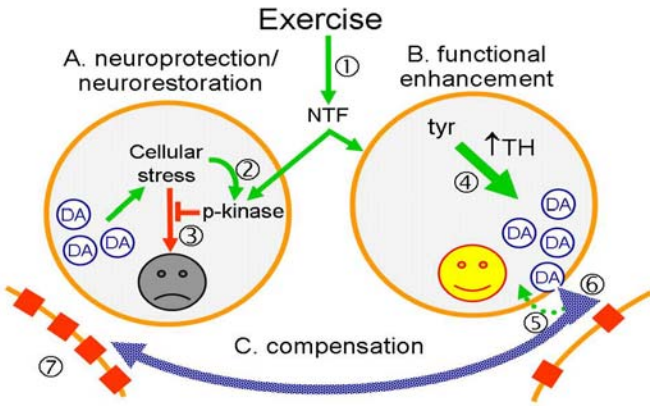

Figure 1: A schema for the impact of exercise on DA neurons. Cellular stress can result from many factors including ROS, mitochondrial deficiency, and proteasomal dysfunction. These insults can, in turn, be initiated as a result of environmental or genetic factors and be influenced by variables such as diet and physical activity. We hypothesize that (1) Exercise increases expression of several neurotrophic factors (NTFs), including GDNF and BDNF. These, in turn (2) activate intracellular signaling cascades including Ras/ERK and PI3K/Akt, leading to the phosphorylation of protein kinases (p-kinase) and activation of downstream elements. (3) Mild cellular stress can lead to a similar activation of survival cascades, which we and others have termed *preconditioning*. Together, these actions can often **(A) *protect DA neurons from death.*** NTFs can also **(B) *increase the capacity of remaining DA neurons*** by (4) both activating and inducing TH, thereby increasing DA synthesis. This, coupled with (5) a decrease in DAT activity, leads to (6) increase DA overflow. Moreover, if the loss of DA neurons is large (typically >90%), there will be an (7) increase in DA receptors. Together with the increased DA overflow, this is to **(C) *compensate for DA neuron loss***. Some elements of our model are not shown, including a transfer of some functions to other systems (e.g., serotonin) and an alteration in synaptic number.

Below we summarize our studies performed during the tenure of this research program, 2003-2008.

Body

1. Exercise can protect DA neurons from toxin-induced stress

Casting: Although the hypothesis that forced exercise via unilateral casting reduces the behavioral and biological effects of DA-specific neurotoxins has now been supported by three papers from our group (Tillerson et al., 2001; 2002; Cohen et al., 2003), our additional unpublished experiments, and a number of reports from several labs, we recently have not been able to replicate the effect. Several attempts to resolve this problem, as well as efforts by our collaborator Dr. Tim Schallert, have not been successful. There are several possible reasons for this, though none are very satisfying. First, our animals may be experiencing more stress and, if so, this might be potentiating the effects of the toxin. Possible origins of the stress include an infection (our animal quarters has had a problem with pin-worms from time to time) and the chemicals being used to eradicate that infection, being housed in a room with female rats (due to a temporary shortage of space), and a tighter cast (employed to reduce the number of animals who are able to remove their cast). Second, we noticed in retrospect that our lesions have become somewhat larger – perhaps we have reached a lesion size against which exercise is ineffective. We hope to resolve the problem in the future. However, we have moved to other forms of exercise for the time being.

Treadmill: We have also examined the effect of treadmill running on the vulnerability of DA neurons in the SN against 6-OHDA. As mentioned earlier, infusion of 6-OHDA into the striatum produces a progressive degeneration of the nigrostriatal pathway that occurs over months. Additionally, 2-4 weeks of treadmill running has been shown to protect against other forms of toxicity, particularly ischemic damage. Thus, in the next experiment animals were trained for 3 days on the treadmill and then forced to run for 5 day/wk at 15 m/min for 30 min for 2 weeks. At the end of the 2 week running period, animals received an infusion of 16 µg 6-OHDA into the striatum. After a 3-day recovery period, animals were run on the treadmill for 4 days, perfused, striatum sectioned and assayed by immunohistochemistry (IHC). Unfortunately, the was small. This could have been caused by our inability to get male Sprague-Dawley rats to run on a treadmill without the use of a mild shock to encourage them to move out of the start box during the training period. This may have resulted in enough stress to block the effects of the exercise. Second we may have been using the wrong strain and or sex.

After consulting with two other researchers who have used treadmill running, we have decided to use female Long Evans rats, which are reported to require less coaxing to run on the treadmill than male rats previously used (Sprague Dawley). These studies were promising. The animals appear to learn to run on the treadmill with little if any coaxing and the mild shock during training was unnecessary. However, because of a lack or resources, these studies are also not on hold. However, in collaboration with Dr. Judy Cameron and with support from NINDS we have begun to explore the effects of treadmill running in MPTP-treated rhesus monkey. These studies are extremely promising

We have examined six monkeys (age 16-20 y). Two of these ran 1 hr/day, 5 days/wk for 3 mo before and 7 more weeks after a unilateral dose of MPTP (0.8 mg via the right carotid). One of these ran at 60% max heart rate, the other at 80% max, intensities that our colleagues at the University of Colorado have shown can be tolerated by patients with PD (Schenkman et al., 2008); M. Schenkman, personal communication). A third monkey was run at 80% max heart rate but only ***after*** MPTP injection. Results were compared with comparably aged monkeys removed from their home cages each day for 60 min but not otherwise exercised. Behavioral analysis using the Motor Assessment Panel (mMAP) indicated that the sedentary monkey did

not use the left hand after MPTP, whereas the exercised monkeys showed a significant behavioral protection. Each animal was assessed using the PET ligand ^{11}C-DTBZ for vesicular monoamine transporter, type 2 (VMAT2) (results not shown) and then sacrificed for biochemical assessment of tyrosine hydroxylase (TH), the high affinity DA transporter (DAT), and VMAT2. These results showed show that exercise significantly reduced the MPTP-induced loss of TH, DAT, and VMAT protein (**Figure 2**). Collectively, these findings in a limited number of animals support the hypothesis that running not only reduced the functional deficit caused by MPTP but also attenuated the loss of DA terminals and increased the capacity for the net efflux of DA into extracellular space.

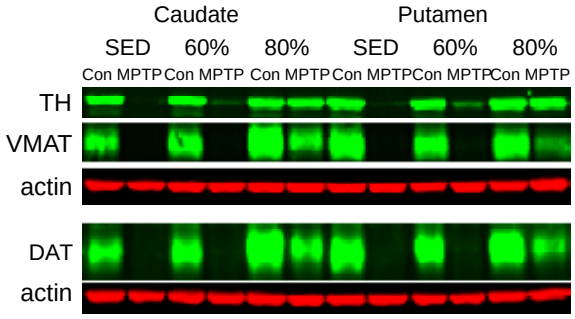

Figure 2: The immunoblot of monkey caudate and putamen from Project 3. Shown is the side of the MPTP injection and the control side of a sedentary (SED) animal and ones who ran at 60% and 80% max heart rate. β-Actin levels were assessed as an equal protein loading control.

Running wheel*:* The most common form of exercise used for rodents is running in a wheel, typically attached to the home cage and available ad libitum. Thus, in 2005 we began to use this approach in our models of PD. This work has been a collaborative venture with Dr. Richard Smeyne at St. Jude Children's Research Hospital, Memphis. In one of these experiments, performed under the direction of Dr. Smeyne, ***female mice*** were housed for 3 mo with access to running wheels and housed either in standard cages or under environmental enrichment cages. They were then given MPTP and a week later, animals were sacrificed and cell counts for TH^+ cells in SN were obtained. Smeyne observed that access to running wheels ± EE abolished the loss of TH^+ cells normally produced by the toxin. This effect has recently been replicated by us using ***male mice*** allowed unlimited access to running wheels for 3 mo prior to and 3.5 wks after a lower dose of MPTP (7.5 mg/kg x 4). Furthermore, we showed that 3.5 wks of running initiated one week ***after*** MPTP also attenuated loss of TH^+ cells in SN, (**Figure 3**), presumably an example of "neurorescue."

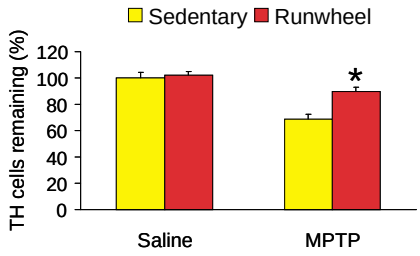

Figure 3: **Neurorescue experiment**: Effect of post-MPTP running on TH^+ neurons in SN. **Male mice** were housed 1/cage either in standard cages or with 24-hr access to a running wheel for 3.5 wks 1 wk post MPTP (4 x 7.5 mg/kg) or saline at 2 hr intervals. MPTP reduced TH^+ SN cells, an effect significantly attenuated by 3.5 wks of running (*p <0.001 ANOVA). Data were collected at Univ. Pittsburgh (Zigmond) and analyzed at St. Jude's (Smeyne).

Parallel experiments in 6-OHDA-treated adult ***male rats*** have yielded comparable results. After 3 months of continuous access to a running wheel, the rats were given a unilateral injection of 6-OHDA into the medial forebrain bundle (MFB) through which the SN-striatal DA projection courses. They were then allowed to run for 5 more weeks after a 1-week interlude, thereby paralleling the protocol used in female monkeys (see above). Brains were then removed for biochemical and histochemical analyses. As shown in representative photomicrographs (**Figure 4, next page**), running dramatically reduced the 6-OHDA-induced loss of TH^+ cells in SN. Moreover, the protection of TH^+ cells in the SN was highly correlated with protection in striatum of TH protein and DAT as assessed by western immunoblotting (WB) (**Figure 5**, $r^2 = 0.753$, next page) and of tissue DA as reflected by HPLC analysis ($r^2 = 0.77$, $p = 0.04$, t-test). No effect of

exercise on contralateral TH, DAT, or DA was observed in these animals, allowing us to express the data as a ratio of ipsilateral to contralateral.

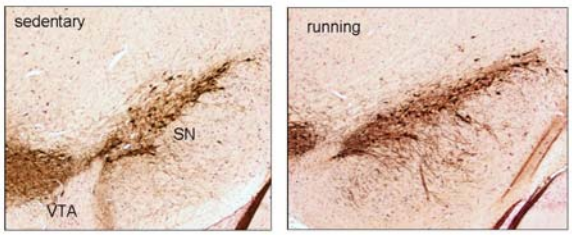

Figure 4: Effect of running on TH^+ cells in rat SN ipsilateral to an intra-MFB injection of 6-OHDA (0.6 μg). Shown are representative sections from animals showing a 50% cell loss (sedentary, left) and 20% cell loss (running, right). Group averages: 52 ± 12 % of contralateral side (no exercise) and 87 ± 7% of control (exercise), p = 0.04 two-tailed t-test; n = 4 and 5 respectively. (See text.)

Collectively, these data reveal that ***the protective effects of exercise are generalized across species (monkeys, rats, mice), gender (males, females), toxins (6-OHDA, MPTP), route (i.p. versus intracranial), and housing location (Pittsburgh vs. St. Jude's).*** Furthermore, the protection of cell bodies is highly correlated with that of terminals (as assessed by multiple, independent assays) and that efficacy can occur when exercise is provided before (***protection***) or after (***rescue***) toxin is applied, thereby avoiding potential confounding effects of exercise on DAT function and paralleling the post-MPTP exercise protection observed in mice.

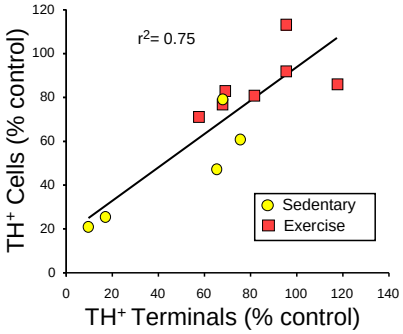

Figure 5: Correlation between loss of TH^+ cells in SN and TH^+ in striatum in 6-OHDA treated rats provided with 3 mo of running exercise (yellow square) or maintained in home cage (red circle). Similar results were obtained for striatal DAT and DA vs. TH^+ cells.

Use of micro-PET in our 6-OHDA model of PD: One of the problems that we and others have in studying interventions in animal models of PD is the inability to examine progressive biological changes in the same animal. We therefore have performed a pilot study to investigate the utility of microPET to monitor changes in DA terminals in rats given unilateral injections of 6-OHDA. The cost of the scans was covered by the PET center itself.

Rats received 6-OHDA (0.75 - 3.0 μg) delivered into the MFB. After 7 or 28 days, the animals underwent PET imaging using ligands for the DA transporter (DAT) ([^{11}C] β-CFT) and/or the D2-receptor ([^{11}C] raclopride). DA release was assessed using D2 receptor imaging before and after amphetamine challenge (4 mg/kg i.p). The extent of striatal denervation was assessed by DA tissue content measured by HPLC. Data were expressed relative to the nonlesioned striatum. [^{11}C] β-CFT binding was reduced in lesioned striatum (range: -18 to -62%) **(Figure 6),** with the reduction being correlated with dose of 6-OHDA and DA depletion. Modest increases in [^{11}C]raclopride binding in lesioned striatum relative to the nonlesioned side were observed in rats that received the highest dose of 6-OHDA (+16 and +35%), suggesting that D2 upregulation occurred only after pronounced DA denervation.

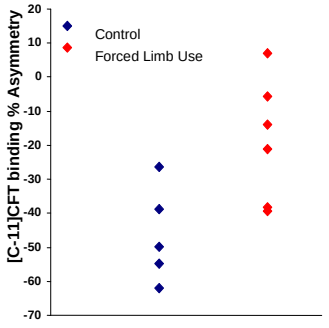

Figure 6. [C-11] β-CFT asymmetry (%) in 6-OHDA treated animals (n=5) and 6-OHDA + exercise (n=6).

Amphetamine pretreatment resulted in greater asymmetry in [^{11}C]raclopride binding between the lesioned and control striatum (range: +7% to +48%), suggesting attenuated DA release in the lesioned striatum. MicroPET was also able to detect a significant attenuation of DAT

loss in animals subjected to forced limb use immediately following 6-OHDA infusion compared to lesioned animals that did not undergo motor therapy ($p<0.001$) (Lopresti et al., 2004). We conclude that microPET is useful for making non-invasive assessments of DA function in rodent models of PD, and may be applied in longitudinal studies to assess the response to putative therapies for PD. Unfortunately, our attempts to obtain funding to continue these studies have not been successful and they are currently on hold.

2. Exercise increases NTFs

Our hypothesis is that exercise confers protection by increasing the availability of trophic factors, including GDNF and BDNF (Figure 1). We have shown that exercise can increase BDNF and GDNF. Indeed, we find that the amount of exercise required for this effect is rather low: We have observed marked increases in these NTFs in mice subjected to a limited amount of motor training: 18 trials on an elevated beam over 11 days was sufficient to increase GDNF and BDNF collected 7 days later. At present, we are examining the time course of changes in NTF message and protein in collaboration with Dr. Smeyne. Our initial observation suggest that exercise increases gene expression for both GDNF and BDNF (**Figure 7**).In the future, we hope to use conditional knockout animals and/or blocking antibodies for these NTFs to determine whether these changes in NTF expression are essential to exercise-induced protection.

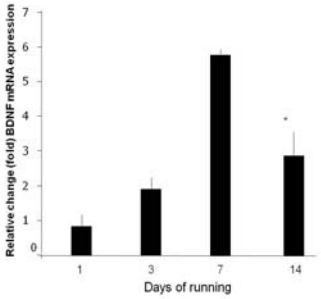

Fig. 7: Changes in mouse striatal mRNA for BDNF as a function of days of running. Mean ± SEM.

3. GDNF can protect in cell-based models

a. MN9D. Many of our studies have used ***MN9D cells*** as models of DA neurons, and in fact we have now accepted the responsibility for distributing these cells to other labs with the approval of Dr. Alfred Heller, who developed these cells (he has retired) and the University of Pittsburgh (which owns the intellectual property rights). These cells have a number of the salient characteristics of DA neurons, including the ability to synthesize and store DA and to respond to GDNF. We find that 6-OHDA produces a concentration- and time-dependent death of these cells, and that these effects are attenuated by the addition of GDNF. Specifically, GDNF (10 ng/ml) protected MN9D cells against 6-OHDA (250 μM) and this was blocked by inhibitors of pERK and pAkt (**Figure 8**; Ugarte et al., 2003; Leak et al, 2007).

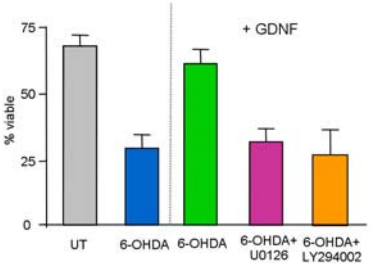

Fig. 8: MN9D cells were treated with 250 μM 6-OHDA for 30 min, alone or with 10ng/ml GDNF. GDNF and 6-OHDA were applied in the absence or presence of the MEK inhibitor U0126 (5-10 μM) or PI3K inhibitor LY294002 (10-50μM). Counts of viable Hoechst stained nuclei were performed 24 hrs after 6-OHDA was removed. Data are mean ± SEM for 4-5 independent experiments.

b. Primary DA: Although cell lines have the advantage that they provide a relatively homogenous population of cells that can be readily transfected and with which stanradr biolchemical analyses can be performed, they are obviously not primary neurons. Thus, we have established the methods necessary for studying ***primary DA neurons*** in culture. Previous studies of such cells failed to obtain specific 6-OHDA-induced DA cell loss; they also have ustilized 6-OHDA in a manner that causes a great deal of non-specific damage. Thus, we have developed a paradigm to obtain such selective effects on primary dissociated cultures of DA neurons from *rats* and *mice*. We prepared dissociated cultures from the SN region of rat pups (P0) and exposed them to 6-OHDA (40-250 μM; 15 min), producing a specific loss of TH^+ cells

while sparing GABAergic neighbors. In this preparation we observed that GDNF (100 ng/ml) blocked 6-OHDA-induced TUNEL labeling at 3 hr (Ding et al., 2004).

4. GDNF can protect in animal models

It has been shown by several previous investigators that GDNF can protect against the effects of 6-OHDA. We have carried out a series of experiments to extend these observations.

Effect of GDNF on the 6-OHDA-induced loss of TH, DAT, and VMAT2 immunoreactivity in the striatum: Rats received the retrograde tracer FluoroGold (FG) into striatum followed 1 wk later by 9 µg GDNF and 6 hr later by 6-OHDA (4 µg). 6-OHDA caused a loss of FG^+ and TH^+ cells in SN 2-8 wk later. At 2 wk post-operative, animals treated with 6-OHDA alone displayed loss of each of the major phenotypic markers for DA neurons as assessed by an IHC analysis of striatum. These markers included tyrosine hydroxylase (TH), the high affinity DA transporter (DAT), and the vesicular monoamine transporter, type 2 (VMAT2). The loss remained constant for the 8-week duration of the study ($p < 0.001$). GDNF alone had no significant effect on the number of TH^+ cells at any time point ($p > 0.05$). Moreover, to our initial surprise, pretreatment with GDNF 6 hrs prior to 6-OHDA infusion did not protect against the loss of these markers at 2 wks. However, these markers gradually recovered over 4-8 wks, with a ~70% reduction in lesion size at 4 wks and an ~80% reduction in lesion size at 8 wks ($p < 0.001$) (**Figure 9**). Treatment with vehicle or GDNF alone had no effect on levels of any of these phenotypic markers.

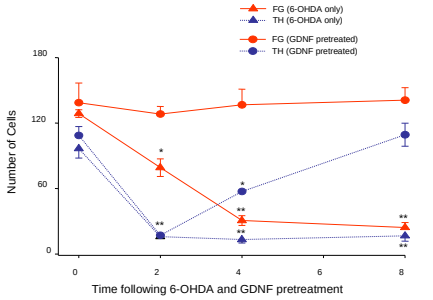

Figure 9. Effect of GDNF (9 µg/3 µl) or vehicle pre-treatment on TH- and FG+ cells in the SN after intrastriatal 6-OHDA (4 µg/0.75 µl) or vehicle infusion in rat. Mean ± SEM of 6-9/group

6-OHDA-induced loss of TH^+ cells in the SN could have been a result of a loss of the DA phenotype rather than actual cell death or degeneration. Indeed, our studies with FG suggest that initially there is a loss of the DA phenotype; however, this is accompanied by a slower but inexorable loss of the cells themselves. A 57% loss of FG^+ cells was observed at 2 wks in animals given 6-OHDA alone ($p < 0.001$), which was even greater at 4 wks (78%; $p < 0.05$) and 8 wks (83%; $p < 0.001$), indicating that 6-OHDA caused a gradual but profound loss of the DA cells projecting from SN to striatum.

In summary, GDNF given just prior to 6-OHDA protects the DA neurons from 6-OHDA. However, whereas no significant loss of cells was detected over the period examined (2 – 8 wk), it took 8 weeks for the restoration of the major phenotypic markers of DA neurons. (In our summary of accomplishments last year, we alluded to this work. However, since we were still completing the project no data were presented.)

5. GDNF may act in part through the activation of ERK and Akt

A major focus of our work is to determine the signaling cascades associated with GDNF-induced protection of DA neurons. Early in our studies, we have found that the protection afforded by exposure of ***MN9D*** cells to GDNF (10-100 ng/ml for 15 min) could be blocked by the MEK inhibitor U0126 (5-10µM) as well as the inhibitor of Akt phosphorylati8on LY294002 (10-50 µM) (**Figure 8**, previous page; Ugarte et al., 2003). Later we observed that this was accompanied by an increase in phosphorylated ERK1/2 (pERK), an increase in ERK *activity* as assessed in a kinase activity assay using the transcription factor Elk1, a well-known ERK target, and an increase in pCREB, and an increase in pAkt (data not shown).

We also examined the effect of forced limb use, running, and GDNF on activation of ERK1/2 in our ***animal models*** of the DA loss that accompanies PD. As indicated by WB, forced use of one limb increased pERK1/2 by 4-fold in the contralateral striatum at 24 hr, and levels remained high for the 7-day casting period. In the SN, the increase in pERK1/2 was more gradual but reached a comparable level within 7 days. We have also found that running causes an increase in pERK, as well as pAkt. Moreover, the direct injection of GDNF into either rat and mouse striatum also produced a marked increase of pERK1/2 in both striatum and SN. In each case, the changes occurred primarily within dopamine neurons (i.e., neurons that were TH^+) of the SN as indicated by double label confocal microscopy (e.g., **Figure 10**).

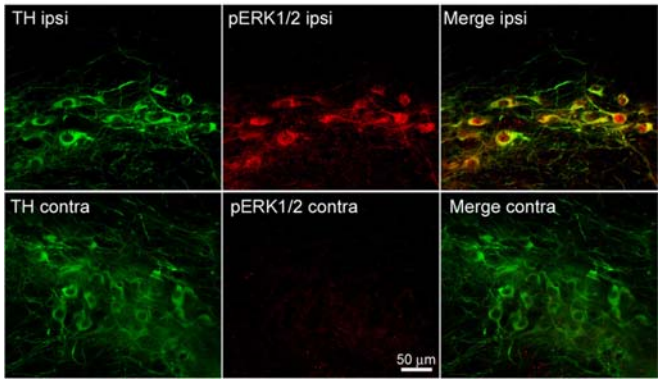

Figure 10: Effect of intrastriatal GDNF on pERK. Animals received intrastriatal GDNF or vehicle. After 24 hrs, the animals were perfused, representative sections of SN labeled with anti-pERK1/2 and anti-TH, and then viewed with confocal microscopy. In ipsilateral SN the vast majority of TH cells were dual-labeled, whereas no pERK staining was observed in the contralateral SN.

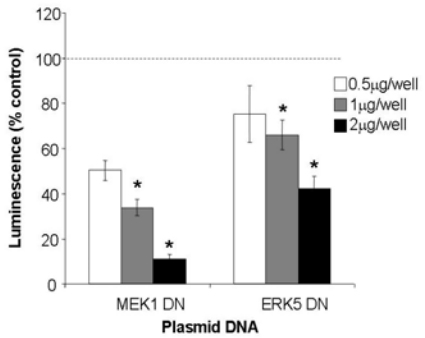

Figure 11: Effects of transfection with dominant negative MEK1 or ERK5 on basal MN9D cell survival. Cells were also co-transfected with a luciferase reporter plasmid and the number of lucerfase-positive cells counted after 24 hr. Shown is the mean ± SEM. Shown are means ± SEM. Results are representative of 3 independent experiments.

Role of ERK 5: ERK5 is also a member of the MAPK family. Although its biological function is poorly defined, it is known to be activated by NTFs and thus may play a role in cell survival. Indeed, our preliminary data indicate that GDNF (10 ng/ml) activates ERK5 in MN9D cells and that U0126 (10 µM), which blocks the protective effects of GDNF, also blocks ERK5 activation. We also observed that U0126 decreased basal survival of these cells. Since U0126 blocks the phosphorylation of ERK5 as well as ERK1/2, we wished to determine which ERK isoform(s) were critical to this effect. Cells were transfected with either dnERK5 or dnMEK1, the specific upstream activator of ERK1/2. Transfection of MN9D cells with either dominant negative construct reduced basal cell survival (**Figure 11**). Moreover, transfection of the cells so as to increase ERK1/2 activity inhibited 6-OHDA-induced cell death. A similar trend was observed for treatments that increased ERK5 activity but the effect was not significant (data not shown). These studies demonstrate a role for ERK5 in basal DA cell survival, and may also point to a difference between ERK1/2 and 5 in influencing protection of DA cells from oxidative stress (Cavanaugh, 2006).

Effect of GDNF on pERK levels in mouse striatum: We have also established a mouse model in which to examine the effects of GDNF in order to take advantage of the availability of mouse lines in which one or more NTF or NTF receptor is knocked out. In these studies, GDNF was infused into the striatum and striatal pERK1/2 was analyzed by IHC at 24 hr. GDNF caused a unilateral dose-dependent increase in the phosphorylation of ERK1/2 in the striatum that was significant at 0.045 µg GDNF and peaked at 0.45 µg, reaching 330% of vehicle control. At 4.5 µg of GDNF, the rise in phosphorylation appeared to decrease slightly

from the effect at 0.45 µg. However, this decrease was not significant. Comparable data were obtained via Western blot analysis.

The temporal effects of high and low GDNF on pERK1/2: The infusion of 0.45 µg GDNF caused a time-dependent increase in pERK1/2 in the ipsilateral striatum analyzed by IHC that was detectable by 3 hr ($p < 0.01$), reached 420% above control by 7 days but was back to basal levels by 4 weeks. Infusion of 4.5 µg GDNF also caused a time-dependent increase in pERK1/2 that appeared slightly lower than the effect of 0.45 µg GDNF, although the difference was not significant. Seven days after administration of 4.5 µg GDNF there was a small region of downregulation of ERK1/2 phosphorylation around the needle track despite the fact that pERK1/2 was still increased in the remaining ipsilateral striatum (Lindgren et al., 2008; **Figure 12**). In contrast, only the higher dose of GDNF activated Akt, raising the possibility that Akt played a critical role.

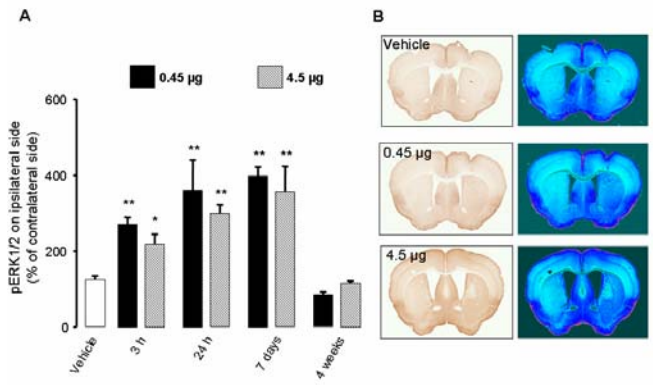

Figure 12: Effect of intrastriatal GDNF on striatal pERK1/2 as a function of time. Animals received vehicle, 0.45 µg GDNF or 4.5 µg GDNF into the striatum. After 3h, 24h, 7 days, or 4 weeks the animals were perfused and brain sections were labeled with anti-pERK1/2. A. The labeled sections were scanned and quantified using Metamorph software. The measured immunoreactivity in the ipsilateral striatum is expressed as a percent of the non-injected contralateral striatum in all animals, including vehicle controls. Data are mean ± SEM. *P<0.05, **P<0.01 vs. vehicle, ANOVA followed by Dunnett's. B. Representative slides of a vehicle injected animal (top), an animal injected with 0.45 µg of GDNF (middle), and an animal injected with 4.5 µg of GDNF (bottom). The slides to the left are unaltered scanned images, whereas the images on the right were modified with Metamorph software to visualize intensity differences.

Effect of high and low dose GDNF on toxicity induced by 6-OHDA: Mice injected with vehicle, 0.45 µg or 4.5 µg GDNF received 6-OHDA (0.5 µg) into the striatum 6 hr later. After 4 weeks, the mice were sacrificed, and the presence of DA terminals in the striatum was analyzed by IHC for TH, a marker for these neurons. 6-OHDA by itself caused a large loss of TH immunoreactivity at the site of toxin injection. Injection of 4.5 µg GDNF significantly reduced the 6-OHDA-induced loss of TH immunoreactivity by 75%. In contrast, 0.45 µg GDNF did not have any apparent effect on the 6-OHDA-induced TH loss (Lindgren et al., 2008; **Figure 13**). In summary, GDNF protected against the effects of 6-OHDA in the mouse as in the rat. However, contrary to our in vitro results, whereas 0.45 µg GDNF produced a maximal increase in striatal pERK levels, it did not protect against 6-OHDA – a significantly higher concentration of GDNF was required for the latter effect. We will

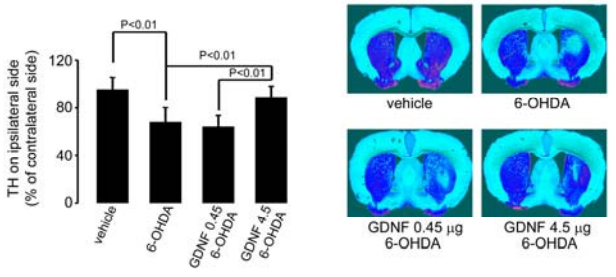

Figure 13. Effect of GDNF on TH^+ loss induced by 6-OHDA. Mice received vehicle or GDNF into striatum. Six hr later, 6-OHDA (0.5 µg/0.5µl at 0.1 µl/min) or saline was infused in the striatum at the same site. Images obtained from tissue obtained 4 wk later, sectioned, stained for TH, and quantified using Metamorph software. Mean ± SEM for 6/group. *P<0.01 vs. vehicle. Note that GDNF-induced protection was observed at 4.5 µg but not 0.45 µg.

be examining other possible explanations for the cellular basis of GDNF protection, beginning with a possible role for Akt as suggested by our initial data.

6. The effects of pERK depend in part on it localization; its neuroprotective actions may involve a suppression of BimEL

Developing constitutively active (CA) forms of ERK. The capacity to over-express active ERK isoforms is essential to our research objectives. It has been shown, however, that substituting T183 and Y185 on ERK2 with glutamate does not mimic phospho-T183 and phospho-Y185. The resulting double mutant cannot function as the constitutively active version of the kinase. To circumvent this problem, we employed co-expression of caMEK with wt ERK1 or 2 respectively, and have shown that we can over-express pERK1 and pERK2 (**Figure 14**).

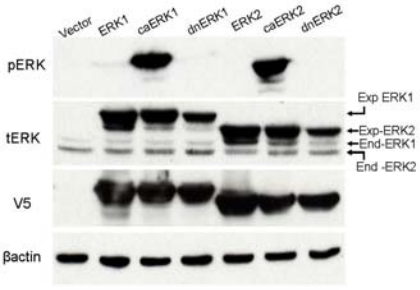

Figure 14. Ca and dnERK1 and ERK2 expression in HEK293 cells. The coding sequences of each construct was first cloned into pcDNA3.1 with V5 and His tags and transfected. Exp, expressed; End,

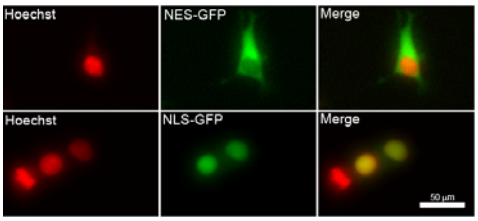

Figure 15: Localization of GFP fused with NES or NLS, and transfected into MN9D cells using Lipofectamine (Invitrogen). Nuclei were stained for Hoechst (red) and GFP was visualized by green immunofluoresence.

Directing the cellular localization of key molecules: It is important that we be able to control the localization of pERK isoforms if we are to determine conclusively whether the compartment within which pERK resides is a crucial factor in determining its impact on cell survival. As a first step in accomplishing this, we created constructs in which either the NLS or NES sequences were fused to EGFP or to ERK. We then expressed them in HEK293 cells and in MN9D cells. These sequences successfully directed the fused proteins to the nucleus (NLS) or cytoplasm (NES) **(Figure 15**). Furthermore, we have mutated the leucine residues at 33 and 37 to alanine on the caMEK1 gene to disrupt the NES motif and the aspartic acid at 316 to alanine on the ERK2 gene (termed 316A) to abrogate its association to MEK1 without affecting its capacity to be phosphorylated (activated) and function as a kinase. This construct was then co-expressed in HEK293 cells with the ERK2-316A gene fused with NLS sequence. Twenty-four hours post-transfection, the cells were immunostained with pERK and counter-stained with Hoechst staining. The wt ERK2 gene with NLS sequence was used as control. Without the NLS sequence, the pERK2 was localized largely in the cytoplasm. However, after the modification, the pERK2 in the nucleus was significantly increased, reflecting the expected function of NLS sequence. Moreover, the co-expression of these two constructs resulting in a significant increase in cell death, both under basal conditions and in response to H_2O_2. We also can separate nuclear from cytoplasmic proteins by subcellular fractionation. This work is being readied for publication.

The role of BimEL: Neurotrophic factors such as GDNF or BDNF are able to protect against stress-induced cell death. However, the cellular events that underlie this protection are not well understood. In this study, we examine the protective characteristics of individual and combined treatments with GDNF and BDNF in SH-SY5Y cells under the insult of H_2O_2. Our observations indicate that the ability of GDNF and BDNF is accompanied by a decrease in pERK and in BimEL **(Figure 16**, next page). Inhibition of ERK activation with U0126 reversed the decrease in BimEL and abolished the protection, suggesting that ERK is a key MAP kinase regulating BimEL and that this interaction played a significant role in protection by the trophic factors. Finally, clones in which BimEL was constitutively knocked down had higher tolerance towards H_2O_2 and an attenuated protection by the trophic factors. Collectively, the results

suggest that GDNF and BDNF can act via a pERK-mediated regulation of BimEL to reduce the vulnerability of SH-SY5Y cells to oxidative stress.

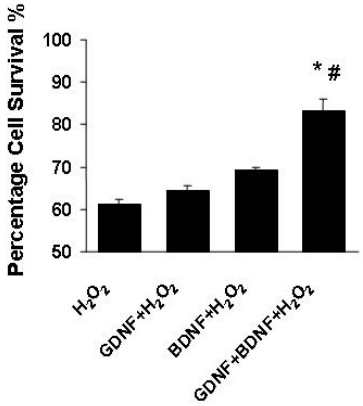

Figure 16: Comparison of protection by GDNF (20 ng), BDNF (20 ng), and the combination in SH-SY5Y cells exposed to H_2O_2. (60 μM) for 24 hrs. Viability was assayed with the WST-1 reagent. Shown are means ± SEM from 3 independent experiments. (Adding NTFs at 2x concentration did not produce further protection.)

7. Prior exposure to low levels of stress can lead to a protective, "preconditioning" effect

***a. Short-term studies with MN9D and 6-OHDA*:** Our basic assumption is that protective treatments alter both post-translational and translational events so as to reduce the vulnerability of the affected cells. Such treatments include GDNF and 6-OHDA (despite its neurotoxic consequences) Given our observation that the 6-OHDA-induced phosphorylation of ERK serves to reduce the cell death caused by that toxin, it seemed reasonable to predict that low concentrations of 6-OHDA could actually precondition cells against later higher concentrations of 6-OHDA. We have, indeed, shown that this was the case. Brief exposure to subtoxic 6-OHDA (2.5 – 10 μM) significantly reduced the vulnerability of MN9D cells to a 30 min-exposure to a toxic 6-OHDA concentration (50-200 μM) delivered 6 hr later when viability was measured 24 hr later by Hoechst staining (**Figure 17**) (Leak et al., 2007).

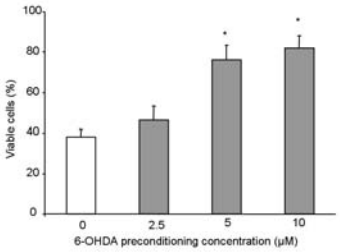

Figure 17: Effect of prior exposure of MN9D cells to subtoxic concentrations of 6-OHDA on the subsequent response to a concentration of 6-OHDA that normally represents the approximate LD_{50} (50 μM).

We have gone on to show that 6-OHDA preconditioning was associated with fundamental changes in the protein profile of the MN9D cells, which included changes in gene expression, alterations in protein synthesis, and post-translational state. Although we have not yet examined the effects of GDNF on gene expression in these cells, we have performed preliminary analyses of the effects of 6-OHDA alone. MN9D cells, when exposed to 6-OHDA, show a rapid, robust change in expression profile using MG430 whole genome oligonucleotide microarrays. For example, 6 hr after a 30-min exposure to a sub-toxic concentration of 6-OHDA (5 μM) we identified a number of gene expression changes related to cellular signaling, apoptosis, oxidative phosphorylation, chaperone molecules and structural proteins. In addition, there was increased phosphorylation of ERK, Akt, and JNK, and inhibitors of the phosphorylation of each kinase blocked preconditioning. These results have been published (Leak et al., 2007).

b. *Longer-term studies with PC12 and MG132*: We have selected PC12 cells, a line more generally available than MN9D cells and about which considerably more is known. PC12 cells have the added advantage that they do not change with successive passages as much as do MN9D cells and thus seem a better model for longer experimental time frames. In our initial studies, we found as expected that PC12 cells did not take up ^{3}H-DA. Thus, we chose to make use of PC12 cells stably transfected with human DA transporter (kind gift of Dr. Gonzalo Torres at the University of Pittsburgh) to ensure rapid high affinity uptake of 6-OHDA into the cell within a short exposure interval. We first confirmed a high expression of TH and nomifensine-sensitive DA uptake. Given that cellular stress is often chronic, we decided to examine a long-term treatment to test the hypothesis that otherwise healthy cells exposed even to a chronic insult would be protected against subsequent insults. 6-OHDA was not suitable for long-term exposures because it rapidly oxidizes under culture conditions. Thus, we applied the

proteasome inhibitor MG-132 chronically to PC12 cells.

Cells were grown for 2 weeks in 0.1μM MG-132 and then continuously maintained in the presence of this inhibitor. The treatment reduced chymotrypsin-like proteasome activity by 47% and was associated with protection against both 6-OHDA (100 mM) (**Figure 18**) and higher dose MG132 (40 mM). Protection developed slowly over the course of the first 2 weeks of exposure and was chronic thereafter. There was no change in total glutathione levels after MG132. Buthionine sulfoximine (100 mM) reduced glutathione levels by 60% and exacerbated 6-OHDA toxicity to the same extent in both MG132-treated and control cells, without reducing MG132-induced protection. Chronic MG132 resulted in elevated antioxidant proteins CuZn superoxide dismutase (SOD, +55%), MnSOD (+21%), and catalase (+15%), as well as chaperone heat shock protein 70 (+42%). Examination of SOD enzyme activity revealed higher levels of CuZnSOD (+40%), without any change in MnSOD activity. We further assessed the mechanism of protection by reducing CuZnSOD levels with two independent siRNA sequences, both of which successfully attenuated protection against 6-OHDA.. Previous reports suggested that artificial overexpression of CuZnSOD in dopaminergic cells is protective. Our data complement such observations, revealing that dopaminergic cells are also able to use endogenous CuZnSOD in self-defensive adaptations to chronic stress, and that they can even do so in the face of extensive glutathione loss. These results have now been published (Leak et al., 2008).

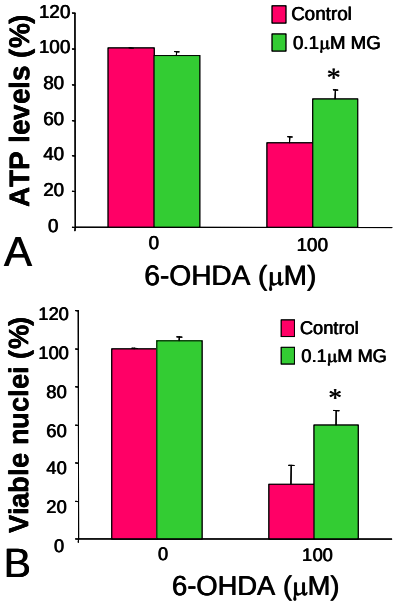

Figure 18: PC12 cells chronically treated with 0 or 0.1 μM MG-132 were exposed to a challenge of 100 μM 6-OHDA. Cells were lysed and assayed for ATP levels (A) or stained with Hoechst reagent (B) 24 hrs after the challenge. * $p < 0.05$ compared to non-MG-132 treated control cells, Bonferroni post-hoc.

c**. *Studies of methamphetamine***: Mild stress can protect against a subsequent larger insults, a phenomenon termed “preconditioning” or “tolerance.” We sought to determine if a mild stressor could also protect cells in a model of the dopamine deficiency associated with Parkinson's disease. We used methamphetamine and 6-hydroxydopamine (6-OHDA) as sources of oxidative stress and MN9D cells as a model of dopamine neurons. We observed that prior exposure to subtoxic concentrations of methamphetamine (0.1 - 0.5 mM) protected these cells against 6-OHDA toxicity, whereas higher concentrations of methamphetamine (3 – 5 mM) did not. The protection by methamphetamine was accompanied by a decrease in uptake of both [^{3}H]dopamine and 6-OHDA into the MN9D cells, which may have accounted for some of the apparent protection. However, a number of other effects of methamphetamine exposure suggested that the drug also affected basic cellular survival mechanisms. First, although preconditioning with methamphetamine decreased pERK levels, it also enhanced the 6-OHDA-induced increase in pERK1/2. Second, this was accompanied by an increase in the apparent activity of MEK1/2 and a decrease in the apparent activity of protein phosphatase 2A. Third, the pro-survival protein Bcl-2 was upregulated by methamphetamine exposure. Our observations suggest that exposure to subtoxic methamphetamine concentrations can cause a complex change in dopamine cells, resulting in a decrease in the vulnerability of those cells to subsequent oxidative stress. These observations are consistent with other studies involving exposure of dopamine cells to stress and may have implications for the development of new therapies for the prevention or treatment of PD. A manuscript is in the final stages of submission for publication.

8. 6-OHDA may trigger a defensive increase in phosphokinase levels.

In our in early vitro studies with ***MN9D cells***, we also observed that ERK was activated by 6-OHDA itself. This initially appeared to us to be paradoxical since it suggested that a toxic stimulus initiating a *neuroprotective* response. One possibility was that pERK served as a *pro-survival* response after GDNF and a *pro-death* response after 6-OHDA. A precedent for such a dichotomy exists, and our studies of 6-OHDA preconditioning are consistent with this formulation (see above). However, it was also possible that the pERK response to 6-OHDA we saw represented a defensive reaction to oxidative stress, and this appears to be the case: MN9D cells were treated with 6-OHDA (250 µM) and the time course of changes in pERK isoforms was determined. We observed that pERK1 and pERK2 were increased 25-fold at 15 min but returned to baseline by 30 min. After removing 6-OHDA, a smaller sustained peak in pERK1/2 arose between 3-6 hr and persisted for several more hr. This late pERK peak was temporally associated with activation of caspase-3 and cell death. Phosphorylation of CREB, one of the molecules that ERK phosphorylates through its action on RSK, also occurred during both the transient and sustained 6-OHDA-induced pERK activation. Addition of U0126 (5 µM) before and during toxin exposure to block the first pERK peak, significantly increased cellular vulnerability to 6-OHDA (50-250 µM) . No such effect was seen if U0126 was provided after this initial peak. These data suggest that the initial transient activation of ERK after oxidative stress is a compensatory response to reduce cellular vulnerability. Inhibiting the second, sustained pERK peak had no detectable effect on cell viability (Lin et al., 2008).

Next, 6-OHDA (3 µg in 2 µl) was injected into ***rats*** along the MFB and increased activation of pERK1/2 was assessed in the SN and striatum after sacrificing our animals by focused microwave irradiation. Again, a combination of WB and ICC was used. The activation of ERK1/2 in response to 6-OHDA was observed in cells as early as 15 min in the SN and persisted for at least 24 hrs post-infusion. Double labeling for pERK1/2 and TH revealed that the increase in pERK1/2 was in DA neurons in the SN (**Figure 19**). In the striatum, increases in pERK1/2 were first observed at 1 hr and persisted for at least 24 hrs. Activation of ERK1/2 was observed in fibers as well as cells in the striatum. We believe that the increase in pERK1/2 in fibers in the *striatum* is in TH immunoreactive terminals; however, double labeling is still needed to show co-localization of pERK1/2 and TH in the striatum. As in the case of the MN9D cells, we hypothesize that the activation of pERK1/2 within DA cells of SN and DA fibers within the striatum is a self-protective response to counteract the effects of 6-OHDA-induced oxidative stress. Experiments are ongoing to determine the precise role of pERK1/2 in oxidative-induced damage to the nigrostriatal pathway after infusion of 6-OHDA into the MFB (Smith et al., 2004; Castro et al., 2005). We anticipate completing this work within the next few months.

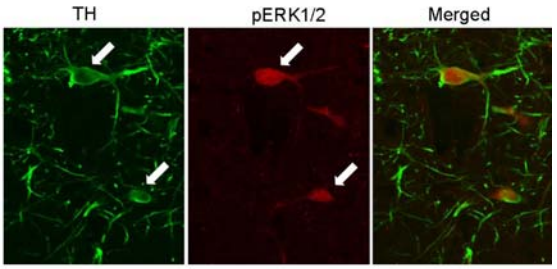

Figure 19: Endogenous pERK1/2 (red) in rat SN 24 hr after intra-MFB injection of 6-OHDA (3 µg/ 2 ul). Note absence of TH (green) in the nucleus of the two large cells in the left hand panel contrasted by the presence of pERK throughout the cell in the middle panel (arrows).

We also observed an increase in pERK1/2 when rats were given ***intrastriatal*** 6-OHDA (6 µg in 1 µl). This increase could be detected by 15 min and persisted for several hours. A similar temporal profile was observed for pJNK, although the peak increase was lower than for pERK. The morphology of the cells containing the increased activated MAP kinases suggests that they were the principal target neurons for the DA projection from SN, the medium spiny

neurons, although this has not yet been confirmed by double labeling. The increases in MAP kinases were accompanied by a delayed increase in cfos, which was first detectable at 1 hr and remained for at least 3 hr. No changes in activated MAP kinases or cfos were observed in the substantia nigra (Smith et al., 2004, Fischer et al., 2005). Activation of ERK1/2 and cfos induction has previously been reported following administration of drugs that activate DA receptors, and the induction of cfos can be attenuated by the administration of a DA antagonist. Thus, we hypothesize that changes in activated MAP kinases and in cfos represent the effects of endogenous DA being released in response to the neurotoxic actions of 6-OHDA. This suggests that initial changes in striatal pERK and cfos would be useful as short-term indices of the efficacy of neuroprotective treatments. This work is being prepared for publication.

9. The product of the LRRK2 gene protects DA neurons due in part of ERK activation; this does not occur with the Y1699C mutation.

As indicated in our Introduction, PD is likely to involve interactions between environment and genetics. Recently, mutations in LRRK2 have been identified as a major factor in PD. Moreover, LRRK2 contains a kinase domain, raising the possibility that its actions are related in some way to the NTF-kinase axis that is central to our interests. Thus, we have decided to characterize functional differences between wild-type LRRK2 and Y1699C mutant in response to oxidative stress. The constructs containing human LRRK2 wild-type gene and Y1699C mutant fused with GFP at the C-terminal in the mammalian expression vector pCDNA3.1 were kind gifts from Dr. Matthew Farrer and the Neurogenetics Laboratories, Mayo Clinic, Jacksonville. In our initial characterization, we have selected HEK293 cells as the host for the wild-type LRRK2 and Y1699C mutant and H_2O_2 as the stressor. This allows us to achieve high transient transfection efficiency and a readily reproducible insult in order to begin to examine the initial interaction between LRRK2 and oxidative stress.

Changes in basal cell physiology due to expression of wild-type LRRK2 and Y1699C mutant: First, we examine changes in basal cell viability and basal levels of pERK and pJNK due to expression of wild-type LRRK2 or Y1699C mutant in HEK293 cells. To ensure high transfection efficiency, we monitored the expression of each LRRK2 gene by fluorescence microscopy via their GFP moiety fused to their C-terminal, finding that at least 70% of our cells exhibited the green fluorescence demonstrating the efficacy of this approach. The presence of wild-type LRRK2 and Y1699C mutant in HEK293 cells was also visualized by probing immunoblots with an antibody recognizing GFP. No band was detected in lysate derived from cells transfected with the empty vector (pcDNA3.1). We have also failed to detect endogenous wild-type LRRK2 in HEK293 cells with several commercially available antibodies.

Expression of either wild-type or mutant LRRK2 decreased the pERK level, with the mutant producing a larger decrease than the wild-type when compared to cells transfected with pcDNA3.1. These changes were not associated with alterations in total ERK. Moreover, no visible changes in the expression level of pJNK and total JNK were detected. Expression of wild-type LRRK2 and the Y1699C mutant for 24 hours consistently resulted in a 40% drop in basal cell viability of HEK293 cells. A similar observation has also been reported in studies where wild-type and mutant LRRK2 were expressed in other cell types, suggesting that over-expression of these proteins in mammalian cells could be toxic.

Cells expressing wild-type LRRK2 are more resistant to oxidative stress than cells expressing Y1699C mutant: Next, we examined the interaction of LRRK2 and H_2O_2, using a concentration of the peroxide that is roughly at the EC50 for toxicity (150 μM). At 4 hr after the plasmid transfection process no visible cell death was observed. However, at 18 hr of H_2O_2 treatment, we observed that cells expressing LRRK2 wild-type gene exhibited higher resistance towards H_2O_2 toxicity with 27% cell death as opposed to 50% cell death in cells expressing

Y1699C mutant under the same treatment (**Figure 20a**). Cells expressing wild-type LRRK2 elicited a significantly higher pERK level in response to H_2O_2 toxicity than cells expressing Y1699C mutant (**Figure 20b**). No such change was observed for pJNK. Thus, the results suggest potential cross-talk between LRRK2 and the ERK pathway. Moreover, the observed higher level of pERK consistently correlated with a lower H_2O_2-induced cell death in cells expressing wild-type LRRK2 as compared to those expressing Y1699C mutant. We intend to perform subsequent experiments to examine any causative relationship between ERK activation and attenuation in cell death.

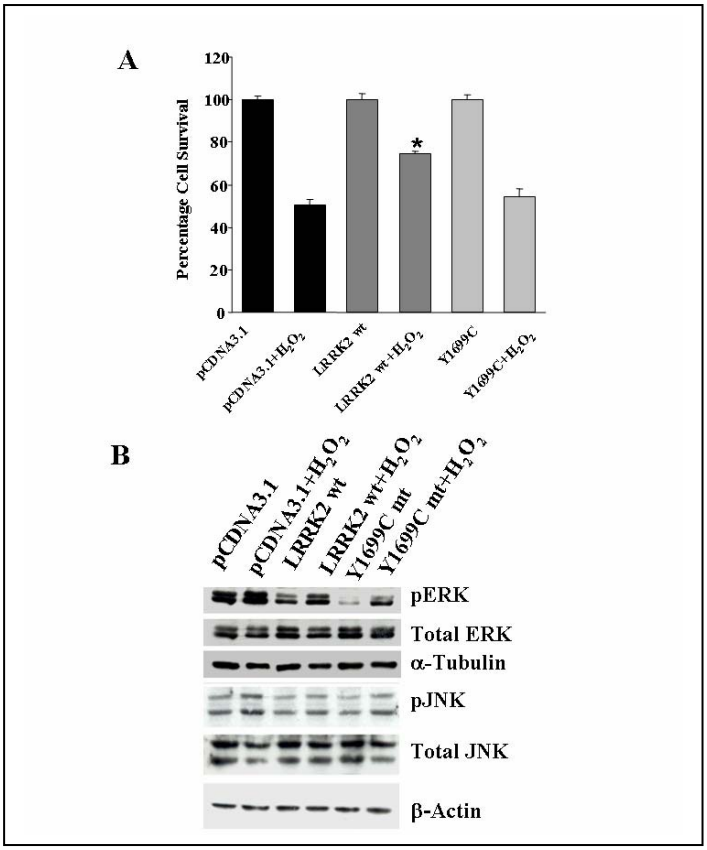

Figure 21: Impact of LRRK2 wild-type gene and Y1699C mutant gene expression on H2O2-induced cell death. (A) Attenuation of H_2O_2-induced cell death for cells expressing LRRK2 wild-type gene, but not in cells expressing Y1699C mutant gene. Percentage cell death induced by H_2O_2 among cells transfected with pCDNA3.1, expressing LRRK2 wild-type or Y1699C mutant gene is normalized against untreated cells transfected with the same vector or expressing the same proteins. Data are means ± SEM, at least 24 readings per data point, from six independent experiments. * $p < 0.05$ versus viability of cells transfected with pCDNA3.1 after 150 μM of H2O2 treatment for 18 hours. (B) Corresponding changes in activated ERK, total ERK, activated JNK, and total JNK in HEK293 cells expressing LRRK2 wild-type gene or Y1699C mutant gene with and without chronic treatment with 150 μM of H_2O_2 for 18 hours. β-Actin was used as loading control.

In summary, it appears that the wild-type form of LRRK2, but not the Y1699C mutant reduces the vulnerability of HEK293 cells to the oxidative stress imposed by H_2O_2. This is associated with an increase in pERK, which also is produced by wild-type gene expression.

Key Research Accomplishments

- Physical exercise increases the resistance of DA neurons in mouse and rat to the specific neurotoxins 6-OHDA (mouse, rat) and MPTP (mouse)
- The effects of exercise could be mimicked by GDNF. However, full restoration of the DA phenotype required 4-8 weeks.
- Increases in pERK1/2 and pAkt were associated with the neuroprotective effects of exercise and GDNF, and comparable effects of GDNF could be seen in in DA cells studied in culture.

- The nature of the actions of pERK depend on the amplitude of the change, its time course, and its subcellular localization.
- Inhibition of proteasomal function increased the resistance of MN9D and PC12 cells to the toxic effects of proteasome inhibition (MG-132) and oxidative stress (6-OHDA). This may be due in part to changes in phosphokinases and in the expression of SOD.
- LRRK2 increased resistance of HEK293 cells to oxidative stress (H_2O_2) more effectively that did the Y1699C mutant. This was associated with an increase in pERK1/2 cells produced by the wild-type but not the mutant form of the gene.

Reportable Outcomes

Manuscripts (* = PDF file provided at end of this report)

Cohen AD, Tillerson JL, Smith AD, Schallert T, **Zigmond MJ.** Neuroprotective effects of prior limb use in 6-hydroxydopamine-treated rats: Possible role of GDNF. *J. Neurochem*, **85**: 299-305, 2003.

Ugarte SD, Lin, E, Klann E, **Zigmond MJ**, Perez RG. The effects of GDNF on 6-hydroxydopamine-induced death in a dopaminergic cell line: Modulation by inhibitors of PI3 kinase and MEK. *J. Neurosci. Res,* **73**: 105-112, 2003.

Juranyi Z, **Zigmond MJ**, Harsing LG. [^{3}H] Dopamine release in a striatum in response to cortical stimulation in a corticostriatal slice preparation. *J. Neuroscience Methods*, **126**: 57-67, 2003.

Smith AD, Antion MD, **Zigmond MJ**, Austin MC. Effect of 6-hydroxydopamine-induced lesions of the nigrostraital projections on GDNF and its receptor mRNA in the adult rat. *Molecular Brain Research*, **117**: 129-138, 2003.

Ding YM, Jaumotte JD, Signore, AP, **Zigmond MJ**. Effects of 6-hydroxydopamine on primary cultures of substantia nigra: Specific damage to dopamine neurons and the impact of glial cell line-derived neurotrophic factor. *J. Neurochem*, **89**: 776-787, 2004.

Jaumotte JD, **Zigmond MJ**. Dopaminergic innervation of forebrain by ventral mesencephalon in organotypic slice co-cultures: Effects of GDNF. *Mol Brain Res*. 134: 139-146, 2005.

Smith AD, Kozlowski DA, Bohn MC, **Zigmond MJ.** Effect of AdGDNF on dopaminergic neurotransmission in the striatum of 6-OHDA-treated rats. *Exp. Neurol*, **193**: 420-426, 2005.

Leak RK, Liou, AKF, **Zigmond MJ**. Effect of sublethal 6-hydroxydopamine on the response to subsequent oxidative stress in dopaminergic cells: evidence for preconditioning. *J Neurochem*., **99**: 1151-1163., 2006.

*Cavanaugh JE, Jaumotte JD, Lakoski JM, **Zigmond MJ**. Neuroprotective role of ERK1/2 and ERK5 in a dopaminergic cell line under basal conditions and in response to oxidative stress. *J Neurosci Res*., 84:1367-1375, 2006.

Venneti S, Lopresti BJ, Wang G, Slagel SL, Mason NS, Mathis CA, Fischer ML, Larsen NJ, Mortimer AD, Hastings TG, Smith AD, **Zigmond MJ**, Suhara T, Higuchi M, Wiley, CA. A comparison of the high-affinity peripheral benzodiazepine receptor ligands DAA1106 and ®-PK11195 in rat models of neuroinflammation: Implications for PET imaging of microglial activation. *J Neurochem*, **102**:2118-31, 2007.

*Lin E, Cavanaugh JE, Leak RK, Perez RG, **Zigmond MJ**. Rapid activation of ERK by 6-hydroxydopamine promotes survival of dopaminergic cells. *J Neurosci Res* **86**:108-117, 2008.

*Lindgren N, Leak RK, Carlson KM, Smith AD, **Zigmond MJ.** Activation of the extracellular signal-regulated kinases 1 and 2 by glial cell line-derived neurotrophic factor and its relation to

neuroprotection in a mouse model of Parkinson's disease. *J Neurosci Res*, **86**:2039-2049, 2008.

Pienaar IS, Kellaway LA, Russell VA, Smith AD, Stein DJ, **Zigmond MJ**, Daniels WMU. Maternal separation exaggerates the toxic effects of 6-hydroxydopamine in rats: Implications for neurodegenerative disorders. *Stress*, **11**:448-56, 2008.

*Leak RK, **Zigmond MJ**, Liou AKF. Adaptation to chronic MG132 reduces oxidative toxicity by a CuZnSOD-dependent mechanism. *J Neurochem*, **106**:860-874, 2008.

*Liou AK, Leak RK, Li L, **Zigmond MJ**. Wild-type LRRK2 but not its mutant attenuates stress-induced cell death via ERK pathway. *Neurobiol Dis*. **32**:116-24, 2008.

Abstracts

Stachowiak, EK, Jaumotte, JD, **Zigmond, MJ**, Buzanska, L, Stachowiak, MK. Differentiation of human umbilical cord blood-derived neural stem cells in co-cultures with rat brain basal ganglia cells. Program No. 151.12. *2003 Abstract Viewer and Itinerary Planner*. Washington, DC: Society for Neuroscience, 2003. Online.

Harsing, LG, Juranyi Z, **Zigmond, MJ**. Cortical stimulation influences striatal dopamine release via gabaergic neurons in corticostriatal slices of the rat. Program No. 705.8. *2003 Abstract Viewer and Itinerary Planner*. Washington, DC: Society for Neuroscience, 2003. Online.

Jaumotte JD, Cavanaugh JE, Nufer MA, Lakoski JM, **Zigmond MJ**. The role of extracellular signal-regulated kinases 1 and 2 and phosphatidylinositol-3-kinase pathways in GDNF-mediated neuroprotection of primary substantia nigra neurons from 6-OHDA toxicity. Program No. 946.2. *2003 Abstract Viewer and Itinerary Planner*. Washington, DC: Society for Neuroscience, 2003. Online.

Lin E, Stanciu M, **Zigmond MJ**, Perez RG. The role of ERK in dopaminergic cell survival after exposure to oxidative stress. Program No. 946.3. *2003 Abstract Viewer and Itinerary Planner*. Washington, DC: Society for Neuroscience, 2003. Online.

Mirnics ZK, Mirnics K, Smith AD, Lin E, Jaumotte JD, Douglass KC, Macioce M, Lewis DA, Schor NF, **Zigmond MJ**. Striatal expression change in transferring is associated with exercise-induced protection against 6-hydroxydopamine. Program No. 948.9. *2003 Abstract Viewer and Itinerary Planner*. Washington, DC: Society for Neuroscience, 2003. Online.

Cohen AD, Jaumotte JD, **Zigmond MJ**, Smith AD. Impact of forced limb use on 6-OHDA-induced degeneration of the DA nigrostriatal pathway. Program No. 948.12. *2003 Abstract Viewer and Itinerary Planner*. Washington, DC: Society for Neuroscience, 2003. Online.

Cavanaugh JE, Jaumotte JD, Pinchevsky D, Ganabathi R, Lakoski JM, **Zigmond MJ**. The role of ERK5 in GDNF-mediated neuroprotection of dopaminergic neurons from oxidative stress. . Program No. 221.3. *2004 Abstract Viewer and Itinerary Planner*. Washington, DC: Society for Neuroscience, 2004. Online.

Lindgren N. Chelluri J, Cohen AD, **Zigmond MJ**. The effect of exercise on a striatal, rat model of Parkinson's disease. Program No. 221.2. *2004 Abstract Viewer and Itinerary Planner*. Washington, DC: Society for Neuroscience, 2004. Online.

Cohen AD, El Ayadi A, Smith AD, **Zigmond MJ**. Forced limb use prior to 6-OHDA reduces vulnerability of dopamine neurons to oxidative stress. Program No. 221.1. *2004 Abstract Viewer and Itinerary Planner*. Washington, DC: Society for Neuroscience, 2004. Online.

Leak RK, Lin E, DeFranco D, Smith AD, **Zigmond MJ**. Sublethal concentrations of 6-OHDA preconditions dopaminergic cells against lethal exposure. Program No. 562.21. *2004 Abstract Viewer and Itinerary Planner*. Washington, DC: Society for Neuroscience, 2004. Online.

Lin E, Perez RG, **Zigmond MJ**. Role of ERK1/2 activation in dopaminergic cell survival in response to oxidative stress. Program No. 93.9. *2004 Abstract Viewer and Itinerary Planner*. Washington, DC: Society for Neuroscience, 2004. Online.

Lopresti BJ, Mathis CA, Mason NS C, Bohnen NI, Fischer M, Ruszkiewicz JA, Smith AD, **Zigmond MJ**. The use of positron emission tomography to measure dopamine nerve terminal degeneration. Program No. 562.14. *2004 Abstract Viewer and Itinerary Planner*. Washington, DC: Society for Neuroscience, 2004. Online.

Zigmond MJ. Triggering endogenous neuroprotective mechanisms in Parkinson's disease. 16th International Congress on Parkinson's Disease and Related Disorders. Berlin, Germany. 2005.

Fukuwatari T, Wu HQ, Koenig JI, **Zigmond, MJ**, Schwarcz R. Acute stress increases kynurenate and reduces dopamine levels in striatal microdialysate of adrenalectomized rats. Program 186.3. *2005 Abstract Viewer and Itinerary Planner*. Washington, DC: Society for Neuroscience, 2005. Online.

Fisher JL, Leak RK, **Zigmond MJ**, Smith AD. 6-hydroxydopamine causes an acute increase in CFOS and MAP kinases in the rat striatum. Program 424.10. *2005 Abstract Viewer and Itinerary Planner*. Washington, DC: Society for Neuroscience, 2005. Online.

Jaumotte JD, Smith AD, Lin E, Lakoski JM, **Zigmond MJ**. ERK5 protects dopaminergic cells from oxidative stress. Program 552.30. *2005 Abstract Viewer and Itinerary Planner*. Washington, DC: Society for Neuroscience, 2005. Online.

Lindgren N, Leak RK, Smith AD, **Zigmond MJ**. GDNF-induced phosphorylation of ERK and tyrosine hydroxylase in the basal ganglia of mice: implications for cell survival. Program 899.9. *2005 Abstract Viewer and Itinerary Planner*. Washington, DC: Society for Neuroscience, 2005. Online.

Cohen AD, **Zigmond MJ**, Smith AD. Changes in the PI3 kinase/AKT pathway by GDNF and 6-OHDA: Implications for neuroprotection. Program 899.10. *2005 Abstract Viewer and Itinerary Planner*. Washington, DC: Society for Neuroscience, 2005. Online.

Leak RK, Macioce M, Tyurina YY, Mirnica K, Liou AKF, Kagan VE, **Zigmond MJ**. Exposure of dopaminergic cells to sublethat 6-hydroxydopamine protects againse subsequent lethal exposure. Program 1006.18. *2005 Abstract Viewer and Itinerary Planner*. Washington, DC: Society for Neuroscience, 2005. Online.

El Ayadi A, Lin E. **Zigmond MJ**. Methamphetamine preconditions dopaminergic cells to oxidative stress. Program 1007.15. *2005 Abstract Viewer and Itinerary Planner*. Washington, DC: Society for Neuroscience, 2005. Online.

Cavanaugh JE, Bravo GL, Lakoski JM, **Zigmond MJ**. Motor impairments and dopamine neurodegeneration increase with age and MPTP. Program 469.16. *2006 Abstract Viewer and Itinerary Planner*. Atlanta, GA: Society for Neuroscience, 2006. Online.

Cohen AD, **Zigmond MJ**, Mirnics K, Smith AD. Temporal kinetics of phenotypic markers following 6-OHDA: impact of GDNF. Program 756.6. *2006 Abstract Viewer and Itinerary Planner*. Atlanta, GA: Society for Neuroscience, 2006. Online.

El Ayadi A, Liou, AJKF, **Zigmond MJ**. Methamphetamine preconditioning against oxidative stress: Role of MAPK pathway. Program 471.20. *2006 Abstract Viewer and Itinerary Planner*. Atlanta, GA: Society for Neuroscience, 2006. Online.

Li L, **Zigmond MJ**. Liou AJKF. The role of ERK is dependent on its sub-cellular localization in the cell. Program 471.16. *2006 Abstract Viewer and Itinerary Planner*. Atlanta, GA: Society for Neuroscience, 2006. Online.

Lindgren, N, Leak RK, Smith AD, **Zigmond, MJ**. Role of MAP kinases in the neuroprotective effects of GDNF in vivo. Program 756.7. *2006 Abstract Viewer and Itinerary Planner*. Atlanta, GA: Society for Neuroscience, 2006. Online.

Liou AJKF, Leak RK, Li L, Kotevski L, **Zigmond MJ**. Characterization of functional differences between LRRK2 wild-type and mutant. Program 173.9. *2006 Abstract Viewer and Itinerary Planner*. Atlanta, GA: Society for Neuroscience, 2006. Online.

Russell VA, Mabandla MV, Johnson S, Dobson B, Kellaway LA , Daniels WMU , **Zigmond MJ**. Beneficial effects of exercise on motor function following intracerebral 6-OHDA are decreased in prenatally stressed rats. Program 469.5. *2006 Abstract Viewer and Itinerary Planner*. Atlanta, GA: Society for Neuroscience, 2006. Online.

Smith AD, **Zigmond MJ**, El Ayadi A. Intra-striatal IGF-1 protects dopamine terminals against oxidative stress. Program 470.12. *2006 Abstract Viewer and Itinerary Planner*. Atlanta, GA: Society for Neuroscience, 2006. Online.

Weisz OA, Zellers DF, Woodward JE, Seltzer DL, Baty CJ, **Zigmond MJ**, Kapoor WN, Lakoski JM. AAMC Group on Faculty Affairs Professional Development Conference. San Diego, CA. 2007.

Lindgren N, Carlson KM, Leak RK, Smith AD, **Zigmond MJ**. Role of ERK1/2 and Akt in the neuroprotective effects of GDNF in a model of Parkinson's disease. Dopamine @ 50 years. Goteborg, Sweden, May 29 – June 2, 2007.

Carlson KM, Kearney SM, **Zigmond MJ**. Impact of GDNF/GFR*α*-gene deletion on spontaneous locomotor activity and MPTP toxicity in mice. Program 371.7. *2007 Abstract Viewer and Itinerary Planner*. San Diego, CA Society for Neuroscience, 2007. Online.

Leak RK. Wong MS, **Zigmond MJ,** Liou AKF, Proteasome inhibition induces protection against oxidative stress in catecholaminergic cells. Program 382.7. *2007 Abstract Viewer and Itinerary Planner*. San Diego, CA Society for Neuroscience, 2007. Online.

Russell VA, Mabandla, Kellaway LA, Daniels WMU, **Zigmond MJ**. Effect of exercise on neuron survival in the nigrostriatal pathway. Program 589.4. *2007 Abstract Viewer and Itinerary Planner*. San Diego, CA Society for Neuroscience, 2007. Online.

Mirnics K, Garbett KA, Mitchess AC, Sullivan E, Leak RK, **Zigmond MJ**, Cameron JL. Spontaneus activity and neocortical gene expression in non-human primates. Program 589.9. *2007 Abstract Viewer and Itinerary Planner*. San Diego, CA Society for Neuroscience, 2007. Online.

El Ayadi A, **Zigmond MJ**, Smith AD. Signaling pathways underlying IGF-1 induced protection of DA terminals against oxidative stress. Program 882.1. *2007 Abstract Viewer and Itinerary Planner*. San Diego, CA Society for Neuroscience, 2007. Online.

Li L, Liou AK, **Zigmond MJ**. Influences of expression level and localization of perk on cell survival in response to oxidative stress. Program 382.19. *2007 Abstract Viewer and Itinerary Planner*. San Diego, CA Society for Neuroscience, 2007. Online.

Kohler SJ, Dong WK, Stanton GB, Todd SL, Smith AD, **Zigmond MJ**, Greenough WT. Independent effects of enriched environment on behavior and TH loss in a rat model of Parkinson's disease. Program 139.3. *2008 Abstract View and Itinerary Planner*. Washington, DC, Society for Neuroscience, 2008. Online.

Allen EN, Carlson KM, **Zigmond MJ**, Cavanaugh JE. Locomotor deficits are reversed by levodopa in a mouse model of normal aging. Program 145.21. *2008 Abstract View and Itinerary Planner*. Washington, DC, Society for Neuroscience, 2008. Online.

Russell VA, Mabandla MV, Kellaway LA, Daniels WMU, **Zigmond MJ**. Effect of maternal separation stress and exercise on dopamine neuron function in a rat model for Parkinson's disease. Program 341.3. *2008 Abstract View and Itinerary Planner*. Washington, DC, Society for Neuroscience, 2008. Online.

Leak RK, Jaumotte JD, **Zigmond MJ**. Responses to low and high cellular stress in cortical neuronal cultures. Program 343.21. *2008 Abstract View and Itinerary Planner*. Washington, DC, Society for Neuroscience, 2008. Online.

Liou AK, He K, **Zigmond MJ**. GDNF and BDNF act synergistically to protect against cellular stress via down-regulation of BimEL. Program 544.5. *2008 Abstract View and Itinerary Planner*. Washington, DC, Society for Neuroscience, 2008. Online.

Jaumotte JD, **Zigmond MJ**. The effect of GDF-5 on postnatal dissociated cultures of the ventral midbrain. Program 818.5. *2008 Abstract View and Itinerary Planner*. Washington, DC, Society for Neuroscience, 2008. Online.

Presentations

In this section, I have list most presentations not represented in the list of abstracts above.

PRESENTATION	VENUE AND DATE
Waking up the brain's capacity for self protection: Studies in models of PD	The Neurobiology of Exercise, 12/6/04 – 12/7/04
Waking up the brain's own mechanisms for self-protection: Studies in models of Parkinson's Disease	NE Ohio University College of Medicine Grass Lecture, 1/13/05
Why does Parkinson's disease progress? (panel chair)	Winter Conference on Brain Research 1/22/05 – 1/28/05
Alternative therapies to treat Parkinson's disease (panelist)	Parkinson's Action Network, 2/6/05
Eliciting endogenous neuroprotection in models of PD	Mt. Sinai Medical Center, 5/4/05
Triggering endogenous neuroprotective mechanisms in Parkinson's disease: Studies with a cellular model	16th International Congress on Parkinson's Disease and Related Disorders. Berlin, Germany, June, 2005
Endogenous mechanisms of neuroprotection in cellular and animal models of Parkinson's disease	Banbury Center Conference on Parkinson's Disease: Insights from Genetic and Toxin Models 5/14/06 – 5/17/06
Update on degenerative disease	The University Medical Center – Ho Chi Min City, HCMC, Vietnam, 9/22/06 – 10/2/06
Keynote lecture on neuroscience research in developing nations; workshop on stress, exercise, and brain	University of Cape Town Brain Behavior Initiative Inauguration, Cape Town, South Africa 11/6/06

Endogenous neuroprotective mechanisms: Implications for etiology and treatment	Lexington Conference on Trophic Factor Therapy for Parkinson's Disease Lexington, KY 4/17/07 – 4/19/07
Taking advantage of the brain's endogenous neuroprotective mechanisms	American Society for Neural Therapy and Repair Clearwater, FL 5/3/07 – 5/7/07
Moderator of session on the history of dopamine research	Dopamine 2007 Congress Goteborg, Sweden, 5/30/07 – 6/2/07
Endogenous neuroprotection in PD (3 lectures)	S. Korea (several sites), 6/21/07 – 7/2/07
CNS changes with exercise	Bedside-to-Bench Conference September 5-7, 2007
Triggering protection in PD	Parkinson's Disease Foundation 50th Anniversary Educational Symposium New York, NY, 10/11/07 – 12/12/07
Research in developing countries	Fogarty International Center meeting San Diego, CA, 11/2/07
Exercise as an intervention in neurodegenerative disorders: studies with models of Parkinson's disease	Jefferson University, 2/7/08 Philadelphia, PA
Promoting neuroprotection through exercise and neurotrophic factors: studies in models of Parkinsonism	Boston University School of Medicine February 14, 2008
Promoting neuroprotection through exercise and trophic factors: studies in models of Parkinson's disease	St. Jude Children's Research Hospital Brain Club Seminar, March 6, 2008 Memphis, Tennessee
Exercise, neurotrophic factors, and Parkinson's disease	National Center for Brain Research, Delhi; February 25, 2008
Exercise, neurotrophic factors, and Parkinson's disease	All India Institute for Medical Science; both in Delhi, India February 26, 2008
Toward reducing the progression and preventing disease: A basic scientist's view	Brain Awareness Week, Bowling Green State University March 12, 2008, Bowling Green, Ohio
Promoting self-protection of CNS neurons: Studies in models of Parkinson's disease	Department of Psychology Bowling Green State University March 13, 2008 Bowling Green, Ohio

Employment received based on experience/training supported by award:

ElAyadi, Amina: Postdoc Fellow, Univ of Texas Medical Branch, Neuroscience and Cell Biology, Galveston

He, Kunyen: Postdoc, Emory U with Dr. Keqiang Ye

Fischer, Michele: Student in Physician Assistant Program, Philadelphia, PA

Leak, Rehana: Research Asst Prof, Dept of Neurology, U of Pittsburgh

Li, Lihua: Postdoc, Dept of Surgery, University of Pittsburgh

Lin, Eva: Research Associate, Dept of Surgery, University of Pittsburgh

Lindgren, Niklas: Postdoc trainee with Angela Cenci-Nilsson, MD, PhD, Dept. of Experimental Medical Science, Sweden

Ugarte, Susana: Instructor, Dept of Biology, Loyola U

LIST OF PERSONNEL RECEIVING PAY FROM THE RESEARCH EFFORT

2003-2004

Michelle Fischer
Juliann Jaumotte
J. Niklas Lindgren
Amanda Smith
Michael Zigmond

2004-2005

Sandy Castro
Amina Elayadi
Michelle Fischer
Julianne Jaumotte
J. Nicklas Lindgren
Kian-Fong Liou
Dongzhu Ma
Susan Slagel
Michael Zigmond

2005-2006

Sandy Castro
Amina Elayadi
Michelle Fischer
Shannon Kearney
Leonard Kotevski
Julianne Jaumotte
Rehana Leak
Lihua Li
Kian-Fong Liou
Niklas Lindgren
Michael Zigmond

2006-2007

Sandy Castro
Amina Elayadi
Michelle Fischer
Kunyan He
Julianne Jaumotte
Shannon Kearney
Rehana Leak
Lihua Li
Kian-Fong Liou
Niklas Lindgren
Michael Zigmond

2007-2008

Kirsten Carlson
Jordan Carr
Sandy Castro
Rachel Galioto
Kunyan He
Juliann Jaumotte
Shannon Kearney
Rehana Leak
Lihua Li
Eva Lin
Kian-Fong Liou
Michael Zigmond

Conclusions

Physical exercise is a viable approach to the treatment of PD. This is made clear by our own work and that of several other groups studying both animal models and humans. It is likely to involve a preconditioning phenomenon whereby exercise triggers an increase in neurotrophic factor expression, which in turn produces a variety of translational and post-translational modifications. Understanding the parameters of protective exercise will be critical to proscribing an effective exercise regimen. Moreover, understanding the mechanism of action of exercise should provide insights into the development of drug therapies.

References

The references referred to in this document are all from our research group and can be found on pp. 18-19. References to work from other laboratories are provided in our published papers.

Appendices

Attached is a selection of the papers that derived in part from funding from this grant. They include the following:

Cavanaugh JE, Jaumotte JD, Lakoski JM, Zigmond MJ. Neuroprotective role of ERK1/2 and ERK5 in a dopaminergic cell line under basal conditions and in response to oxidative stress. *J Neurosci Res*., **84**:1367-1375, 2006.

Lin E, Cavanaugh JE, Leak, RK, Perez RG, Zigmond MJ. Rapid activation of ERK by 6-hydroxydopamine promotes survival of dopaminergic cells. *J Neurosci Res* **86**:108-117, 2007.

Lindgren N, Leak RK, Carlson KM, Smith AD, Zigmond MJ. Activation of the extracellular signal-regulated kinases 1 and 2 by glial cell line-derived neurotrophic factor and its relation to neuroprotection in a mouse model of Parkinson's disease. *J Neurosci Res*, **86**:2039-2049, 2008.

Leak RK, Zigmond MJ, Liou AKF. Adaptation to chronic MG132 reduces oxidative toxicity by a CuZnSOD-dependent mechanism. *J Neurochem*, **106**:860-874, 2008.

Liou AK, Leak RK, Li L, Zigmond MJ. Wild-type LRRK2 but not its mutant attenuates stress-induced cell death via ERK pathway. *Neurobiol Dis*. **32**:116-24, 2008.

Journal of Neuroscience Research 84:1367–1375 (2006)

Neuroprotective Role of ERK1/2 and ERK5 in a Dopaminergic Cell Line Under Basal Conditions and in Response to Oxidative Stress

Jane E. Cavanaugh,[1]* Juliann D. Jaumotte,[2] Joan M. Lakoski,[1] and Michael J. Zigmond[1,2]

[1]Department of Pharmacology, University of Pittsburgh School of Medicine, Pittsburgh, Pennsylvania
[2]Department of Neurology, University of Pittsburgh School of Medicine, Pittsburgh, Pennsylvania

Loss of motor function in Parkinson's disease is due in part to degeneration of dopamine (DA) neurons. Pharmacological evidence suggests that the mitogen-activated protein kinase signaling pathways involving extracellular signal-regulated kinases (ERKs) play important roles in neuroprotection of DA neurons. However, the relative roles of the several ERK isoforms in the viability of DA neurons have not yet been determined. In the present study, we investigated the contributions of ERK5, as well as ERK1/2, to MN9D cell survival under basal conditions and in response to 6-hydroxydopamine (6-OHDA). We observed that U0126, an inhibitor of ERK activation, decreased basal survival of these cells. To differentiate between ERK1/2 and ERK5, cells were transfected with a dominant negative form of either ERK5 or MEK1, the upstream activator of ERK1/2. Transfection of MN9D cells with either dominant negative construct mimicked U0126, reducing cell survival. Moreover, transfection of the cells in such a way as to increase ERK5 or ERK1/2 activity inhibited 6-OHDA-induced cell death, although this effect was significant only in the case of ERK1/2 activation. These studies suggest that activations of ERK5 and ERK1/2 both promote basal DA cell survival and that ERK1/2 also protects DA cells from oxidative stress. These are the first studies to demonstrate a role for ERK5 in DA neuronal survival and to investigate the relative roles of ERK1/2 and ERK5 in basal DA survival and neuroprotection from oxidative stress.

Key words: 6-hydroxydopamine; cell death; MAPK; MN9D cells; Parkinson's disease

Parkinson's disease is a debilitating neurodegenerative disease that involves motor deficits attributed to the loss of dopamine (DA) neurons in the substantia nigra pars compacta. Although the cause of DA cell death is not fully understood, there is substantial evidence that oxidative stress is a contributing factor (Lotharius and Brundin, 2002). To develop strategies to prevent DA neuronal cell death, studies are necessary to explore the relevant cellular processes. The present study aims to examine the role of extracellular signal regulated kinase (ERK) isoforms, members of the mitogen-activated protein kinase (MAPK) family, in DA neuronal survival.

The best studied of the ERK isoforms are ERK1 and -2 (ERK1/2), which have been shown to be important for neuroprotection from toxic insults such as DNA damage, trophic factor deprivation, and oxidative stress, all of which are thought to play a role in neurodegeneration (Xia et al., 1995; Hetman et al., 1999). Previously, we have provided evidence indicating that activation of ERK plays a role in growth factor-mediated neuroprotection from 6-hydroxydopamine (6-OHDA) toxicity in a dopaminergic cell line (Ugarte et al., 2003). However, the nature of the ERK isoform involved in this protection is unknown. In 1995, Zhou and coworkers reported the existence of an ERK isoform, ERK5. Although many studies, have implied that ERK1/2 is responsible for the neuroprotection that has been observed, those studies have relied largely on the pharmacological inhibitors PD98059 and U0126, drugs that also inhibit the ERK5 pathway (Kamakura et al., 1999; Mody et al., 2001). Thus, some of the functions attributed to ERK1/2 might actually be carried out by ERK5, which also has been shown to play a role in neuronal survival. Although some support for this possibility exists in other cell types (Watson et al., 2001;

Contract grant sponsor: National Institute on Aging; Contract grant number: AG25848 (to J.E.C.); Contract grant number: AG7476 (to J.M.L.); Contract grant sponsor: National Institute of Neurological Disorders and Stroke; Contract grant number: NS19608 (to M.J.Z.); Contract grant sponsor: U.S. Department of Defense; Contract grant number: ERMS 03281022 (to M.J.Z.).

*Correspondence to: Jane E. Cavanaugh, PhD, Department of Pharmacology, University of Pittsburgh School of Medicine, W1005 Biomedical Science Tower, Lothrop Street, Pittsburgh, PA 15221.
E-mail: jec21@pitt.edu

Received 12 April 2006; Revised 13 June 2006; Accepted 23 June 2006

Published online 28 August 2006 in Wiley InterScience (www.interscience.wiley.com). DOI: 10.1002/jnr.21024

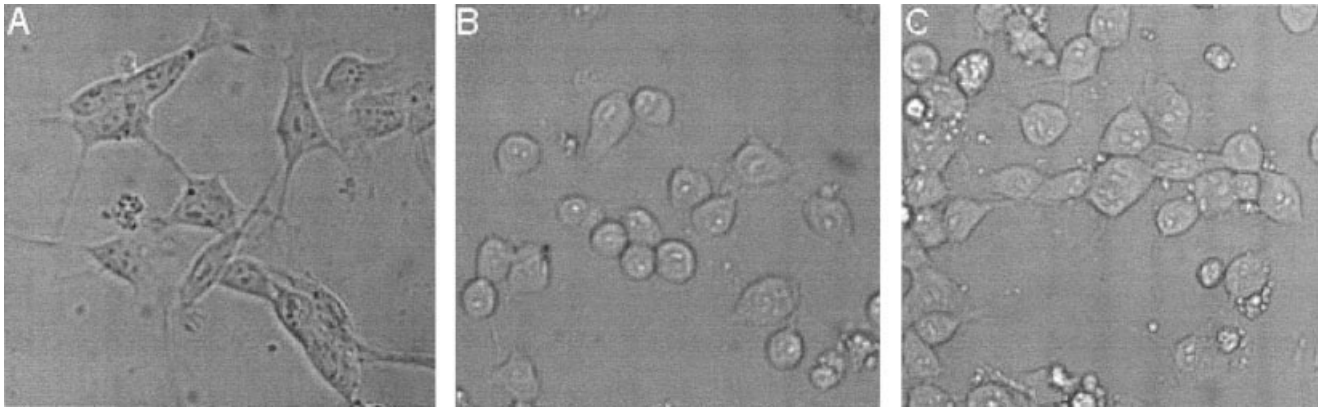

Fig. 1. MN9D cells cultured in various media had distinct morphologies. **A:** MN9D cells cultured in medium containing 10% serum. **B:** MN9D cells cultured in serum-free medium. **C:** MN9D cells cultured in defined medium (Neurobasal with B27 supplement). All pictures were taken with 20× long-working-distance objective with a Retiga 1300R 12-bit cooled CCD digital camera (Q Imagining, Barnaby, British Columbia, Canada).

Liu et al., 2003; Shalizi et al., 2003), a role for ERK5 in DA neuronal survival has not been explored.

In the present study, we examined the roles of ERK1/2 and ERK5 in DA neuronal survival by using 6-OHDA and MN9D cells. 6-OHDA is a structural analog of catecholamines that is concentrated into neurons via uptake by the high-affinity transport system located at catecholaminergic terminals. After uptake, 6-OHDA is rapidly oxidized into the cytotoxic compounds 6-OHDA quinone and hydrogen peroxide and produces oxidative stress, ultimately leading to cell death (Zigmond and Keefe, 1997). MN9D cells are a dopaminergic cell line formed through the fusion of an embryonic dopaminergic cell from the mouse ventral mesencephalon and a neuroblastoma cell. These cells express ERK and tyrosine hydroxylase (TH) and are susceptible to 6-OHDA toxicity (Oh et al., 1995, 1998; Choi et al., 1999, 2000; Ugarte et al., 2003). The results presented here suggest that both ERK1/2 and ERK5 are important for DA neuronal survival under basal conditions and following a toxic insult.

MATERIALS AND METHODS

Materials

The following plasmids were used in this study: the dominant negative and constitutively active MEK1 (Mansour et al., 1994), the wild-type and dominant negative ERK5 (Kato et al., 1997), the dominant negative and constitutively active MEK5 (Kato et al., 1997), the dominant negative and constitutively active MEF2C (Han et al., 1997), and a luciferase reporter plasmid (PUH-luc; Boeckman and Aizenman, 1996; Rameau et al., 2000). The polyclonal ERK5 antibody to the C-terminal 100-amino-acid sequence of ERK5 has been previously described (Cavanaugh et al., 2001). The polyclonal antiphospho-p44/42 MAPK (ERK1/2) antibody was purchased from Cell Signaling Technology, Inc. (Beverly, MA).

Cell Cultures

Drs. A. Heller and L. Won (University of Chicago) kindly provided the MN9D cell line used in these studies (Choi et al., 1992). Cells were maintained in DMEM (Sigma, St. Louis, MO) containing 10% fetal bovine serum (FBS; Hyclone, Logan, UT) for passing cells and experiments in serum-containing medium with 50 U/ml each of penicillin and streptomycin. When indicated, cells were cultured in serum-free DMEM or in a defined medium consisting of Neurobasal medium supplemented with B27 (Invitrogen, Carlsbad, CA).

MN9D cells maintained in serum (10%), serum-free, and defined medium had distinctly different cellular morphologies (see Fig. 1). In serum-containing medium and neurobasal medium, MN9D cells were larger and had processes similar to those of primary neuronal cells. In contrast, cells appeared rounded and had fewer processes when maintained in serum-free medium for 24–48 hr. Therefore, cells maintained in serum-containing medium exhibit a more neuronal-like phenotype and enhanced survival compared with cells maintained in serum-free medium.

6-OHDA Treatment

A stock solution (10 mM) of 6-OHDA (Sigma) was prepared in vehicle containing the metal chelator diethylenetriamine pentaacetic acid (DETAPAC; 10 mM) and ascorbic acid (0.15%) to minimize extracellular oxidation of 6-OHDA (Ding et al., 2004). The stock solution was aliquoted, quickly frozen on dry ice, and stored at −80°C until use. Immediately before each treatment, a small aliquot of 6-OHDA was analyzed by HPLC coupled with electrochemical detection (Smith et al., 2002) and employing a 100 μM 6-OHDA standard made in 0.1 N $HClO_3$ acid to identify the proper peak. The detection limit of the system was 5 nM. 6-OHDA stored at −80°C was stable for at least 6 months as determined by HPLC analysis of the compound.

Cells were treated with 6-OHDA (50–250 μM) for 15 min in serum-free DMEM. After treatment, the 6-OHDA-

containing serum-free medium was removed and replaced with 10% serum-containing DMEM or serum-free DMEM as indicated.

U0126 Treatment

A stock solution (10 mM) of U0126 (Cell Signaling Technology) was prepared in dimethylsulfoxide (DMSO). The stock solution was aliquoted and stored at −20°C until use. U0126 (1–10 μM) was added to the cells, and viability was measured 24 hr following treatment. The final concentration of DMSO for all treatments was 0.1%.

Quantitation of Cell Viability

To visualize nuclear morphology, cells were fixed in 4% paraformaldehyde/4% sucrose and stained with 2.5 μg/ml Hoechst 33258 (bisbenzimide; Sigma) 24 hr following treatment. Because most cells that are dead lift off the culture plates, cell viability is reported as the number of live cells per well. Uniformly stained nuclei were scored as healthy, viable neurons. Condensed or fragmented nuclei were scored as apoptotic.

MN9D cell viability was also measured by using the CellTiter Glo Luminescent Cell Viability Assay (Promega, Madison, WI) as described by the manufacturer. This assay is based on a luciferase reaction that requires ATP. Therefore, the lumination produced is proportional to the amount of ATP and provides an indication of cellular metabolic activity.

Transient Transfection of MN9D cells

MN9D cells were plated (100,000 cells/well; 24 well plate) overnight and transiently transfected with Lipofectamine 2000 (Invitrogen), a lipid-based transfection method (Hetman et al., 2000, 2002). Cells were cotransfected with an expression vector encoding luciferase (PUHluc) as a reporter for transfected cells, and cell death was scored in the transfected cells as a loss of luciferase activity by using the Steadylite luminescence assay as previously described (Boeckman and Aizenman, 1996; Rameau et al., 2000). Transfection efficiency was typically 60–70%.

Western Analysis

MN9D cells were plated (500,000 cells/35-mm plate) overnight in 10% serum-containing medium and treated with U0126 (1–10 μM). After treatment, Western blot analyses of ERK5 and phosphorylated ERK1/2 were performed as previously described (Cavanaugh et al., 2001). The same blots were stripped and reprobed for α-tubulin to test for equal protein loading. An antiphospho-ERK1/2 antibody was used to recognize the phosphorylated form of ERK1/2, indicative of ERK1/2 activation. Phosphorylation of ERK5 was observed as a shift in ERK5 mobility, which we and others have shown is indicative of the formation of pERK5 and ERK5 activation (Kato et al., 1997; Cavanaugh et al., 2001). Furthermore, previous reports have shown that treatment with phosphatases inhibits phosphorylation of ERK5 noted by a loss of the higher molecular weight band (Kamakura et al., 1999; Buschbeck et al., 2002; Garcia et al., 2002).

Statistical Analysis

The data were analyzed with SPSS 12.01 statistical software (SPSS, Chicago, IL) via two-way analysis of variance (ANOVA), followed by post hoc testing with Bonferroni error correction or a univariate analysis of variance (UNIANOVA), followed by pairwise comparisons as indicated.

RESULTS

Survival of MN9D Cells Under Basal Conditions and in Response to 6-OHDA Was Influenced by the Culture Medium

There is ample evidence that the characteristics of cells in culture are highly dependent on the medium in which they are grown (Wolinsky et al., 1985; Brewer, 1995; Ricart and Fiszman, 2001; Ward et al., 2004). Consistently with these observations, we found that MN9D cells maintained in serum-containing (10%), serum-free, or defined medium had distinct cellular morphologies (Fig. 1). Moreover, basal cell viability was significantly higher in the presence of 10% serum than in the absence of serum (Fig. 2). In each medium, 6-OHDA significantly decreased cell viability in a concentration-dependent manner, as measured by nuclear staining (33–67% decrease; Fig. 2A) or ATP levels (23–60% decrease; Fig. 2B). However, toxicity of 6-OHDA was influenced by the nature of the culture medium. Toxicity, as determined by a reduction of ATP levels and bisbenzimide staining, was significantly reduced in cells maintained in 10% serum-containing medium compared with cells in serum-free or defined medium. To be able to distinguish 6-OHDA-induced cell death from that produced by trophic factor withdrawal in cells maintained in serum-free medium, we chose to use 10% serum-containing medium as our standard condition and employed it for the remainder of our studies.

Pharmacological Inhibition of ERK1/2 and ERK5 Activation Decreased Basal Cell Survival in MN9D Cells

We have previously shown that exposure of MN9D cells to U0126 for 1–2 hr had no effect on basal survival (Ugarte et al., 2003; Lin et al., 2004). However, the impact of a longer exposure to U0126 has not been previously explored. After 24 hr of exposure to U0126 (1–10 μM) or vehicle (DMSO), MN9D cell death was determined by bisbenzimide staining. Twenty-four-hour exposure to U0126 significantly decreased the number of live cells in a concentration-dependent manner (Fig. 3A). This increase in cell death correlated with a concentration-dependent decrease in ERK1/2 and ERK5 phosphorylation, indicating a role for ERK1/2 and/or ERK5 activation in survival (Fig. 3B).

Transfection With Dominant Negative MEK1 or Dominant Negative ERK5 Decreased Basal Survival of MN9D Cells

To determine the relative roles of ERK1/2 and ERK5 in basal dopaminergic cell survival, we transiently

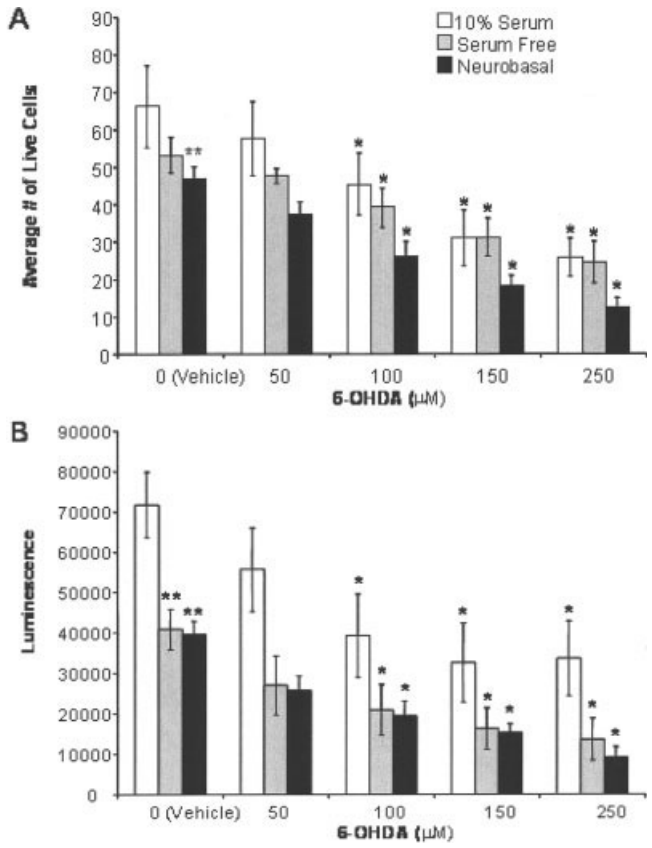

Fig. 2. 6-OHDA increased cell death in a concentration-dependent manner in 10% serum containing, serum-free, and defined media. **A:** At 24 hr following 15 min of stimulation with 6-OHDA (0–250 μM), morphology of MN9D cell nuclei was examined by using bisbenzimide dye (Hoechst). Evenly stained nuclei, characteristic of healthy cells, and condensed or fragmented nuclei, characteristic of apoptotic cells, were quantified. Because late-stage apoptotic cells detached from the culture dish at 24 hr following 15 min of treatment with 6-OHDA, we quantitated cell death by counting the number of live cells remaining. 6-OHDA-induced apoptosis in a dose-dependent manner in all media. Cultures maintained in serum-free or defined medium had fewer live cells under basal conditions (vehicle) than cultures maintained in 10% serum. **B:** Loss of ATP, indicative of cell death, was measured in MN9D cells 24 hr following 15 min of 6-OHDA (0–250 μM) exposure using the CellTiter Glo assay according to the manufacturer's protocol. Similar to the results with bisbenzimide staining, 6-OHDA decreased ATP levels in a dose-dependent manner in all media. Cultures maintained in serum-free or defined medium had lower basal (vehicle) ATP levels than cultures maintained in 10% serum. Results (A,B) are averages of five to seven independent experiments. Error bars show SEM. Raw data were analyzed via two-way ANOVA, followed by Bonferroni post hoc analysis. $^{\star}P < 0.05$ compared with vehicle control in the same medium, $^{\star\star}P < 0.05$ compared with vehicle in 10% serum medium.

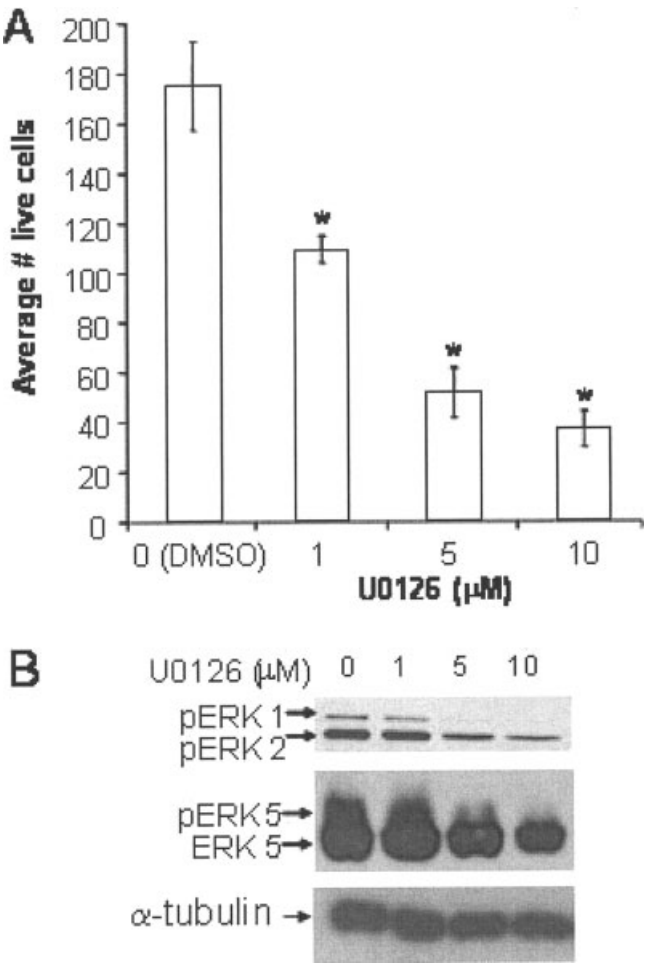

Fig. 3. Inhibitors of ERK1/2 and ERK5 pathways increased basal cell death in MN9D cells. **A:** U0126 (0–10 μM), an inhibitor of the upstream ERK1/2 and ERK5 MAPKKs, MEK1 and MEK5, respectively, increased basal cell death in a dose-dependent manner. MN9D cells were maintained in 10% serum medium. At 24 hr following U0126 treatment, morphology of MN9D cell nuclei was examined by using bisbenzimide dye (Hoechst). The numbers of live cells were quantified as for Figure 2. Error bars show SEM. Raw data were analyzed via two-way ANOVA, followed by Bonferroni post hoc analysis. $^{\star}P < 0.05$ compared with vehicle control. **B:** U0126 inhibited ERK1/2 and ERK5 activation in a dose-dependent manner. Cell lysates were prepared, and 20 μg of total protein was used for Western analysis with antibodies recognizing ERK5 (1:1,000) or phosphorylated (P) ERK1/2 (1:1,000). Phosphorylation of ERK5 was observed as an upward shift in ERK5 mobility, indicative of ERK5 activation. The antiphospho-ERK1/2 antibody recognizes the phosphorylated and activated ERK1/2, indicative of ERK1/2 activation. Western analysis of α-tubulin was used to determine protein loading. Data are representative of three independent experiments.

transfected MN9D cells with a dominant negative MEK1 or a dominant negative ERK5 to block specifically the ERK1/2 or ERK5 pathway, respectively. As a control, cells were transfected with an empty vector (pcDNA3), and all cells were transfected with equal amounts of DNA. Transfection with the dominant negative constructs decreased basal cell survival in a concentration-dependent manner in serum-containing medium, suggesting that both ERK1/2 and ERK5 activity are necessary for serum-promoted survival under basal conditions (Fig. 4).

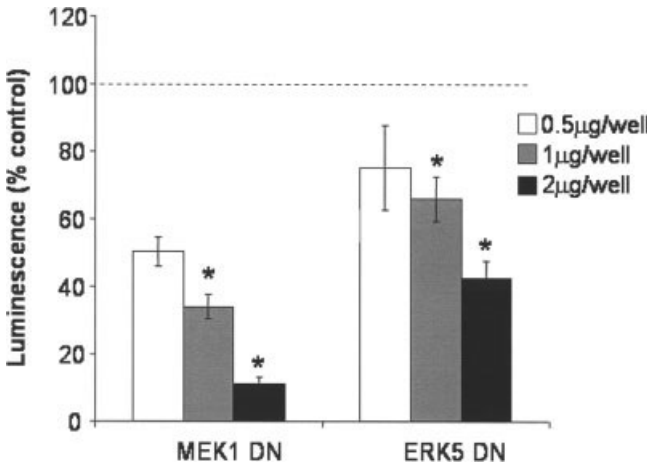

Fig. 4. Transfection with dominant negative MEK1 or ERK5 decreased basal MN9D cell survival. MN9D cells maintained in 10% serum were transfected with a lipid-based transfection (Lipofectamine 2000) method according to the manufacturer's instructions. MN9D cells were transiently transfected with dominant negative MEK1 or dominant negative ERK5 to inhibit the activity of the ERK1/2 and ERK5 pathways, respectively. Cells were also cotransfected with a luciferase reporter plasmid (PUH-luc) and pcDNA3 to keep the total amount of DNA constant. Loss of transfected cells was measured 24 hr following transfection using the Steadylite luciferase reporter assay according to the manufacturer's protocol. Data are expressed as percentage control. Results are representative of three independent experiments. Error bars show SEM. Raw data were analyzed via two-way ANOVA, followed by Bonferonni post hoc analysis. $*P < 0.05$ compared with control.

Transfection With Constitutively Active MEK5 and Wild-Type ERK5 Increased Basal Survival of MN9D Cells

As noted in the introductory paragraphs, the ERK1/2 pathway has been implicated in neuronal survival following several toxic insults. However, such studies have used pharmacological inhibitors that have been shown to block the activation of MEK5 as well as MEK1, thereby inhibiting activation of both ERK5 and ERK1/2. Therefore, to distinguish between the ERK1/2 and the ERK5 pathways and to establish their relative roles in dopaminergic cell survival, MN9D cells were transiently transfected with either a constitutively active MEK1 to activate ERK1/2 signaling or a constitutively active MEK5 plus wild-type ERK5 to activate ERK5 signaling. Cotransfection of a constitutively active MEK5 and wild-type ERK5 was necessary to activate the ERK5 pathway effectively (Cavanaugh et al., 2001; Kondoh et al., 2006; Namakura et al., 2006; Ranganathan et al., 2006).

Cotransfection with a constitutively active MEK5 and wild-type ERK5 increased basal cell survival (28%) of MN9D cells. In contrast, transfection with constitutively active MEK1 decreased basal cell survival, suggesting that, among the three isoforms, it is ERK5 that serves to promote the basal survival of MN9D cells.

Transfection With Constitutively Active MEK1 or Constitutively Active MEK5 and Wild-Type ERK5 Decreased 6-OHDA-Induced MN9D Cell Death

To examine the relative roles of the ERK1/2 and ERK5 pathways in cell survival following oxidative stress, MN9D cells transfected with constitutively active members of these pathways were briefly exposed to 6-OHDA and examined 24 hr later (see Fig. 6). Transfection with these constructs tended to decrease 6-OHDA-induced toxicity, suggesting that the ERK1/2 and ERK5 pathways might both play an important role in the neuroprotection of dopaminergic cells following oxidative stress. However, the protection was significant only following transfection with constitutively active MEK1.

MEF2C May Be a Critical Downstream Target in ERK5-Mediated Survival

The targets for ERK1/2 and ERK5 overlap but are not identical. For example, they both activate the transcription factors c-Myc and Sap1a in neuronal and non-neuronal cell types (Kato et al., 1997; English et al., 1998; Yang et al., 1998; Kamakura et al., 1999; Marinissen et al., 1999); however, ERK1/2 phosphorylates and activates Elk-1, whereas ERK5 does not. Similarly, ERK5, but not ERK1/2, phosphorylates and activates MEF2A and MEF2C (Gille et al., 1992; Marais et al., 1993; Kato et al., 1997; English et al., 1998; Yang et al., 1998; Marinissen et al., 1999; Cavanaugh et al., 2001).

To examine a possible downstream target for ERK5 in dopaminergic neuronal survival, we transiently transfected MN9D cells with a constitutively active MEF2C and examined basal cell survival and 6-OHDA-induced toxicity 24 hr later (Figs. 5, 6). Transfection with constitutively active MEF2C increased basal cell survival and inhibited 6-OHDA-induced cell death, suggesting that MEF2C is important for MN9D cells survival and may be the downstream target of ERK5 in these cells.

DISCUSSION

In the present study, we examined the role of ERK1/2 and ERK5 in basal and 6-OHDA-induced death of dopaminergic MN9D cells. Transfection with constitutively active components of the ERK5 pathway increased basal survival but did not significantly inhibit 6-OHDA-induced toxicity. In contrast, transfection with constitutively active MEK1, the upstream kinase of ERK1/2, decreased basal survival but significantly inhibited further cell death produced by 6-OHDA. Inhibition of either ERK pathway with appropriate dominant negative constructs decreased basal MN9D cell survival. These data suggest that ERK5 may play a larger role in basal survival of dopaminergic cells and that ERK1/2 is more important for survival of dopaminergic cells during exposure to acute oxidative stress. Our data also suggest that the MEF2C transcription factor, a downstream target of ERK5, may play a role in MN9D cell survival. To our knowledge, this is the first study to show evidence that ERK1/2 and

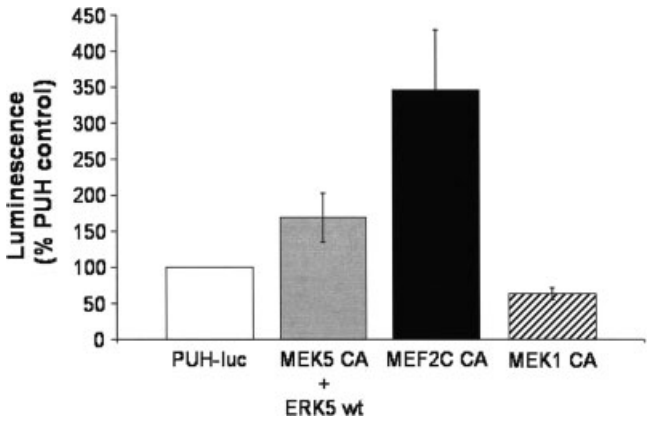

Fig. 5. Transfection with constitutively active components of the ERK5 pathway increased basal survival in MN9D cells. MN9D cells maintained in 10% serum were transfected by using a lipid-based transfection (Lipofectamine 2000) method according to the manufacturer's instructions. MN9D cells were transiently transfected with constitutively active MEK1 or constitutive active MEK5 and wild-type ERK5 to activate the ERK1/2 and ERK5 pathways, respectively, or constitutively active MEF2C, a downstream target of ERK5. In all cases, cells were cotransfected with a luciferase reporter plasmid (PUH-luc). The total amount of DNA was kept equal for each transfection condition with addition of pcDNA3 when necessary. MN9D cell viability was measured 48 hr following transfection by using the Steadylite luciferase reporter assay according to the manufacturer's protocol. Data are expressed as percentage control (cotransfection of PUH-luc and pcDNA3 set as 100%). Transfection with constitutively active MEK5 + wild-type ERK5 or constitutively active MEF2C increased basal survival. In contrast, transfection with constitutively active MEK1 decreased basal survival. Results are representative of four or five independent experiments. Error bars show SEM.

ERK5 play distinct roles in the survival of a dopaminergic neuronal cell type following oxidative stress and under basal conditions.

Influence of Serum on Survival of MN9D Cells

Previous results from our laboratory have shown that 6-OHDA increases MN9D cell death in a concentration-dependent manner (Ugarte et al., 2003). However, in that previous study, MN9D cells were maintained in serum-free medium that by itself increased basal cell death. In the present study, we examined spontaneous and 6-OHDA-induced cell death in medium containing 10% serum as well as in serum-free medium. Cells maintained in the presence of serum had a higher level of survival and a lower vulnerability to 6-OHDA. The increased a toxicity of 6-OHDA in serum-free medium may be a result of the cells being in an already compromised state because of growth factor withdrawal. In defined medium, MN9D cells did not proliferate as rapidly as when they were maintained in 10% serum medium. Therefore, the increase in 6-OHDA-induced toxicity in cells cultured in defined medium may be due to this decrease in proliferation. These results are consistent with the well-known effects of trophic factors on various neurons, including those of dopaminergic origin.

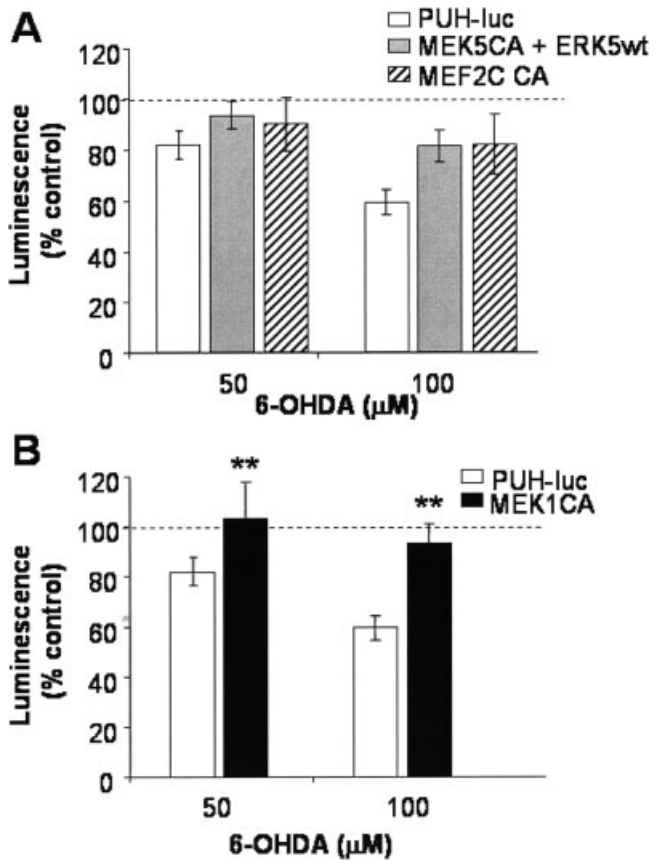

Fig. 6. Transfection with constitutively active components of the ERK1/2 or ERK5 pathways decreased 6-OHDA-induced toxicity in MN9D cells. MN9D cells maintained in 10% serum were transfected with constitutively active members of the ERK1/2 and ERK5 signaling cascades, as noted for Figure 5. On the day following transfection, MN9D cells were treated with 0, 50, or 100 μM 6-OHDA for 15 min. Loss of transfected cells was measured 24 hr following 6-OHDA treatment by using the Steadylite luciferase reporter assay according to the manufacturer's protocol. Data are expressed as percentage control (vehicle treatment for each transfection condition set as 100%). Transfection with constitutively active MEK1, constitutively active MEK5 + wild-type ERK5, or constitutively active MEF2C decreased 6-OHDA toxicity. Results are representative of four or five independent experiments. Error bars show SEM. Raw data were analyzed via UNIANOVA, followed by pairwise comparison of the means. $^{**}P < 0.05$ compared with PUH-luc-transfected cells.

Role of ERK1/2 in Basal Survival

The MAPK intracellular signaling pathways appear to play a key role in the regulation of the cell survival of many cells, including neurons. As noted in the introductory paragraphs, the best studied of these kinases, ERK1/2, has been shown to be important for neuroprotection from a variety of toxic insults thought to play a role in neurodegeneration (Xia et al., 1995; Hetman et al., 1999). ERK1/2 also has been implicated in trophic factor-induced protection from insults (Hetman et al., 1999, 2000). Furthermore, the recent literature suggests that sustained activation of the ERK1/2 signaling cascade might also contribute to

neuronal cell death, insofar as activated ERK1/2 retained in the nucleus increased cell death (Kulich and Chu, 2001; Stanciu and DeFranco, 2002). In the present study, activation or inhibition of the ERK1/2 pathway via transfection with a constitutively active or a dominant negative MEK1, respectively, decreased basal MN9D cell survival. These data suggest that the role of the ERK1/2 pathway in basal dopaminergic cell death may be dependent on the maintenance of a delicate balance between activated and nonactivated ERK1/2 within the cell. Overstimulation of the ERK1/2 pathway may lead to nuclear retention of activated ERK1/2 and subsequently to cell death. Similarly, inhibition of basal ERK1/2 activity via transfection with a dominant negative MEK1 might also tip the balance in favor of cell death. Future studies will be conducted to examine the localization of ERK1/2 within dopaminergic cells.

Influence of ERK1/2 in Response to Oxidative Stress

We observed that transfection of MN9D cells with constitutively active MEK1 blocked the toxic effects of 6-OHDA. In contrast, sustained activation of ERK1/2 has been shown to contribute to 6-OHDA-induced neurotoxicity in the CNS-derived dopaminergic B65 cell line (Kulich and Chu, 2001; Zhu et al., 2002, 2003). This apparent discrepancy may be due to the use of a different cell line and/or protocol for exposing cells to the neurotoxin. For example, whereas many previous studies have exposed cells to 6-OHDA for relatively long periods, our exposures were limited to 15 min to minimize the oxidation of 6-OHDA prior to its uptake into the MN9D cells (see Ding et al., 2004). In addition, data from our research group have shown that, as in B65 cells, MN9D cells exhibit both transient and sustained peaks of 6-OHDA-induced ERK1/2 and ERK5 activation as indicated by Western blot analysis in MN9D cells (Lin et al., 2004). We find that inhibition of the transient increase of ERK activation by U0126, which peaks at 15 min, increases 6-OHDA-induced toxicity. However, we have not yet identified a role for the second, sustained peak of ERK activation in DA cell survival.

Role of ERK5 and MEF2C in Determining Viability of MN9D Cells

Similar to ERK1/2, recent results from dorsal root ganglion, cortical, and cerebellar neurons suggest a role for ERK5 in neuronal survival (Watson et al., 2001; Liu et al., 2003; Shalizi et al., 2003). In cortical and cerebellar neurons, ERK5 plays a larger role in neuronal survival during embryonic development than during postnatal development. Consistent with these findings, the present studies suggest that activation of ERK5 contributes to basal DA cell survival. Although activation of the ERK5 pathway also provided some neuroprotection from acute 6-OHDA toxicity in MN9D cells, our data suggest that this role was less than that of ERK1/2. Thus, maintenance of basal survival by ERK5 may be more important for protection from chronic exposure to toxins. Current studies in our laboratory are being conducted to explore the effect of the ERK5 pathway neuronal survival following chronic exposure to a neurotoxin.

The MEF2 proteins constitute a family of transcription factors that includes MEF2C as a downstream target of ERK5 (Kato et al., 1997; English et al., 1998; Marinissen et al., 1999). MEF2C has been shown to play a role in the survival of some types of neurons (Bonni et al., 1999; Mao et al., 1999); however, a role for MEF2C in DA neuronal survival has not been previously reported. We have now shown that constitutive activation of MEF2C significantly increases basal cell survival and decreases 6-OHDA-induced cell death in MN9D cells. These data further support a role for ERK5 in basal dopaminergic cell survival and suggest that MEF2C might be a target of the ERK5 signaling pathway in DA neuronal cells.

Interactions Between ERK1/2 and ERK5

Our studies support the hypothesis that ERK1/2 and ERK5 are important for DA neuronal survival. Inhibition of these pathways, either pharmacologically or by using transient transfection with dominant negative mutants, decreased MN9D cell survival in a concentration-dependent manner. These data suggest that the ERK1/2 and ERK5 pathways may interact to promote basal survival of DA neuronal cells. Although ERK1/2 and ERK5 activate distinct downstream targets, such as Elk-1 and MEF2C, respectively, they also act on common targets, such as the cMyc and Sap1a transcription factors (Gille et al., 1992; Kato et al., 1997; English et al., 1998; Kamakura et al., 1999; Marinissen et al., 1999; Cavanaugh et al., 2001). Therefore, it is possible that these pathways activate common targets such as cMyc or Sap1a in DA neuronal cells to promote cell survival, and maximal activation of these transcription factors may require both ERK pathways. Alternatively, DA neurons may require simultaneous activation of the distinct ERK1/2 and ERK5 transcription factors Elk-1 and MEF2C, respectively, for survival.

Knowledge of these signaling mechanisms in DA neurons should greatly aid in the development of new therapeutic approaches for neurodegenerative diseases, specifically, Parkinson's disease. Results from this study provide new information on the ERK signaling pathways that play a role in the neuroprotection and basal survival of DA neurons. Future studies will examine whether there is cross-talk between the ERK1/2 and the ERK5 pathways or whether these kinases are working independently to increase DA neuronal survival.

ACKNOWLEDGMENTS

We thank Drs. Alfred Heller and Lisa Won for a gift of the MN9D cells and Drs. Donald DeFranco and Elias Aizenman for critical discussion of the manuscript. Some of these results have previously been presented at the 16th

International Congress on Parkinsonism and Related Disorders (June, 2005; Berlin) and the 35th annual meeting of the Society for Neuroscience (November, 2005; Washington, DC).

REFERENCES

Boeckman FA, Aizenman E. 1996. Pharmacological properties of acquired excitotoxicity in Chinese hamster ovary cells transfected with N-methyl-D-aspartate receptor subunits. J Pharmacol Exp Ther 279:515–523.

Bonni A, Brunet A, West AE, Datta SR, Takasu MA, Greenberg ME. 1999. Cell survival promoted by the Ras-MAPK signaling pathway by transcription-dependent and -independent mechanisms. Science 286:1358–1362.

Brewer GJ. 1995. Serum-free B27/neurobasal medium supports differentiated growth of neurons from the striatum, substantia nigra, septum, cerebral cortex, cerebellum, and dentate gyrus. J Neurosci Res 42:674–683.

Bushbeck M, Eickhoff J, Sommer MN, Ullrich A. 2002. Phosphotyrosine-specific phosphatase PTP-SL regulates the ERK5 signaling pathway. J Biol Chem 277:29503–29509.

Cavanaugh JE, Ham J, Hetman M, Poser S, Yan C, Xia Z. 2001. Differential regulation of mitogen-activated protein kinases ERK1/2 and ERK5 by neurotrophins, neuronal activity, and cAMP in neurons. J Neurosci 21:434–443.

Choi HK, Won L, Roback JD, Wainer BH, Heller A. 1992. Specific modulation of dopamine expression in neuronal hybrid cells by primary cells from different brain regions. Proc Natl Acad Sci U S A 89:8943–8947.

Choi WS, Yoon SY, Oh TH, Choi EJ, O'Malley KL, Oh YJ. 1999. Two distinct mechanisms are involved in 6-hydroxydopamine- and MPP^+-induced dopaminergic neuronal cell death: role of caspases, ROS, and JNK. J Neurosci Res 57:86–94.

Choi WS, Yoon SY, Chang II, Choi EJ, Rhim H, Jin BK, Oh TH, Krajewski S, Reed JC, Oh YJ. 2000. Correlation between structure of Bcl-2 and its inhibitory function of JNK and caspase activity in dopaminergic neuronal apoptosis. J Neurochem 74:1621–1626.

Ding YM, Jaumotte JD, Signore AP, Zigmond MJ. 2004. Effects of 6-hydroxydopamine on primary cultures of substantia nigra: specific damage to dopamine neurons and the impact of glial cell line-derived neurotrophic factor. J Neurochem 89:776–787.

English JM, Pearson G, Baer R, Cobb MH. 1998. Identification of substrates and regulators of the mitogen-activated protein kinase ERK5 using chimeric protein kinases. J Biol Chem 273:3854–3860.

Garcia L, Garcia F, Llorens F, Unzeta M, Itarte E, Gomez N. 2002. PP1/PP2A phosphatases inhibitors okadaic acid and calyculin A block ERK5 activation by growth factors and oxidative stress. FEBS Lett 523:90–94.

Gille H, Sharrocks AD, Shaw PE. 1992. Phosphorylation of transcription factor p62TCF by MAP kinase stimulates ternary complex formation at c-fos promoter. Nature 358:414–417.

Han J, Jiang Y, Li Z, Kravchenko VV, Ulevitch RJ. 1997. Activation of the transcription factor MEF2C by the MAP kinase p38 in inflammation. Nature 386:296–299.

Hetman M, Kanning K, Cavanaugh JE, Xia Z. 1999. Neuroprotection by brain-derived neurotrophic factor is mediated by extracellular signal-regulated kinase and phosphatidylinositol 3-kinase. J Biol Chem 274:22569–22580.

Hetman M, Cavanaugh JE, Kimelman D, Xia Z. 2000. Role of glycogen synthase kinase-3beta in neuronal apoptosis induced by trophic withdrawal. J Neurosci 20:2567–2574.

Hetman M, Hsuan SL, Habas A, Higgins MJ, Xia Z. 2002. ERK1/2 antagonizes glycogen synthase kinase-3beta-induced apoptosis in cortical neurons. J Biol Chem 277:49577–49584.

Kamakura S, Moriguchi T, Nishida E. 1999. Activation of the protein kinase ERK5/BMK1 by receptor tyrosine kinases. Identification and characterization of a signaling pathway to the nucleus. J Biol Chem 274:26563–26571.

Kato Y, Kravchenko VV, Tapping RI, Han J, Ulevitch RJ, Lee JD. 1997. BMK1/ERK5 regulates serum-induced early gene expression through transcription factor MEF2C. EMBO J 16:7054–7066.

Kondoh K, Terasawa K, Morimoto H, Nishida E. 2006. Regulation of nuclear translocation of extracellular signal-regulated kinase 5 by active nuclear import and export mechanisms. Mol Cell Biol 26:1679–1690.

Kulich SM, Chu CT. 2001. Sustained extracellular signal-regulated kinase activation by 6-hydroxydopamine: implications for Parkinson's disease. J Neurochem 77:1058–1066.

Lin E, Perez RG, Zigmond MJ. 2004. Role of ERK1/2 activation in dopaminergic cell survival in response to oxidative stress. Program No. 93.9. Abstract Viewer/Itinerary Planner. Washington, DC: Society for Neuroscience.

Liu L, Cavanaugh JE, Wang Y, Sakagami H, Mao Z, Xia Z. 2003. ERK5 activation of MEF2-mediated gene expression plays a critical role in BDNF-promoted survival of developing but not mature cortical neurons. Proc Natl Acad Sci U S A 100:8532–8537.

Lotharius J, Brundin P. 2002. Pathogenesis of Parkinson's disease: Dopamine, vesicles and α-synuclein. Nat Neurosci Rev 3:932–942.

Mansour SJ, Resing KA, Candi JM, Hermann AS, Gloor JW, Herskind KR, Wartmann M, Davis RJ, Ahn NG. 1994. Mitogen-activated protein (MAP) kinase phosphorylation of MAP kinase kinase: determination of phosphorylation sites by mass spectrometry and site-directed mutagenesis. J Biochem 116:304–314.

Mao Z, Bonni A, Xia F, Nadal-Vicens M, Greenberg ME. 1999. Neuronal activity-dependent cell survival mediated by transcription factor MEF2. Science 286:785–790.

Marais R, Wynne J, Treisman R. 1993. The SRF accessory protein Elk-1 contains a growth factor-regulated transcriptional activation domain. Cell 73:381–393.

Marinissen MJ, Chiariello M, Pallante M, Gutkind JS. 1999. A network of mitogen-activated protein kinases links G protein-coupled receptors to the c-jun promoter: a role for c-Jun NH2-terminal kinase, p38s, and extracellular signal-regulated kinase 5. Mol Cell Biol 19:4289–4301.

Mody N, Leitch J, Armstrong C, Dixon J, Cohen P. 2001. Effects of MAP kinase cascade inhibitors on the MKK5/ERK5 pathway. FEBS Lett 502:21–24.

Nakamura K, Uhlik MT, Johnson NL, Hahn KM, Johnson GL. 2006. PB1 domain-dependent signaling complex is required for extracellular signal-regulated kinase 5 activation. Mol Cell Biol 26:2065–2079.

Oh JH, Choi WS, Kim JE, Seo JW, O'Malley KL, Oh YJ. 1998. Overexpression of HA-Bax but not Bcl-2 or Bcl-XL attenuates 6-hydroxydopamine-induced neuronal apoptosis. Exp Neurol 154:193–198.

Oh YJ, Wong SC, Moffat M, O'Malley KL. 1995. Overexpression of Bcl-2 attenuates MPP^+, but not 6-OHDA, induced cell death in a dopaminergic neuronal cell line. Neurobiol Dis 2:157–167.

Rameau GA, Akaneya Y, Chiu L, Ziff EB. 2000. Role of NMDA receptor functional domains in excitatory cell death. Neuropharmacology 39:2255–2266.

Ranganathan A, Pearson GW, Chrestensen CA, Sturgill TW, Cobb MH. 2006. The MAP kinase ERK5 binds to and phosphorylates p90 RSK. Arch Biochem Biophys 449:8–16.

Ricart KC, Fiszman ML. 2001. Hydrogen peroxide-induced neurotoxicity in cultured cortical cells grown in serum-free and serum-containing media. Neurochem Res 26:801–808.

Shalizi A, Lehtinen M, Gaudilliere B, Donovan N, Han J, Konishi Y, Bonni A. 2003. Characterization of a neurotrophin signaling mechanism that mediates neuron survival in a temporally specific pattern. J Neurosci 23:7326–7336.

Smith AD, Amalric M, Koob GF, Zigmond MJ. 2002. Effect of bilateral 6-hydroxydopamine lesions of the medial forebrain bundle on reaction time. Neuropsychopharmacology 26:756–764.

Stanciu M, DeFranco DB. 2002. Prolonged nuclear retention of activated extracellular signal-regulated protein kinase promotes cell death generated by oxidative toxicity of proteasome inhibition in a neuronal cell line. J Biol Chem 277:4010–4017.

Ugarte SD, Lin E, Klann E, Zigmond MJ, Perez RG. 2003. Effects of GDNF on 6-OHDA-induced death in a dopaminergic cell line: modulation by inhibitors of PI3 kinase and MEK. J Neurosci Res 73:105–112.

Ward CM, Barrow KM, Stern PL. 2004. Significant variations in differentiation properties between independent mouse ES cell lines cultured under defined conditions. Exp Cell Res 293:229–238.

Watson FL, Heerssen HM, Bhattacharyya A, Klesse L, Lin MZ, Segal RA. 2001. Neurotrophins use the Erk5 pathway to mediate a retrograde survival response. Nat Neurosci 4:981–988.

Wolinsky EJ, Landis SC, Patterson PH. 1985. Expression of noradrenergic and cholinergic traits by sympathetic neurons cultured without serum. J Neurosci 5:1497–1508.

Xia Z, Dickens M, Raingeaud J, Davis RJ, Greenberg ME. 1995. Opposing effects of ERK and JNK-p38 MAP kinases on apoptosis. Science 270:1326–1331.

Yang CC, Ornatsky OI, McDermott JC, Cruz TF, Prody CA. 1998. Interaction of myocyte enhancer factor 2 (MEF2) with a mitogen- activated protein kinase, ERK5/BMK1. Nucleic Acids Res 26:4771–4777.

Zhu JH, Kulich SM, Oury TD, Chu CT. 2002. Cytoplasmic aggregates of phosphorylated extracellular signal-regulated protein kinases in Lewy body diseases. Am J Pathol 161:2087–2098.

Zhu JH, Guo F, Shelburne J, Watkins S, Chu CT. 2003. Localization of phosphorylated ERK/MAP kinases to mitochondria and autophagosomes in Lewy body diseases. Brain Pathol 13:473–481.

Zigmond MJ, Keefe KA. 1997. Highly selective neurotoxins: basic and clinical applications. New York: Humana Press.

Journal of Neuroscience Research 86:108–117 (2008)

Rapid Activation of ERK by 6-Hydroxydopamine Promotes Survival of Dopaminergic Cells

Eva Lin, Jane E. Cavanaugh, Rehana K. Leak, Ruth G. Perez, and Michael J. Zigmond*

Pittsburgh Institute for Neurodegenerative Diseases, University of Pittsburgh, Pittsburgh, Pennsylvania

Isoforms of the mitogen-activated protein kinase ERK have been implicated in both cell survival and cell death. In the present study we explored their role in cell viability in response to oxidative stress. Using the dopaminergic MN9D cell line, we determined that cell death occurred in a concentration-dependent manner after exposure to 6-hydroxydopamine (6-OHDA). The toxicity of 6-OHDA was mediated through generation of reactive oxygen species and was accompanied by a large increase in phosphorylated ERK1/2 but no significant increase in phosphorylated ERK5. 6-OHDA produced a distinct temporal pattern of ERK1/2 activation, with phosphorylated ERK1/2 peaks occurring after 10–15 min (25-fold increase) and 6–24 hr (13-fold increase). Inhibition of the early phosphorylated ERK1/2 peak with U0126 increased the generation of reactive oxygen species by 6-OHDA as well as 6-OHDA-induced toxicity, whereas inhibition of the late peak did not affect 6-OHDA-induced cell death. The time course of phosphorylation of the prosurvival protein CREB mimicked the temporal profile of ERK1/2 activation after 6-OHDA, and blocking the early phospho-ERK1/2 peak also abolished CREB activation. In contrast, activation of caspase-3 by 6-OHDA was delayed, occurring after about 6 hr, and this activation was increased by inhibition of the first phosphorylated ERK1/2 peak. These results suggest that the rapid activation of ERK1/2 in dopaminergic cells by oxidative stress serves as a self-protective response, reducing the content of reactive oxygen species and caspase-3 activity and increasing downstream ERK1/2 substrates.

Key words: cell death; MAPK; MN9D; oxidative stress; Parkinson's disease

Although the cause of idiopathic Parkinson's disease (PD) is unknown, signs of heightened oxidative stress and reduced antioxidant capacity are present in post-mortem PD brains; this and other evidence suggest a role for oxidative stress (Jenner and Olanow, 1998; Olanow and Tatton, 1999). Thus, determining how dopamine (DA) neurons protect themselves from oxidative stress may be of considerable clinical significance because PD may result from a failure of these defense mechanisms, and boosting the defenses may protect DA neurons. In previous studies we have used the neurotoxin 6-hydroxydopamine (6-OHDA) to produce selective oxidative stress in a DA cell line and have studied how exogenous glial cell line–derived neurotrophic factor (GDNF) protects against such oxidative stress (Zigmond, 1997; Ugarte et al., 2003; Ding et al., 2004). In this report we explore the presence of intrinsic mechanisms for defending against oxidative stress.

Mitogen-activated protein kinases (MAPKs), including extracellular signal–regulated kinases (ERKs), have been implicated in the response to reactive oxygen species (Guyton et al., 1996a; Dudek et al., 1997; Bonni et al., 1999; Harada et al., 2004). Mitogens, growth factors, and other extracellular stimuli activate MEK1/2 through the Ras/Raf pathway; MEK1/2 then phosphorylates and activates ERK1/2 (Seger and Krebs, 1995). To promote survival, phosphorylated ERK1/2 (pERK1/2) activates transcription factors such as cAMP response element–binding protein (CREB) and Elk, thereby increasing transcription of neurotrophic factors such as brain-derived neurotrophic factor (BDNF) and GDNF, as well as prosurvival genes such as *Bcl-2* (Finkbeiner et al., 1997; Finkbeiner, 2000).

Oxidative stress itself can stimulate phosphorylation of the ERK family of MAPKs. Once phosphorylated, the activated ERK can affect cellular responses in either a prosurvival or a prodeath manner depending on the

Contract grant sponsor: National Institute of Neurological Disorders and Stroke; Contract grant number: NS19608; Contract grant sponsor: National Institute on Aging; Contract grant number: AG25848; Contract grant sponsor: U.S. Army; Contract grant number: ERMS 03281022; Contract grant sponsor: Michael J. Fox Foundation; Contract grant sponsor: Parkinson Chapter of Greater Pittsburgh.

Ruth G. Perez and Michael J. Zigmond contributed equally to the work.

*Correspondence to: Michael J. Zigmond, Department of Neurology, Pittsburgh Institute for Neurodegenerative Diseases, 3501 Fifth Avenue, 7016 Biomedical Science Tower 3, University of Pittsburgh, Pittsburgh, PA 15260. E-mail: zigmond@pitt.edu

Received 20 March 2007; Revised 17 June and 22 June 2007; Accepted 25 June 2007

Published online 10 September 2007 in Wiley InterScience (www.interscience.wiley.com). DOI: 10.1002/jnr.21478

kinetics and duration of its activation (Pouyssegur et al., 2002). For example, when activation is rapid and transient, pERK tends to enhance survival (Xia et al., 1995; Guyton et al., 1996b; de Bernardo et al., 2004; Luo and DeFranco, 2006), but when activation is delayed and sustained, pERK can lead to cell death (Kulich and Chu, 2001; Seo et al., 2001; Stanciu and DeFranco, 2002; Canals et al., 2003). Thus, in the present study, we assessed how increased pERK caused by oxidative stress affected cell viability in MN9D cells, a cell line with dopaminergic characteristics. The cells were exposed to the dopaminergic toxin 6-OHDA, and both pERK and cellular viability were monitored. We conclude that in our system, the stress-induced increase in pERK exerted a self-protective influence through a reduction of reactive oxygen species (ROS), an increase in activated CREB, and inhibition of caspase-3 activation.

MATERIALS AND METHODS

Cell Culture

MN9D cells, a fusion of rostral mesencephalic neurons from embryonic C57BL/6J (E14) mice with N18TG2 mouse neuroblastoma cells (Choi et al., 1991), were a gift from Drs. Alfred Heller and Lisa Won. For all experiments, cells were grown on Primaria plates (BD-Falcon Biosciences, Bedford, MA) in Dulbecco's Modified Eagle's Medium [DMEM; D5648 (containing pyridoxol HCl); Sigma, St. Louis, MO] at a pH of 7.2, supplemented with 50 units/mL penicillin, 50 mg/mL streptomycin, and 10% fetal bovine serum (Hyclone, Logan, UT). Cells were maintained at 37°C with 5% CO_2 and used in their undifferentiated state between passages 8 and 20.

Experimental Treatments

Cells were plated the day before treatment at 15,000 cells/well in triplicate in 96-well Primaria plates (0.32 cm^2 surface area) for viability determination or at 500,000 cells/well in six-well Primaria plates (9.6 cm^2 surface area) for lysate collection. 6-OHDA (Sigma, St. Louis, MO), a readily oxidizable analogue of dopamine, was prepared in a vehicle containing DETAPAC (diethylenetriamine pentaacetic acid, 10 mM; Sigma, St. Louis, MO) and 0.015% ascorbic acid and bubbled with nitrogen gas for 10 min to reduce oxidative degradation. Using this protocol, we noted little oxidation of 6-OHDA after 30 min, ensuring that the effects of 6-OHDA on cells would be a result of generation of intracellular ROS rather than a general cytotoxic effect (Ding et al., 2004). There appeared to be lot-to-lot variability in the 6-OHDA, which over time shifted the EC_{50} for MN9D cells in different experiments. We have seen this before (Ding et al., 2004), and others have reported this as well. Nonetheless, regardless of the EC_{50}, we found that a given treatment always had comparable effects on viability and ERK phosphorylation over the course of the experiments when those effects were expressed as percentages of the impact of the proper vehicle control. The medium was changed to serum-free medium (SFM) for 4–6 hr to reduce basal pERK levels; the cells were then treated with 6-OHDA. To prevent cell division, the cells remained in serum-free media until evaluation 24 hr later.

In experiments designed to block ERK phosphorylation at particular times, we used U0126 (Calbiochem, San Diego, CA), a reversible inhibitor of ERK (Dudley et al., 1995; Favata et al., 1998; Appert-Collin et al., 2005; Yuan et al., 2006). U0126 (5 μM) was prepared in dimethyl sulfoxide (Sigma, St. Louis, MO) and added to the cells 1 hr prior to 6-OHDA delivery. After exposure to 6-OHDA, the medium was replaced with SFM for 24 hr.

Cell Viability Measurement

Cell viability was determined by two methods. First, to determine *nuclear condensation* using Hoechst stain, the cells were fixed in 4% formaldehyde/4% sucrose for 20 min. The fixative was removed, and 1 μg/mL of Hoechst 33258 (Sigma, St. Louis, MO) was added for 20 min. Stained cells were stored in PBS with 0.02% azide at 4°C. Analysis of stained cells was performed by counting five independent fields in each well at 20× magnification. Cells were considered viable if their nuclei exhibited a rounded morphology without fragmentation or nuclear condensation, whereas cells were classified as dead if their nuclei were fragmented or condensed and more brightly stained. Second, as a test for loss of cell membrane integrity, *lactate dehydrogenase (LDH) release* was measured using the CytoTox96 Non Radioactive Cytotoxicity Assay (Promega, Madison, WI), performed according to the manufacturer's protocol. Cells were plated and treated in 96-well plates as described above. Twenty-four hours after removal of 6-OHDA, 50 μL of media from each experimental well was transferred to a new 96-well plate. The remaining cells in the wells were lysed with the manufacturer's lysis buffer, and 50 μL from each well was also transferred to the same 96-well plate. A substrate mix provided by the manufacturer was next added to each well and incubated for 30 min at room temperature, and then a stop solution was added to terminate the reaction. Absorbance readings were taken at 490 nm. The percentage of cell death was determined by the formula

$$\text{Percent cytotoxicity} = [\text{media } (OD_{490})/(\text{media } (OD_{490}) + \text{remaining cells } (OD_{490})] \times 100.$$

Some cell death was observed even in the absence of any treatment. This was probably in large part a result of serum deprivation.

Western Blot

At varying times after exposure to 6-OHDA exposure, as described above, the cells were washed with Dulbecco's PBS and then lysed in either 1% Nonidet P40 buffer containing aprotinin, leupeptin, and AEBSF or 1% Triton X-100 buffer containing 20 mM Tris (pH 6.8), 137 mM NaCl, 25 mM beta glycerophosphate, 2 mM NaPPi, 2 mM EDTA, 1 mM Na_3VO_4, 10% glycerol, 5 μg/mL leupeptin, 5 μg/mL aprotinin, 2 mM benzamidine, 0.5 mM DTT, and 1 mM PMSF. The lysates were centrifuged at 15,000 rpm for 10 min at 4°C. Protein content of the supernatant was determined by the BCA assay (Pierce, Rockford, IL). Equal amounts of protein (20 μg) from each treatment were then separated on SDS gels and transferred to nitrocellulose membrane (BioRad Laboratories, Hercules, CA) for Western blot analysis. Blots were blocked in

5% nonfat milk in TBS for 1 hr prior to incubation overnight at 4°C in primary antibody (pERK1/2, total ERK5, cleaved caspase 3, pCREB, Cell Signaling, Beverly, MA; β-actin or α-tubulin, Sigma, St. Louis, MO). Blots were then incubated with secondary antibody (horseradish peroxidase–conjugated antirabbit or -mouse, Calbiochem, San Diego, CA). Proteins were visualized with enhanced chemiluminescence (NEN, Boston, MA). Signal was quantified using the MCID Elite program (Imaging Research, St. Catharines, Ontario, Canada). Blots were stripped and reprobed for total ERK and total CREB (Cell Signaling, Beverly, MA) in order to normalize the phosphoprotein levels.

ERK1/2 Kinase Assay

Cells were plated in six-well plates, treated, and lysed as noted above for Western blot analysis. Immunoprecipitation and kinase assays of pERK1/2 were performed according to the manufacturer's protocol (p44/p42 Kinase Assay Kit, Cell Signaling, Beverly, MA). In brief, pERK1/2 was immunoprecipitated from lysates collected after 6-OHDA treatment on beads coupled to pERK1/2 antibody. The bead-bound pERK1/2 was then incubated with exogenous Elk (Elk-1 Fusion Protein, Cell Signaling, Beverly, MA), and phospho-Elk levels were determined by Western blot analysis of assay samples as described above (p-Elk, Cell Signaling, Beverly, MA).

ROS Assay

Cells were plated as described above in 96-well Primaria plates and were preincubated with 5 μM H_2DCF [5-(and-6)-chloromethyl-2′,7′-dichlorodihydrofluorescein diacetate acetyl ester; Molecular Probes, Carlsbad, CA] for 1 hr prior to treatment with 6-OHDA. This cell-permeant indicator remained nonfluorescent until converted to DCF by removal of the acetate groups by intracellular esterases after oxidation in the cell. The uninternalized H_2DCF reagent was washed out, and the cell medium was replaced with SFM before 6-OHDA treatment. After removal of 6-OHDA, cells received fresh SFM, and readings (excitation 480/emission 530) were taken on a Cytofluor 2300 fluorescent plate reader 24 hr later to measure the fluorescent cleavage product dichlorofluorescein (DCF), an index of ROS formation.

Statistical Analysis

Data represent the mean ± SEM for each experimental condition. All experiments were repeated on separate occasions a minimum of three times using duplicate or triplicate samples for each treatment condition. Data from all experimental conditions were analyzed by analysis of variance (ANOVA) using SPSS V10.1 (SPSS Inc., Chicago, IL) or GraphPad Prism (San Diego, CA). When the ANOVA results were significant at $P < 0.05$, post hoc tests were carried out using the methods of Bonferroni, Tukey, and Dunnets.

RESULTS

Concentration-Dependent MN9D Cell Death in Response to 6-OHDA

6-OHDA caused the death of MN9D cells in a concentration-dependent manner, as measured by Hoechst staining 24 hr after a 30-min exposure to the toxin (Fig. 1A, black bars). For example, 24 hr after exposure to 100 μM 6-OHDA, cell loss was approximately 50%, as measured by Hoechst staining. In contrast, 6-OHDA-induced LDH release, a measure of the loss of membrane integrity that characterizes necrosis, was not significantly increased in the cells except at the highest concentration of 6-OHDA (1,000 μM, $P < 0.05$; Fig. 1B). These results suggest that under our conditions, cell death by 6-OHDA resulted primarily from apoptotic-like cell death involving nuclear condensation rather

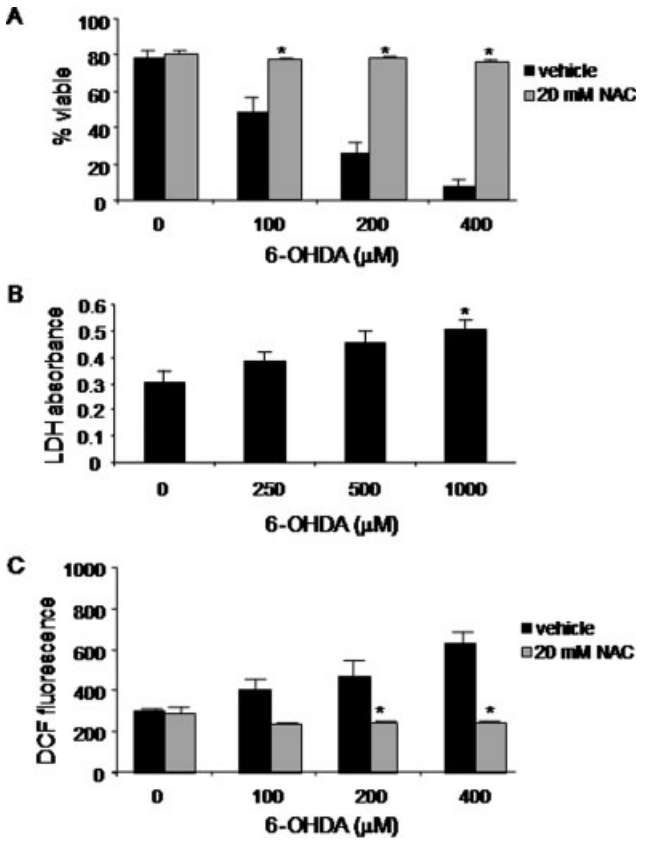

Fig. 1. 6-OHDA killed MN9D cells in a concentration-dependent manner and increased ROS generation. Cells were treated for 30 min with 6-OHDA. **A:** Cell viability as determined by Hoechst staining 24 hr after 6-OHDA removal showing that 6-OHDA increased apoptotic-like cell death in a concentration-dependent manner and that the addition of the antioxidant NAC (20 mM) protected against 6-OHDA-induced cell death. Data represent the mean ± SEM of three independent experiments. $^{\star}P < 0.05$. Significance of differences between vehicle and 20 mM NAC at each 6-OHDA concentration determined. **B:** Minimal necrotic-like cell death resulting from 6-OHDA at low concentrations. LDH assays conducted on cells treated with increasing concentrations of 6-OHDA. LDH release was measured 24 hr after 6-OHDA removal. Data represent the mean ± SEM of three independent experiments. **C:** Cells treated with increasing concentrations of 6-OHDA (100–400 μM); ROS levels after 24 hr monitored with the DCF assay. Addition of NAC (20 mM) blocked the 6-OHDA-induced generation of ROS. Data represent the mean ± SEM of three independent experiments; $^{\star}P < 0.05$, significant difference between 0 and 20 mM NAC at the 6-OHDA concentration indicated.

than from the necrotic-like cell death associated with loss of membrane integrity.

Toxicity of 6-OHDA Was Mediated through Generation of ROS

To determine whether the addition of 6-OHDA resulted in the generation of ROS in our cells, we used H_2DCF, a cell-permeant indicator, to measure the production of ROS 24 hr after 6-OHDA treatment. 6-OHDA (100–400 μM) caused a concentration-dependent increase in intracellular ROS ($P < 0.05$; Fig. 1C, black bars). Next, to confirm the role of ROS production in 6-OHDA-induced toxicity, we applied the antioxidant *N*-acetyl-cysteine (NAC; 20 mM) to cells 1 hr prior to a 30-min treatment with 6-OHDA (100–400 μM). NAC was also present in the media during the 24 hr after removal of 6-OHDA. The presence of NAC significantly protected the cells against death at each concentration of 6-OHDA, as determined by Hoechst stain ($P < 0.05$; Fig. 1B, gray bars). In addition, NAC significantly decreased the amount of ROS generated by 200 and 400 μM 6-OHDA, as measured by DCF ($P < 0.05$; Fig. 1C, gray bars). These data suggest that 6-OHDA-induced toxicity was associated with the generation of ROS as has previously been suggested (Choi et al., 1999).

6-OHDA Produced a Distinct Temporal Pattern of ERK Phosphorylation with Two pERK Peaks

The addition of a toxin to cells should activate various prodeath cascades but might also activate prosurvival cascades as the cells respond to protect themselves. ERK1/2 can be activated in a biphasic pattern after an insult (Stanciu et al., 2000; Cavanaugh et al., 2001; Kulich and Chu, 2001). To investigate the temporal profile of ERK isoform activation after a brief exposure of MN9D cells to 6-OHDA, the cells were treated for 30 min with 6-OHDA (250 μM), and pERK levels were monitored before, during, and after removal of the toxin. We found that 6-OHDA elicited two distinct peaks of pERK1/2 formation: the first peak was large (25-fold), early, and transient (10–15 min); the second was smaller (13-fold) and sustained, for 6–24 hr (Fig. 2A).

Like ERK1/2, ERK5, a member of the MAPK family, is activated by growth factors and has been implicated in neuronal survival (Cavanaugh et al., 2001; Watson et al., 2001; Liu et al., 2003; Shalizi et al., 2003). ERK5 has been shown to promote survival of embryonic cortical neurons via stimulation of the MEF2C transcription factor (Liu et al., 2003). Thus, we also evaluated the activation pattern of this ERK isoform. Following 6-OHDA, there was not a significant increase in pERK5, although a small, 20% activation may have occurred after 30 min (Fig. 2B).

Increased pERK1/2 Levels Were Associated with Increased ERK Activity

To determine whether the phosphorylated ERK was indeed an active kinase, we examined the activity of

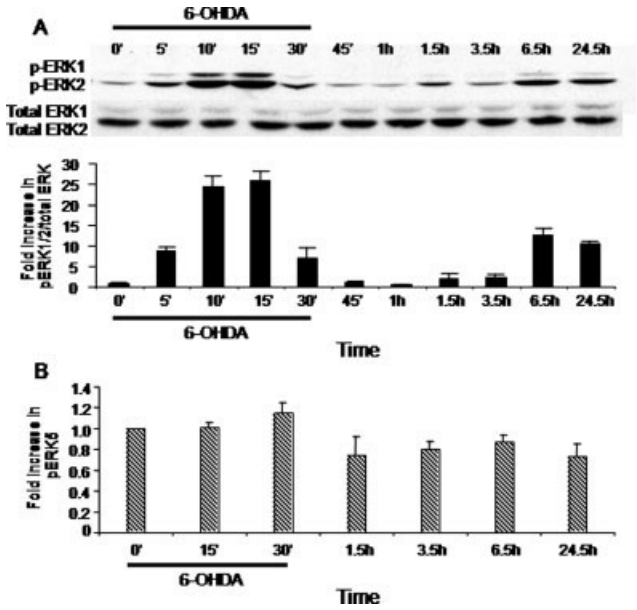

Fig. 2. Two 6-OHDA-induced peaks of ERK1/2 and ERK5. Western blot analysis showing pERK1/2 and pERK5 levels during and up to 24 hr after 6-OHDA removal. **A:** A representative Western blot showing the two distinct peaks of pERK1/2: one early and transient, peaking at 15 min and returning to near baseline by 30 min, and the second delayed and sustained, starting 3–6 hr after removal of 250 μM 6-OHDA removal and persisting up to 24 hr. Data are from three independent experiments. Vehicle controls for each time showed no effect on pERK1/2 (not shown). The corresponding bar graph represents data quantified from three independent experiments. **B:** No significant activation of ERK5 in response to 250 μM 6-OHDA, although there was suggestion of a pattern similar to that of pERK1/2. Data are from three independent experiments. Vehicle controls for each time showed no effect on pERK5 (data not shown).

ERK1/2 following 6-OHDA by measuring its ability to phosphorylate the downstream substrate Elk. pERK1/2 was immunoprecipitated from cell lysates collected after 15 and 30 min of exposure to 250 μM 6-OHDA. The immunoprecipitated pERK was then incubated with exogenous Elk. As before, a 15-min exposure to 6-OHDA treatment caused an increase in pERK1/2, which returned to basal levels by 30 min (Fig. 3A). This was associated with a parallel increase in the ability of the lysate to phosphorylate exogenous Elk (Fig. 3B). The addition of the MEK inhibitor U0126 (5 μM) successfully blocked phosphorylation of ERK1/2 (Fig. 3A) and completely prevented the subsequent activation of Elk (Fig. 3B). Therefore, ERK1/2 phosphorylated in response to 6-OHDA was an active kinase able to phosphorylate a specific downstream target.

Inhibition of Early pERK1/2 Peak Increased 6-OHDA Toxicity and Increased ROS Generation, But Inhibition of Late Peak Had No Effect on 6-OHDA-Induced Cell Death

Short-lived activation of ERK is associated with cell survival (Xia et al., 1995; Guyton et al., 1996b; de

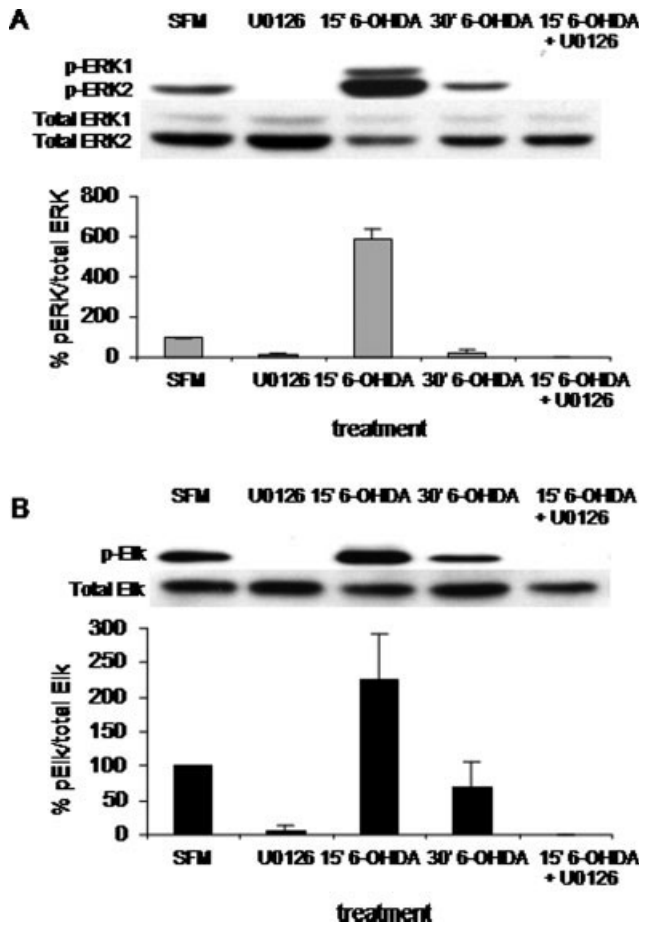

Fig. 3. pERK1/2, an active kinase, generated during 6-OHDA treatment. Kinase assays with exogenous Elk were carried out after immunoprecipitation of pERK1/2 from cells treated with 6-OHDA. **A:** Western blot analysis confirming immunoprecipitation of pERK1/2 from lysates and blocking of phosphorylation of ERK by addition of MEK inhibitor U0126. **B:** Representative Western blot of pElk levels showing paralleling of activation of pElk. The addition of U0126 also blocked phosphorylation of Elk. The corresponding bar graph represents data quantified from three independent experiments.

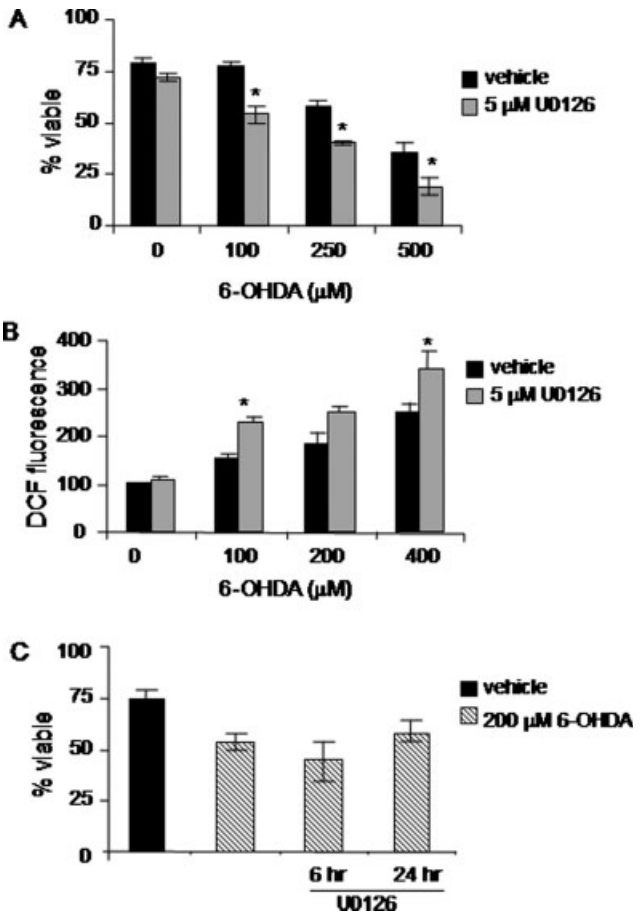

Fig. 4. Increased cell death and generation of ROS from blocking of first pERK1/2 peak, no detectable effect on cell viability from inhibition of second pERK1/2 peak. **A:** Decreased cell viability at all 6-OHDA concentrations after adding U0126 1 hr prior to and during 6-OHDA treatment to block the first pERK1/2 peak ($\star P < 0.05$, significant difference between 0 and 5 μM U0126 at the 6-OHDA concentration indicated). **B:** Generation of ROS after 24 hr as determined by the DCF assay in cells treated with 6-OHDA with and without the addition of 5 μM U0126 to block the early peak of ERK1/2 activation. ROS increased at all 6-OHDA concentrations (100–400 μM) after application of U0126 to block the early peak. Data represent the mean ± SEM of three independent experiments ($\star P < 0.05$, significant difference between vehicle and U0126 at the 6-OHDA concentration indicated). **C:** No detectable affect on cell viability from 1-hr application of U0126 6 and 24 hr after removal of 6-OHDA to block the delayed sustained pERK peak, measured by the Hoechst stain. Data represent the mean ± SEM of three independent experiments.

Bernardo et al., 2004). However, sustained pERK activation has been correlated with cell death (Kulich and Chu, 2001; Seo et al., 2001; Stanciu and DeFranco, 2002; Canals et al., 2003). To study the impact of both pERK1/2 peaks on cell survival in our model, we again measured the effect of the MEK inhibitor U0126 on viability at various times before and after exposure to 6-OHDA. The addition of U0126 (5 μM) 1 hr prior to and during the 30-min 6-OHDA exposure in order to block the first ERK1/2 activation peak significantly reduced cell viability by 24 hr at all 6-OHDA concentrations ($P < 0.05$; Fig. 4A, gray bars), suggesting the first pERK peak was associated with a self-protective response.

To determine if the increased sensitivity to 6-OHDA was associated with an increase in ROS, MN9D cells loaded with H_2DCF were treated for 30 min with 6-OHDA (100–400 μM) with or without U0126. Inhibition of the first 6-OHDA-induced pERK1/2 peak significantly increased the amount of cellular ROS generated in a concentration-dependent manner at 100 and 400 μM ($P < 0.05$; Fig. 4B), suggesting that the early activation of ERK promotes cell survival, at least in part, through its ability to suppress an accumulation of ROS.

To determine if the second peak of pERK was associated with the toxic response to 6-OHDA, we exposed cells to U0126 for 1 hr beginning either 5 or 23 hr after treatment with 6-OHDA and then measured cell survival after 24 hr. This treatment did not cause any significant change in cell viability compared to the viability of cells treated with 6-OHDA alone (Fig. 4C), suggesting that the late peak of ERK1/2 activation did not further contribute to cell death under our conditions.

CREB Phosphorylation Paralleled 6-OHDA-Induced Temporal Activation of ERK

Many prosurvival effects of ERKs are partly mediated via CREB. For example, increased pCREB facilitates the actions of pERK1/2 at least in part by increasing the transcription of neuroprotective proteins BDNF and Bcl-2 (Finkbeiner et al., 1997; Finkbeiner, 2000). To determine whether CREB might also be involved in the response to 6-OHDA, the activation state of CREB was evaluated by Western blot analysis. After 6-OHDA treatment, the temporal pattern of phosphorylation of CREB (Fig. 5A) mimicked the activation profile of pERK1/2, showing two peaks of activation, one early and transient and the other delayed and sustained. This suggested that CREB might be involved in the downstream prosurvival signaling of ERK after 6-OHDA exposure. Moreover, the addition of U0126 for 30 min beginning with the addition of 6-OHDA blocked not only the initial peak of pCREB but also the later peak (Fig. 5B, C, gray bars), further supporting the idea that rapid activation of ERK1/2 by oxidative stress serves as a self-protective response for the cells by increasing activation of prosurvival ERK1/2 substrates.

Activation of Caspase-3 Was Correlated with Cell Death, and Inhibition of the First pERK1/2 Peak Increased Caspase-3 Activation

Caspase-3 is activated by cleavage. In many cell types this event signals the cell to enter a path of programmed cell death. To further assess the mechanism of ROS-induced cell death mediated by 6-OHDA, levels of the cleaved and uncleaved forms of caspase-3 were measured in cells exposed to 6-OHDA (250 μM) for 30 min. Caspase-3 activation could be detected within 3 hr and was sustained up to 24 hr (Fig. 6A, B, black bars). Inhibition of the early pERK1/2 peak by U0126 (5 μM) led to a significant increase in cleaved caspase-3 level as measured 3 and 6 hr after 6-OHDA removal ($P < 0.05$; Fig. 6B, gray bars). These results suggest that 6-OHDA-induced cell death occurs at least in part through the caspase-3 pathway, which could be suppressed by ERK1/2 activation.

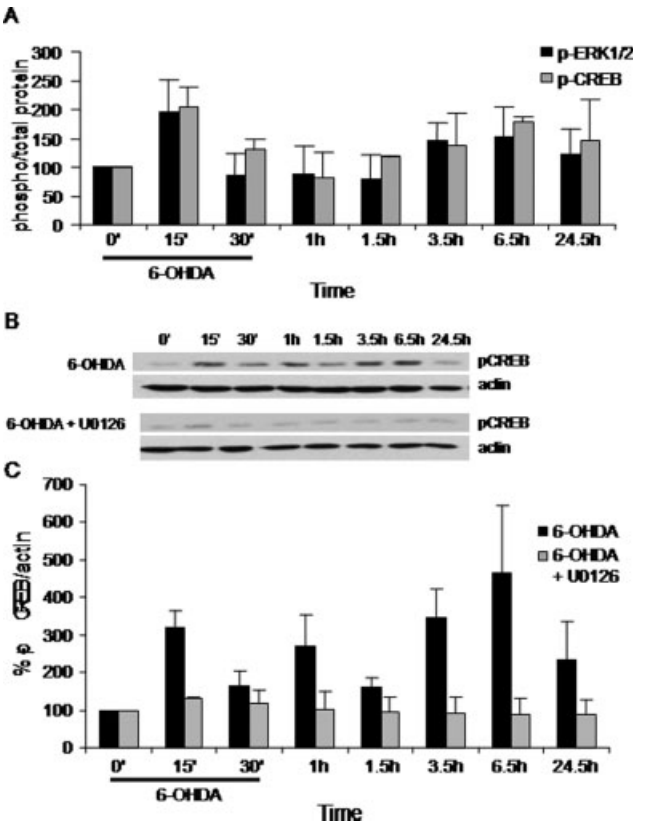

Fig. 5. CREB phosphorylation following 6-OHDA-induced ERK activation and inhibition of activation after first pERK peak. **A:** Western blot analysis of cells treated with 250 μM 6-OHDA for 30 min using pCREB antibody. Phosphorylation of ERK substrate CREB mimicked temporal activation pattern of ERK over the time evaluated. Data are from three independent experiments. **B, C:** Western blot analysis of cells treated with 250 μM 6-OHDA with and without the addition of 5 μM U0126 for 30 min using pCREB antibody. Inhibition of the early pERK peak blocked CREB activation throughout. Actin was included as a control. Data are from three independent experiments.

DISCUSSION

Because increased oxidative stress in DA neurons is a central component of PD pathophysiology, our study focused on the functional significance of increased pERK resulting from oxidative stress in an in vitro model of DA loss using the dopaminergic cell line MN9D and the selective neurotoxin 6-OHDA. After the 6-OHDA treatment regimen, cells responded by rapidly increasing pERK1/2 levels. This was accompanied by increased ERK activity (as measured by a kinase assay), increased CREB phosphorylation, reduced ROS production, and reduced caspase-3 cleavage. These findings suggest that dopaminergic neuronal cells can respond to oxidative insults in a defensive fashion in order to protect themselves from injury, even in the absence of pharmacological intervention.

6-OHDA Stimulates ROS and Apoptosis in MN9D Cells

6-OHDA caused an increase in ROS in MN9D cells. That this ROS increase played a causal role in the

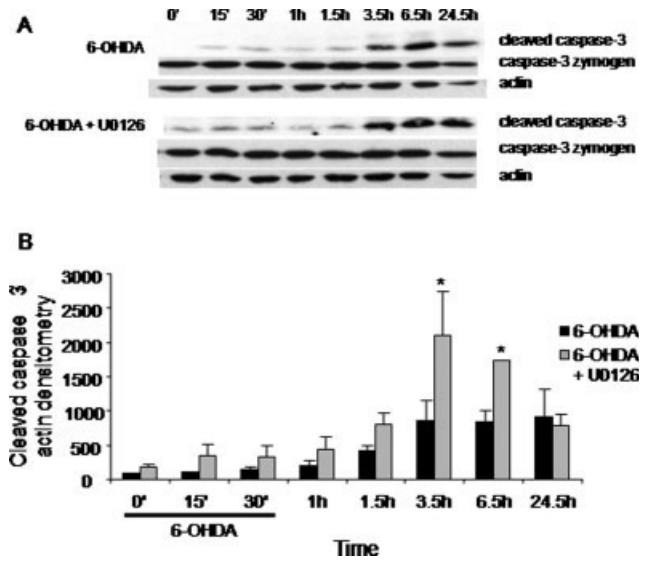

Fig. 6. Late activation of caspase, involvement in 6-OHDA-induced cell death, and increase after inhibition of first pERK peak. **A, B:** Western blot analysis of lysates collected from cells treated with 250 μM 6-OHDA with and without the addition of 5 μM U0126 for cleaved caspase-3, caspase-3 zymogen, and actin. Capase-3 activation began approximately 3 hr after removal of 6-OHDA, and inhibition of the first pERK peak increased caspase-3 activation ($\star P < 0.05$, significant difference between 6-OHDA and 6-OHDA + U0126 at the time indicated).

cell death is suggested by our finding that the antioxidant NAC reduced cell death and that the neuroprotective effects of ERK were accompanied by a reduction in ROS. Several observations indicated that cell death was largely apoptotic: 6-OHDA produced nuclear condensation rather than swelling, little if any LDH release was measurable after 6-OHDA in our cells, and caspase-3, an executioner caspase, was activated, particularly in the presence of U0126. In addition, we have preliminary data indicating that MN9D cells exposed to 6-OHDA also showed biphasic activation of the MAP kinase c-jun N-terminal kinase (JNK), a kinase implicated in apoptosis (Luo et al., 1998; Choi et al., 1999). Collectively, these findings suggest that in our model 6-OHDA-induced increase in intracellular ROS can lead to cell death mainly via apoptosis but that this is attenuated as a result of a rapid increase in ERK activation and a subsequent increase in a cascade of neuroprotective events, leading to reduced oxidative stress.

Increased pCREB and Decreased Caspase-3 Cleavage Modulate ERK-Induced Protection

Our data raise the possibility that ERK-dependent suppression of vulnerability to 6-OHDA results in part from increased phosphorylation of CREB. CREB phosphorylation is assumed to be a nuclear event. Thus, although we did not observe translocation of pERK to the nucleus after short-term 6-OHDA treatment at any time after toxin exposure (data not shown), the CREB data may indicate that a small or transient translocation of pERK into the nucleus occurred or that cytoplasmic pERK can act indirectly on CREB through an intermediary, as previously suggested (Ranganathan et al., 2006). Increased pCREB facilitates the prosurvival actions of pERK1/2 by increasing the transcription of the neuroprotective proteins BDNF and Bcl-2 (Finkbeiner et al., 1997; Finkbeiner, 2000). CREB phosphorylation has also been linked to inhibition of caspase 3, and thus CREB may serve as an intermediary between the increase in pERK and the caspase 3 cleavage that we observed, as supported by others (Allan et al., 2003).

Functional Significance of 6-OHDA-Induced Activation of ERK

Our findings suggest that dopaminergic neuronal cells have the inherent capacity to resist the toxic effects of oxidative stress. Our research group also has observed the activation of ERK1/2 in dopaminergic neurons in the substantia nigra after intracerebral injection of 6-OHDA into rats (Castro and Smith, 2005), suggesting that the hypothesis we derived from our cell culture data also holds true for the intact animal. These in vivo data complement our MN9D data and focus further attention on pERK1/2 as a potential neuroprotective candidate in PD.

Transient Activation of ERK Protects MN9D Cells

Blocking ERK phosphorylation using the MEK inhibitor U0126 effectively blocks phosphorylation of both ERK1/2 and ERK5 (Davies et al., 2000). We noted that ERK activation occurred in a biphasic manner after 6-OHDA exposure in our cells, with the first phase of ERK activation occurring within a few minutes of 6-OHDA exposure. Whereas that initial phosphorylation of ERK1/2 was dramatic, the activation of ERK5 was not significant, leading us to hypothesize that most if not all the effects of U0126 in our study were attributable to a blockade of ERK1/2 phosphorylation. A primary role for ERK1/2 isoforms in protecting against oxidative stress was further supported by our recent findings using both dominant-negative and constitutively active ERK constructs. In that study, we demonstrated that transfection of constitutively active MEK1 inhibited 6-OHDA-induced cell death, suggesting that elevated expression of ERK1/2 can protect against 6-OHDA toxicity. Our current study found that 6-OHDA itself activates ERK1/2 in a biphasic manner and that the large early and transient peak contributes to the survival of the cells in a self-protective response to the toxin. Because of the necessarily chronic nature of dominant-negative or constitutively active ERK constructs, this methodology could not be used to distinguish between the two peaks of ERK activation, one of which was complete within 30 min of 6-OHDA exposure. Thus, transient U0126 treatment

allowed us to dissect out the relative role of the two pERK peaks in a manner not possible with traditional molecular biological techniques.

We noted that the ability of U0126 to increase the toxic effects of 6-OHDA was greatest at the highest concentration of 6-OHDA, with a further loss of 50% more cells as a result of ERK inhibition. At lower 6-OHDA doses, the effect was more modest. It is possible that the 6-OHDA-induced increase in pERK coincided with activation of other signaling cascades, such as PI3K/Akt, particularly at lower doses. Indeed, in a preliminary experiment we also observed 6-OHDA-induced activation of Akt under the same paradigm as that in the present study. Furthermore, we have also demonstrated that inhibitors of either ERK or Akt activation caused loss of protection for GDNF against 6-OHDA (Ugarte et al., 2003). Another signaling molecule that may have compensated against 6-OHDA when U0126 was applied is NF-κB (Park et al., 2004). Coordinated regulation of multiple signaling cascades occurs in many cell types and is consistent with the idea that cells can mount an endogenous defense via multiple signaling pathways.

In contrast to the effects of blocking the early pERK peak, blocking the later pERK peak did not produce a measurable effect on cell viability after short exposure to 6-OHDA. The rather modest difference in viability depending on whether U0126 was present with the late peak may be because the later induction was only inhibited for 1 hr. We added U0126 1 hr prior to each collection time in part because exposure to U0126 for long periods caused cells to die even without the addition of 6-OHDA, confounding interpretation of the data (unpublished data and Cavanaugh et al., 2006). However, a preliminary experiment with chronic U0126 suggested that there was no additional effect on 6-OHDA toxicity when U0126 remained for the entire time beyond the drop in basal viability.

Our observations contrast with those of a previous study, which found that 6-OHDA induced sustained ERK1/2 activation that led to cell death (Kulich and Chu, 2001). However, the protocols of the two studies differed significantly in concentration and duration of 6-OHDA exposure and cell lines and pERK inhibitors used, and thus a direct comparison is not possible. On the other hand, these studies serve as a reminder that ERK activation and its functional significance are influenced by differences in cell type, stimuli, and details of the protocol. It is likely that further understanding of these influences will provide critical insight into how changes in ERK1/2 activation influence the resiliency of DA neurons. Our efforts to characterize ERK1/2 in dopaminergic cells under various conditions that elevate ROS, as initiated in the present study, might be important for understanding the role of ERK1/2 in human DA cell survival. For example, it is possible that ERK1/2 levels may vary as a function of stage of PD and of the precise topographical region in the substantia nigra, as these are known to have varying inherent vulnerabilities (Damier et al., 1999; Braak et al., 2003).

In conclusion, ERK can play a regulatory role in both cell survival and cell death depending on the conditions of the study. This has ramifications for the clinical application of findings related to this pathway and underscores the importance of characterizing the role of ERK1/2 and its spatiotemporal profile in each system being targeted. In our system, pERK1/2 appeared to play a prosurvival role in cells exposed to oxidative stress. These results are consistent with many previous studies on this important, ubiquitous kinase. For example, the involvement of pERK in fundamental processes related to cell survival is strongly suggested by studies of ERK knockout animals (Pages et al., 1999; Mazzucchelli et al., 2002; Saba-El-Leil et al., 2003) and by recent studies demonstrating the involvement of ERK in the neuroprotective effects of granulocyte colony-stimulating factor and erythropoietin in response to 6-OHDA (Signore et al., 2006; Huang et al., 2007). Finally, our data highlight the role of ERKs in the most basic life and death decisions in cells and indicate their relevance to the protection of DA neurons against the type of insults that occur during PD pathogenesis. Knowing the mechanisms underlying this self-protective activity should not only elucidate the role of ERK activation in cell viability decisions but may also identify points of intervention for enhancing dopaminergic neuronal survival in human conditions.

ACKNOWLEDGMENTS

A postdoctoral fellowship from the National Institutes of Health went to E.L. The observations reported in this article were presented in preliminary form at a meeting of the Society for Neuroscience. Our thanks to Alfred Heller and Lisa Won for the gift of MN9D cells and advice regarding their use, Juliann D. Jaumotte for assistance with the statistical analysis, Donald B. DeFranco and Anthony K. F. Liou for helpful comments, Susan M. Giegel for technical editing, and Emma L. Culligan for secretarial assistance.

REFERENCES

Allan LA, Morrice N, Brady S, Magee G, Pathak S, Clarke PR. 2003. Inhibition of caspase-9 through phosphorylation at Thr 125 by ERK MAPK. Nat Cell Biol 5:647–654.

Appert-Collin A, Duong FH, Passilly Degrace P, Warter JM, Poindron P, Gies JP. 2005. MAPK activation via 5-hydroxytryptamine 1A receptor is involved in the neuroprotective effects of xaliproden. Int J Immunopathol Pharmacol 1:21–31

Bonni A, Brunet A, West AE, Datta SR, Takasu MA, Greenberg ME. 1999. Cell survival promoted by the Ras-MAPK signaling pathway by transcription-dependent and -independent mechanisms. Science 286:1358–1362.

Braak H, Del Tredici K, Rub U, de Vos RA, Jansen Steur EN, Braak E. 2003. Staging of brain pathology related to sporadic Parkinson's disease. Neurobiol Aging 24:197–211.

Canals S, Casarejos MJ, de Bernardo S, Solano RM, Mena MA. 2003. Selective and persistent activation of extracellular signal-regulated protein kinase by nitric oxide in glial cells induces neuronal degeneration in glutathione-depleted midbrain cultures. Mol Cell Neurosci 24:1012–1026.

Castro S, Smith AD. 2005. Activation of MAPK in DA neurons after 6-hydroxydopamine into the medial forebrain bundle. Abstract Viewer and Itinerary Planner. Washington, DC: Society for Neuroscience; 2005.

Cavanaugh JE, Ham J, Hetman M, Poser S, Yan C, Xia Z. 2001. Differential regulation of mitogen-activated protein kinases ERK1/2 and ERK5 by neurotrophins, neuronal activity, and cAMP in neurons. J Neurosci 21:434–443.

Cavanaugh JE, Jaumotte JD, Lakoski JM, Zigmond MJ. 2006. Neuroprotective role of ERK1/2 and ERK5 in a dopaminergic cell line under basal conditions and in response to oxidative stress. J Neurosci Res 84:1367–1375.

Choi HK, Won LA, Kontur PJ, Hammond DN, Fox AP, Wainer BH, Hoffmann PC, Heller A. 1991. Immortalization of embryonic mesencephalic dopaminergic neurons by somatic cell fusion. Brain Res 552:67–76.

Choi WS, Yoon SY, Oh TH, Choi EJ, O'Malley KL, Oh YJ. 1999. Two distinct mechanisms are involved in 6-hydroxydopamine- and MPP+-induced dopaminergic neuronal cell death: role of caspases, ROS, and JNK. J Neurosci Res 57:86–94.

Damier P, Hirsch EC, Agid Y, Graybiel AM. 1999. The substantia nigra of the human brain. II. Patterns of loss of dopamine-containing neurons in Parkinson's disease. Brain 122:1437–1448.

Davies SP, Reddy H, Caivano M, Cohen P. 2000. Specificity and mechanism of action of some commonly used protein kinase inhibitors. Biochem J 351:95–105.

de Bernardo S, Canals S, Casarejos MJ, Solano RM, Menendez J, Mena MA. 2004. Role of extracellular signal-regulated protein kinase in neuronal cell death induced by glutathione depletion in neuron/glia mesencephalic cultures. J Neurochem 91:667–682.

Ding YM, Jaumotte JD, Signore AP, Zigmond MJ. 2004. Effects of 6-hydroxydopamine on primary cultures of substantia nigra: specific damage to dopamine neurons and the impact of glial cell line-derived neurotrophic factor. J Neurochem 89:776–787.

Dudek H, Datta SR, Franke TF, Birnbaum MJ, Yao R, Cooper GM, Segal RA, Kaplan DR, Greenberg ME. 1997. Regulation of neuronal survival by the serine-threonine protein kinase Akt. Science 275:661–665.

Dudley DT, Pang L, Decker SJ, Bridges AJ, Saltiel AR. 1995. A synthetic inhibitor of the mitogen-activated protein kinase cascade. Proc Natl Acad Sci U S A 92:7686–7689

Favata MF, Horiuchi KY, Manos EJ, Daulerio AJ, Stradley DA, Feeser WS, Van Dyk DE, Pitts WJ, Earl RA, Hobbs F, Copeland RA, Magolda RL, Scherle PA, Trzaskos JM. 1998. Identification of a novel inhibitor of mitogen-activated protein kinase kinase. J Biol Chem 273:18623–18632.

Finkbeiner S, Tavazoie SF, Maloratsky A, Jacobs KM, Harris KM, Greenberg ME. 1997. CREB: a major mediator of neuronal neurotrophin responses. Neuron 19:1031–1047.

Finkbeiner S. 2000. CREB couples neurotrophin signals to survival messages. Neuron 25:11–14.

Guyton KZ, Gorospe M, Kensler TW, Holbrook NJ. 1996a. Mitogen-activated protein kinase (MAPK) activation by butylated hydroxytoluene hydroperoxide: implications for cellular survival and tumor promotion. Cancer Res 56:3480–3485.

Guyton KZ, Liu Y, Gorospe M, Xu Q, Holbrook NJ. 1996b. Activation of mitogen-activated protein kinase by H2O2. Role in cell survival following oxidant injury. J Biol Chem 271:4138–4142.

Harada H, Quearry B, Ruiz-Vela A, Korsmeyer SJ. 2004. Survival factor-induced extracellular signal-regulated kinase phosphorylates BIM, inhibiting its association with BAX and proapoptotic activity. Proc Natl Acad Sci U S A 101:15313–15317.

Huang HY, Lin SZ, Kuo JS, Chen WF, Wang MJ. 2007. G-CSF protects dopaminergic neurons from 6-OHDA-induced toxicity via the ERK pathway. Neurobiol Aging 28:1258–1269.

Jenner P, Olanow CW. 1998. Understanding cell death in Parkinson's disease. Ann Neurol 44:S72–S84.

Kulich SM, Chu CT. 2001. Sustained extracellular signal-regulated kinase activation by 6-hydroxydopamine: implications for Parkinson's disease. J Neurochem 77:1058–1066.

Liu L, Cavanaugh JE, Wang Y, Sakagami H, Mao Z, Xia Z. 2003. ERK5 activation of MEF2-mediated gene expression plays a critical role in BDNF-promoted survival of developing but not mature cortical neurons. Proc Natl Acad Sci U S A 100:8532–8537.

Luo Y, DeFranco DB. 2006. Opposing roles for ERK1/2 in neuronal oxidative toxicity: Distinct mechanisms of ERK1/2 action at early versus late phases of oxidative stress. J Biol Chem 281:16436–16442.

Luo Y, Umegaki H, Wang X, Abe R, Roth GS. 1998. Dopamine induces apoptosis through an oxidation-involved SAPK/JNK activation pathway. J Biol Chem 273:3756–3764.

Mazzucchelli C, Vantaggiato C, Ciamei A, Fasano S, Pakhotin P, Krezel W, Welzl H, Wolfer DP, Pages G, Valverde O, Marowsky A, Porrazzo A, Orban PC, Maldonado R, Ehrengruber MU, Cestari V, Lipp HP, Chapman PF, Pouyssegur J, Brambilla R. 2002. Knockout of ERK1 MAP kinase enhances synaptic plasticity in the striatum and facilitates striatal-mediated learning and memory. Neuron 34:807–820.

Olanow CW, Tatton WG. 1999. Etiology and pathogenesis of Parkinson's disease. Annu Rev Neurosci 22:123–144.

Pages G, Guerin S, Grall D, Bonino F, Smith A, Anjuere F, Auberger P, Pouyssegur J. 1999. Defective thymocyte maturation in p44 MAP kinase (Erk 1) knockout mice. Science 286:1374–1377.

Park SH, Choi WS, Yoon SY, Ahn YS, Oh YJ, 2004. Activation of NF-kappaB is involved in 6-hydroxydopamine-but not MPP+-induced dopaminergic neuronal cell death: its potential role as a survival determinant. Biochem Biophys Res Commun. 322:727–733.

Pouyssegur J, Volmat V, Lenormand P. 2002. Fidelity and spatio-temporal control in MAP kinase (ERKs) signalling. Biochem Pharmacol 64:755–763.

Ranganathan A, Pearson GW, Chrestensen CA, Sturgill TW, Cobb MH, 2006. The MAP kinase ERK5 binds to and phosphorylates p90 RSK. Arch Biochem Biophys 449:8–16.

Riccio A, Ahn S, Davenport CM, Blendy JA, Ginty DD. 1999. Mediation by a CREB family transcription factor of NGF-dependent survival of sympathetic neurons. Science 286:2358–2361.

Saba-El-Leil MK, Vella FD, Vernay B, Voisin L, Chen L, Labrecque N, Ang SL, Meloche S. 2003. An essential function of the mitogen-activated protein kinase Erk2 in mouse trophoblast development. EMBO Rep 4:964–968.

Seger R, Krebs EG. 1995. The MAPK signaling cascade. FASEB J 9: 726–735.

Seo SR, Chong SA, Lee SI, Sung JY, Ahn YS, Chung KC, Seo JT. 2001. Zn2+-induced ERK activation mediated by reactive oxygen species causes cell death in differentiated PC12 cells. J Neurochem 78: 600–610.

Shalizi A, Lehtinen M, Gaudilliere B, Donovan N, Han J, Konishi Y, Bonni A. 2003. Characterization of a neurotrophin signaling mechanism that mediates neuron survival in a temporally specific pattern. J Neurosci 23:7326–7336.

Signore AP, Weng Z, Hastings T, Van Laar AD, Liang Q, Lee YJ, Chen J. 2006. Erythropoietin protects against 6-hydroxydopamine-induced dopaminergic cell death. J Neurochem 96:428–443

Stanciu M, DeFranco DB. 2002. Prolonged nuclear retention of activated extracellular signal-regulated protein kinase promotes cell death generated by oxidative toxicity or proteasome inhibition in a neuronal cell line. J Biol Chem 277:4010–4017.

Stanciu M, Wang Y, Kentor R, Burke N, Watkins S, Kress G, Reynolds I, Klann E, Angiolieri MR, Johnson JW, DeFranco DB. 2000. Persistent activation of ERK contributes to glutamate-induced oxidative toxicity in a neuronal cell line and primary cortical neuron cultures. J Biol Chem 275:12200–12206.

Ugarte SD, Lin E, Klann E, Zigmond MJ and Perez RG. 2003. Effects of GDNF on 6-OHDA-induced death in a dopaminergic cell line: Modulation by inhibitors of PI3 kinase and MEK. J Neurosci Res 73:105–112.

Watson FL, Heerssen HM, Bhattacharyya A, Klesse L, Lin MZ, Segal RA. 2001. Neurotrophins use the Erk5 pathway to mediate a retrograde survival response. Nat Neurosci 4:981–988.

Xia Z, Dickens M, Raingeaud J, Davis RJ, Greenberg ME. 1995. Opposing effects of ERK and JNK-p38 MAP kinases on apoptosis. Science 270:1326–1331.

Yuan LL, Chen X, Kunjilwar K, Pfaffinger P, Johnston D. 2006. Acceleration of K+ channel inactivation by MEK inhibitor U0126. Am J Physiol Cell Physiol 290:C165–C171.

Zigmond MJ, Keefe K. 1997. 6-Hydroxydopamine as a tool for studying catecholamines in adult animals: lessons from the neostriatum. In: Kostrzewa R, editor. Highly selective neurotoxins: basic and clinical applications. Totowa, NJ: Humana Press. p 75–108.

Journal of Neuroscience Research 86:2039–2049 (2008)

Activation of the Extracellular Signal-Regulated Kinases 1 and 2 by Glial Cell Line-Derived Neurotrophic Factor and Its Relation to Neuroprotection in a Mouse Model of Parkinson's Disease

Niklas Lindgren, Rehana K. Leak, Kirsten M. Carlson, Amanda D. Smith, and Michael J. Zigmond*

Pittsburgh Institute for Neurodegenerative Diseases, University of Pittsburgh, Pittsburgh, Pennsylvania

Glial cell line-derived neurotrophic factor (GDNF) has been shown to be neuroprotective in animal models of the dopamine deficiency in Parkinson's disease. To examine the role of the extracellular signal-regulated kinases 1 and 2 (ERK1/2) in this process, we infused a single dose of GDNF into the striatum of mice and analyzed the effect on ERK1/2 by immunohistochemistry and Western blot analysis. GDNF caused an increase in the phosphorylation of ERK1/2 both in the striatum and in tyrosine hydroxylase-positive neurons in the substantia nigra. In the striatum, the increase in ERK1/2 phosphorylation was evident by 3 hr and persisted for at least 7 days, whereas, in the substantia nigra, an increase in phosphorylated ERK1/2 was first evident at 24 hr and persisted for at least 7 days. The increase in phosphorylated ERK1/2 was maximal at 0.45 μg GDNF at the time points examined. GDNF also protected dopamine terminals against the loss of tyrosine hydroxylase immunoreactivity normally associated with the intrastriatal administration of 6-hydroxydopamine (0.5 μg/0.5 μl). However, this was observed only at a much higher dose of GDNF, 4.5 μg. Thus, our results suggest that the ability of GDNF to protect dopamine neurons cannot be explained solely in terms of its influence on ERK1/2 and that the role of other signaling pathways should be explored.

Key words: Akt; 6-hydroxydopamine; dopamine; GRFα1; neuroprotection; neurotrophic factors; striatum; RET

Since the discovery of glial cell line-derived neurotrophic factor (GDNF; Lin et al., 1993), there have been high expectations for its neuroprotective potential, particularly with regard to Parkinson's disease (PD; Bohn, 1999; Kirik et al., 2004). Although clinical observations have been mixed (Sherer et al., 2006), we and others believe that trophic factors such as GDNF represent a promising avenue for the development of therapeutic interventions. Indeed, in addition to positive clinical findings (Patel et al., 2005; Slevin et al., 2005), numerous studies using in vitro (Hou et al., 1996; Nicole et al., 2001; Ugarte et al., 2003; Ding et al., 2004) and in vivo models of PD (Hoffer et al., 1994; Kearns and Gash, 1995; Tomac et al., 1995; Gash et al., 1996; Winkler et al., 1996; Choi-Lundberg et al., 1997; Akerud et al., 2001) have shown that GDNF can protect dopamine (DA) neurons against toxic insults and can even have restorative effects (Love et al., 2005).

GDNF is generally believed to exert its biological effects through its coreceptor complex, GFRα1 and RET (Jing et al., 1996; Treanor et al., 1996; Cacalano et al., 1998), and the mRNAs for these proteins are present within the substantia nigra (SN; Trupp et al., 1996; Golden et al., 1998; Smith et al., 2003). Most of what we know about the intracellular mechanism of action of GDNF comes from in vitro studies, which have focused mainly on the extracellular signal-regulated kinases 1 and 2 (ERK1/2). For example, ERK1/2 appears to mediate the neuritic outgrowth induced by GDNF (Chen et al., 2001; Wiklund et al., 2002; Garcia-Martinez et al., 2006),

The last two authors contributed equally to this work.

Contract grant sponsor: National Institute of Neurological Disorders and Stroke; Contract grant number: NS19608 (to M.J.Z., A.D.S.); Contract grant number: NS45698 (to M.J.Z., A.D.S.); Contract grant sponsor: U.S. Army; Contract grant number: ERMS 03281022 (to M.J.Z., A.D.S.); Contract grant sponsor: Michael J. Fox Foundation (to R.K.L.); Contract grant sponsor: American Parkinson's Disease Association (to N.L.); Contract grant sponsor: Swedish Society for Medical Research (Svenska sällskapet för Medicinsk Forskning; to N.L.); Contract grant sponsor: NIH; Contract grant number: NS45698 (to A.D.S.).

*Correspondence to: Michael J. Zigmond, PhD, Pittsburgh Institute for Neurological Diseases, 3501 Fifth Avenue, 7016 Biomedical Science Tower 3, University of Pittsburgh, Pittsburgh, PA 15261.
E-mail: zigmond@pitt.edu

Received 8 August 2007; Revised 30 November 2007; Accepted 7 December 2007

Published online 25 April 2008 in Wiley InterScience (www.interscience.wiley.com). DOI: 10.1002/jnr.21641

and ERK1/2 also is involved in some of the neuroprotective effects of GDNF according to studies from our group (Ugarte et al., 2003) and others (Nicole et al., 2001; Onyango et al., 2005). However, little is known about the signaling mechanisms underlying the neuroprotective effects of GDNF in animal models.

Salvatore and coworkers (2004) observed that an intrastriatal infusion of GDNF caused a 55% increase in phospho-ERK2 (pERK2) in the striatum and a 26% increase in pERK1 in the SN at 4 weeks postinfusion. However, in their study, as in most studies that examine the neuroprotective potential of the GDNF protein, high concentrations of GDNF were used (10 μg or more; Hoffer et al., 1994; Kearns and Gash, 1995; Tomac et al., 1995; Winkler et al., 1996; Lapchak et al., 1996; Salvatore et al., 2004). These microgram amounts of GDNF can be assumed to yield local concentrations of GDNF in the micromolar range (see Discussion) and are in contrast to in vitro experiments showing high-affinity binding of GDNF to GFRα1/RET in the nanomolar to picomolar range (Jing et al., 1996; Treanor et al., 1996; Sanicola et al., 1997; Trupp et al., 1998). Thus, the goal of the present study was to characterize the effect of GDNF on pERK1/2 as a function of trophic factor concentration and then to relate that concentration to the neuroprotective effects of GDNF against 6-hydroxydopamine (6-OHDA). A portion of these results was presented at the annual meeting of Society for Neuroscience (2005 and 2006) and the Dopamine 50 Years Symposium (May, 2007).

MATERIALS AND METHODS

All reagents were purchased from Sigma-Aldrich (St. Louis, MO) unless indicated otherwise and were of the highest available purity. GDNF and its vehicle were kindly provided by Amgen (Thousand Oaks, CA), and 6-OHDA was obtained from Regis Technologies (Morton Grove, IL).

Animals

We used male C57BL/6 mice (Hilltop Lab Animals Inc., Scottdale, PA) weighing 25 g at 2 months of age. The animals were housed in groups of four in clear Plexiglas cages containing Aspen Sani-Chip bedding (P.J. Murphy Forest Products Corp., Montvillem, NJ), maintained on a 12-hr light/dark cycle and given irradiated Purina rodent chow (TR LAST, Gibsonia, PA) and water ad libitum.

Dose-Response and Temporal Analysis of GDNF Effects on pERK1/2

For the dose-response and temporal analysis experiments, animals (n = 4–10 animals/group in each experiment) were anesthetized with Equithesin (25 mg/kg pentobarbital, P3761, and 150 mg/kg chloral hydrate C8383; Sigma-Aldrich) and placed in a Kopf stereotaxic apparatus (David Kopf Instruments, Tujunga, CA) with a Cunningham mouse adaptor (Stoelting, Wood Dale, IL). GDNF was infused unilaterally (0.1 μl/min) into the striatum (0.8 mm posterior and 2.0 mm lateral to bregma and 3.5 mm ventral to the flat skull) using a Hamilton syringe (Hamilton Company, Reno, NV) in accordance with a stereotaxic mouse brain atlas (Paxinos and Franklin, 1997). Concentrations of GDNF were varied within a fixed volume of 1.5 μl vehicle (citrate buffer, pH 7.2; provided by Amgen). The syringe was left in place for 5 min after the infusion was terminated to allow for diffusion into tissue and to minimize leakage up the needle track. Control animals received injections of vehicle only. Animals were killed by perfusion (for immunohistochemical analysis) or microwave irradiation (for Western blot) at one of up to four different time points after surgery, 3 hr, 24 hr, 7 days, or 4 weeks. In the dose-response study, animals were injected with 0.0045–4.5 μg of GDNF and killed by perfusion (for immunohistochemical analysis) 24 hr later.

GDNF Protection Against 6-OHDA

Animals (6 animals/group) were anesthetized with isoflurane on a gas anesthesia platform (Stoelting), mounted in a Kopf stereotaxic apparatus with a Cunningham mouse adaptor. GDNF (0.1 μl/min) or vehicle was infused into the striatum in a fixed volume of 1.5 μl at one of two different concentrations (0.45 and 4.5 μg) at the same coordinates as described above. Six hours later, 6-OHDA (0.5 μg/0.5 μl at 0.1 μl/min) or 2 mg/ml ascorbic acid in saline was infused in the striatum at the same site as the GDNF infusion. The animals were killed by perfusion 4 weeks after surgery.

Immunohistochemical Analysis

Animals were deeply anesthetized with Equithesin and perfused through the heart with 10 ml of 0.1 M phosphate buffer (pH 7.2) containing 1.0 mM sodium fluoride (a phosphatase inhibitor to stabilize phosphokinases) and 1.0% sodium nitrate (a vasodilator), followed by 20 ml of 4% formaldehyde containing 1.0 mM sodium fluoride. The brain was removed and postfixed in the same solution for 12 hr at 4°C. This was followed by cryoprotection in 30% sucrose in 0.1 M phosphate buffer (pH 7.2) for 48 hr at 4°C. Sections were cut at 40 μm in the coronal plane on a freezing microtome from the front of the striatum to the end of the retrorubral field. Unless otherwise noted, every sixth section was analyzed for a given antibody.

All reagents for immunohistochemistry were diluted in 0.01 M phosphate-buffered saline (PBS; pH 7.6), which was also used for washes between incubations unless specified otherwise. Sections were pretreated with 0.5% sodium borohydride and 0.1% hydrogen peroxide for 15 min each, with several changes of buffer between the pretreatments. As a blocking step, sections were then incubated in 10% normal donkey serum (Jackson Immunoresearch, West Grove, PA) and 0.3% Triton X-100 for 1–2 hr at room temperature on a rotator. This was followed by incubation in primary antibody diluted in 1% normal donkey serum and 0.3% Triton X-100 overnight on a rotator at 4°C. The primary antibodies used were rabbit polyclonal anti-pERK1/2 (Thr202/Tyr204; 1:200; Cell Signaling, Danvers, MA; catalog No. 9101), polyclonal anti-GDNF (1:1,000; R&D Systems, Minneapolis, MN; catalog No. AF-212-Na), and monoclonal anti-tyrosine hydroxylase (TH; 1:1,000; Chemicon International, Temecula, CA; cata-

log No. MAB318). Sections were then exposed to appropriate biotinylated secondary antibodies (Jackson Immunoresearch; 1:200) in the same diluent for 90–120 min on a rotator at room temperature, which was followed by exposure to Vectastain Elite avidin-biotin reagents (Vector, Burlingame, CA) with 0.3% Triton X under the same conditions. After a 10-min preincubation in diaminobenzidine (20 mg in 100 ml Tris buffer, pH 7.2), hydrogen peroxide was added to begin the peroxidase reaction (final dilution 0.01%) and terminated by buffer washes within 10 min. The free-floating sections were mounted and allowed to dry overnight at room temperature. The sections were then exposed to a 0.04% solution of osmium tetroxide (for stabilization of the diaminobenzidine signal against photobleaching) in 0.1 M phosphate buffer for 3–5 sec, washed, dehydrated in a graded series of ethanols, cleared in xylenes, and coverslipped with Permount (Fisher Scientific, Pittsburgh, PA).

Double-Label Immunofluorescence

To determine the extent of pERK1/2 expression in DA neurons, we used double-immunofluorescent labeling with rabbit anti-pERK1/2 (1:150) and mouse anti-TH (1:2,000) in 10 mM PBS with 1% normal donkey serum, 1% normal goat serum, and 0.3% Triton X-100, after a blocking step in 10% normal donkey and 10% normal goat serum. Sections were subsequently labeled with Alexa Fluor 488 (goat anti-mouse) and Alexa Fluor 555 (donkey anti-rabbit) at concentrations of 1:500 each (Molecular Probes, Invitrogen, Carlsbad, CA) in PBS with 0.3% Triton X-100 for 2 hr at room temperature, washed, mounted, coverslipped, and viewed with confocal microscopy for double- or single-labeled profiles (FluoView FV1000; Olympus, Center Valley, PA). All sections were stained at the same time and imaged with the same confocal settings. Omitting either primary antibody (TH or pERK1/2) from these steps resulted in loss of fluorescent signal.

Western Blot Analysis

To maintain in vivo levels of phosphorylation in the brains in post-mortem samples, animals were killed using a TMW-6402C system (Muromachi Kikai Tokyo, Japan), composed of a microwave power generator and applicator unit specialized to restrain a mouse and direct the microwave beam to the head. The animals (n = 8–9/group) were exposed to 4.75 kW of radiation for 1.17 sec to inactivate enzymes that might otherwise dephosphorylate the kinases (O'Callaghan and Sriram, 2004). The striata were then dissected out on an ice-cooled surface, frozen on dry ice, and stored at –80°C. Thawed tissue samples were sonicated in 500 µl of 1% sodium dodecyl sulfate and boiled for 10 min. Aliquots (12.5 µl) of the homogenate were used for protein content determinations. Equal amounts of protein from each sample were loaded onto 10% polyacrylamide gels, and the proteins were separated by sodium dodecyl sulfate-polyacrylamide gel electrophoresis and transferred to polyvinylidine difluoride membranes (Bio-Rad, Hercules, CA). The membranes were probed using polyclonal antibodies that selectively detect pERK1/2 (Thr202/Tyr204; 1:3,000; Cell Signaling; catalog No. 9101) and total ERK1/2 proteins (1:1,000; Cell Signaling; catalog No. 9102). Antibody binding was revealed by incubation with goat anti-rabbit horseradish peroxidase-linked IgG (1:10,000; Calbiochem, San Diego, CA) and the Western Lightning immunoblotting detection method (Perkin Elmer, Boston, MA) on X-ray film (Kodak Bio-Max MR). Quantification of optical density of the bands corresponding to the pERK1/2, total-ERK1/2 bands was done in UnScanIt software (Silk Scientific, Orem, UT).

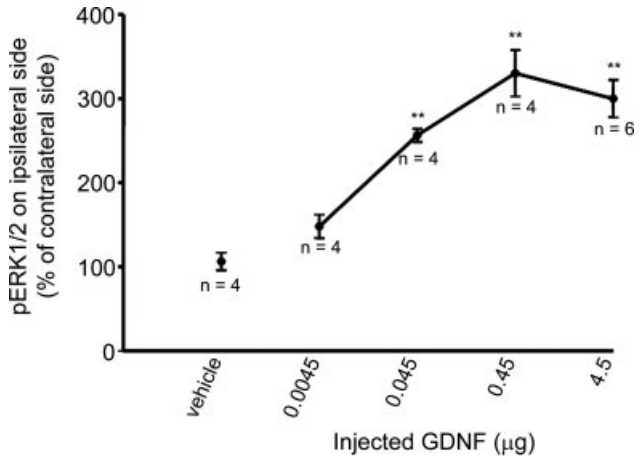

Fig. 1. Effect of intrastriatal GDNF on striatal pERK1/2 as a function of GDNF dose. GDNF was infused into the striatum. Twenty-four hours later, the animals were perfused and brain sections were labeled with anti-pERK1/2. The labeled sections were then scanned and quantified using Metamorph software. The immunoreactivity is expressed as percentage of the noninjected contralateral side for all data points, including vehicle (n = 4–6 animals). Data are mean ± SEM. $^{**}P < 0.01$ vs. vehicle, ANOVA followed by Dunnett's test.

Data and Statistical Analysis

The immunohistological sections were photographed with a Nikon Supercool 9000 scanner (Nikon Inc., Melville, NY) and analyzed in blind fashion in MetaMorph software (Molecular Devices, Sunnyvale, CA). Data were calculated as the average optical density in three sections centered around the needle track. The optical density of the infused striatum was expressed as a percentage of the contralateral striatum, with immunoreactivity in the overlying sensory cortex used for background subtraction. This effectively controlled for minor variability in immunohistochemical staining between runs. The TIFF images (Fig. 3) were pseudocolored in MetaMorph.

The statistical analyses were performed in Prism 3.03 (GraphPad Software, San Diego, CA), using one-way ANOVA, followed by Dunnett's or Newman-Keuls tests. Results were deemed significant at $P < 0.05$.

RESULTS

Effects of Intrastriatal GDNF on Striatal pERK1/2

GDNF was infused into the striatum, and striatal pERK1/2 was analyzed by immunohistochemistry at 24 hr (Fig. 1). GDNF caused a unilateral dose-dependent increase in the phosphorylation of ERK1/2 in the stria-

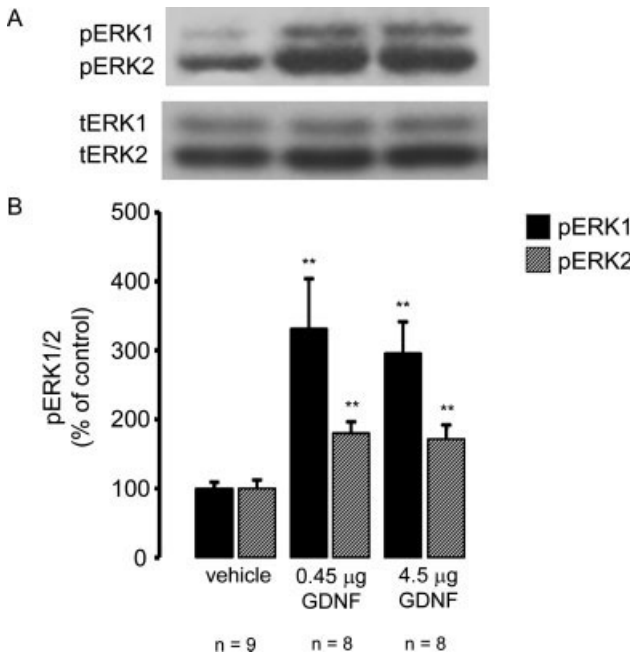

Fig. 2. Effect of intrastriatal GDNF on striatal pERK1/2 as measured by Western blot analysis. Animals received vehicle, 0.45 μg GDNF, or 4.5 μg GDNF into the striatum. After 24 hr, the animals were killed by focused microwave irradiation. Samples were labeled with antibodies to pERK1/2 and total ERK1/2. **A:** Representative blots of pERK1/2 (top) and total ERK1/2 protein levels (bottom). **B:** Quantification of Western blot. The pERK1/2 values are divided by the levels of total ERK1/2 protein in each sample and expressed as percentage of control (n = 8–9 animals). Data are mean ± SEM. $^{**}P < 0.01$ vs. vehicle, ANOVA followed by Newman-Keuls test.

tum that was significant at 0.045 μg GDNF and peaked at 0.45 μg, reaching 330% of vehicle control. At 4.5 μg GDNF, the rise in ERK1/2 phosphorylation appeared to decrease slightly from the effect at 0.45 μg. However, this decrease was not significant. There was no observable effect in the striatum on the contralateral side to the injection in any of the animals.

Effect of High- and Low-Dose of GDNF on pERK1/2 Analyzed Via Western Blot

To validate the data obtained by immunohistochemistry, two doses of GDNF and saline were chosen for analysis by Western blotting. Animals were given intrastriatal GDNF (0.45 or 4.5 μg) or vehicle and killed by microwave irradiation 24 hr after surgery to inactivate protein phosphatases rapidly. Lysates were then prepared and analyzed by Western blotting. In the animals injected with 0.45 μg GDNF, pERK1 in the ipsilateral striatum increased to 331% above that in saline-injected animals, and pERK2 increased to 180%. Comparable results were obtained with 4.5 μg GDNF (Fig. 2). Samples from the contralateral striatum were also analyzed, and the results indicated that GDNF did not produce any change in the level of pERK1/2 on this side of the brain (data not shown).

Temporal Effects of High- and Low-Dose GDNF on pERK1/2

The increase in pERK1/2 caused by the intrastriatal infusion of 0.45 μg GDNF was detectable in the ipsilateral striatum by 3 hr ($P < 0.01$) using immunohistochemistry. The increase reached 420% above control by 7 days, but the level was back to basal by 4 weeks (Fig. 3). Infusion of 4.5 μg GDNF (Fig. 3A) also caused a time-dependent increase in pERK1/2 that actually appeared slightly lower than the effect of 0.45 μg GDNF, although the difference was not significant. Seven days after administration of 4.5 μg GDNF, there was a small region of down-regulation of ERK1/2 phosphorylation around the needle track with a surrounding halo of increased pERK1/2 (Fig. 3B).

Intrastriatal GDNF also increased pERK1/2 in SN, although the effects were delayed relative to the effects in the striatum, insofar as we did not observe any nigral ERK1/2 phosphorylation 3 hr after the injection (data not shown). At 24 hr, pERK1/2-labeled SN neurons appeared ipsilateral to the striatal infusion in all animals (Fig. 4A). No such effect was detected in any animals infused with vehicle (Fig. 4A). Phosphorylation persisted for at least 7 days and was confined to TH-positive cells as shown by immunofluorescent double labeling (Fig. 4B). Vehicle-injected animals showed no pERK1/2 immunolabeling within TH-positive profiles. Similarly, the contralateral nigra had TH-positive profiles without any detectable pERK1/2 signal (shown for the same animal as in upper panels of Fig. 4B, using the same confocal settings). Omission of primary antibody also resulted in loss of pERK1/2 signal. Finally, at 4 weeks, the level of nigral phosphorylation was back to basal, undetectable levels (data not shown).

It was possible that the total amount of ERK1/2 might be altered by GDNF at one or more of the time points examined and thereby partially obscure the real effect on the levels of pERK1/2. Therefore, animals were injected with 0.45 or 4.5 μg GDNF, and total ERK1/2 was assessed by Western blotting. Neither of the doses altered the levels of ERK1/2 proteins at any time examined (data not shown).

Diffusion of GDNF Into Striatum

Three hours after administration of 0.45 μg GDNF, diffusion of GDNF immunoreactivity was limited to the vicinity of the needle track (Fig. 5), whereas the effect of 4.5 μg of GDNF was more widespread. By 24 hr, GDNF immunoreactivity was found throughout the ipsilateral striatum, with spillover into cortex. GDNF immunoreactivity remained high in the striatum at 7 days, albeit at a level that was considerably less than that at 24 hr. At 7 days after 4.5 μg GDNF infusion, GDNF immunoreactivity was lower than that at 24 hr but markedly higher than the effect of 0.45 μg GDNF after 7 days. Four weeks after infusion of either dose, immunoreactivity remained

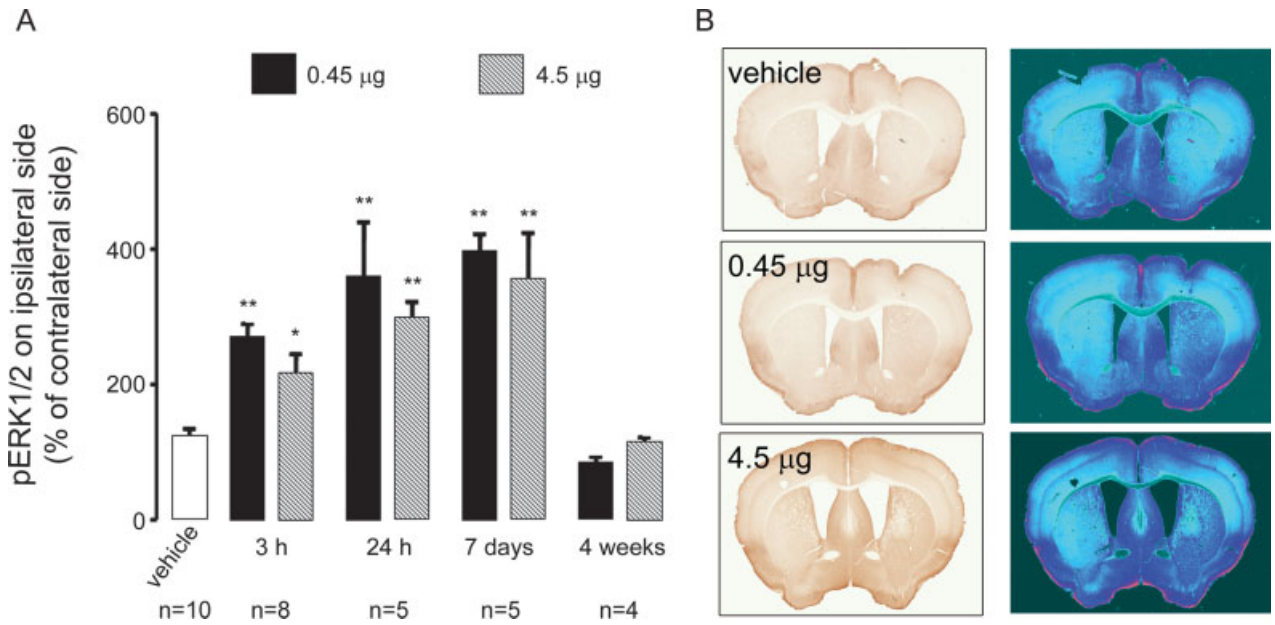

Fig. 3. Effect of intrastriatal GDNF on striatal pERK1/2 as a function of time. Animals received vehicle, 0.45 µg GDNF, or 4.5 µg GDNF into the striatum. After 3 hr, 24 hr, 7 days, or 4 weeks, the animals were perfused and brain sections were labeled with anti-pERK1/2. **A:** The labeled sections were scanned and quantified in Metamorph software. The measured immunoreactivity in the ipsilateral striatum is expressed as a percentage of the noninjected contralateral striatum in all animals, including vehicle controls (n = 4–10 animals). Data are mean ± SEM. $*P < 0.05$, $**P < 0.01$ vs. vehicle, ANOVA followed by Dunnett's test. **B:** Representative slides of a vehicle-injected animal (top), an animal injected with 0.45 µg GDNF (middle), and an animal injected with 4.5 µg GDNF (bottom) on the right side in the picture, sacrificed 7 days after the injection. The slides to the left are unaltered scanned images, whereas the images on the right were modified in Metamorph software to visualize intensity differences.

only around the needle track. The diffusion sphere of GDNF did not reach the midbrain at either dose. However, light anterograde labeling was observed ipsilaterally in the SN pars reticulata at 24 hr (data not shown), as has previously been reported after up-regulation of GDNF in the striatum by lentiviral vectors (Georgievska et al., 2004).

Effect of High- and Low-Dose GDNF on Toxicity Induced by 6-OHDA

Mice injected with vehicle or either 0.45 µg or 4.5 µg GDNF received 6-OHDA (0.5 µg) into the striatum 6 hr later. After 4 weeks, the mice were killed, and the presence of DA terminals in the striatum was analyzed by immunohistochemistry for TH, a marker for these neurons. 6-OHDA by itself caused a large loss of TH immunoreactivity at the site of toxin injection (Fig. 6). Injection of 4.5 µg GDNF reduced the 6-OHDA-induced loss of TH immunoreactivity by 75%. In contrast, 0.45 µg GDNF did not have any apparent effect on the 6-OHDA-induced TH loss (Fig. 6).

DISCUSSION

GDNF and Neuroprotection

Previous studies of neuroprotection by GDNF in 6-OHDA models have involved microgram to high-milligram amounts of GDNF, and this apparent need for high doses of GDNF was supported by our results. With our neuroprotective dose of 4.5 µg (~100 pmoles), the maximal diffusion we observed had a diameter of about 4 mm and thus a volume of ~35 µl. From this we infer that the neuroprotective concentration would be in the low micromolar range (0.1 µmole in 35 µl). Obviously, such a calculation is very rough; nonetheless, it does contrast sharply with the Kd derived from in vitro studies, which is in the picomolar to nanomolar range (Jing et al., 1996; Treanor et al., 1996; Sanicola et al., 1997; Trupp et al., 1998).

If it is true that GDNF is neuroprotective only at relatively high doses, this would have obvious clinical implications. Indeed, it has recently been suggested that the mixed clinical observations with the effects of GDNF in patients with PD may result from differences in the available concentrations of the trophic factor resulting from differences in delivery methods and consequent differences in diffusion (Salvatore et al., 2006). Our results also raise questions about the mechanism of action of the neurotrophic factor.

It is, of course, possible that the discrepancy between the neuroprotective dose of GDNF in animal models and the affinity of the trophic factor for its preferred receptor results from the failure of dissociated cells to reflect the in vivo affinity of the GDNF receptor complex for its ligand. However, it seems equally plausible that there are targets other than or in addition to the

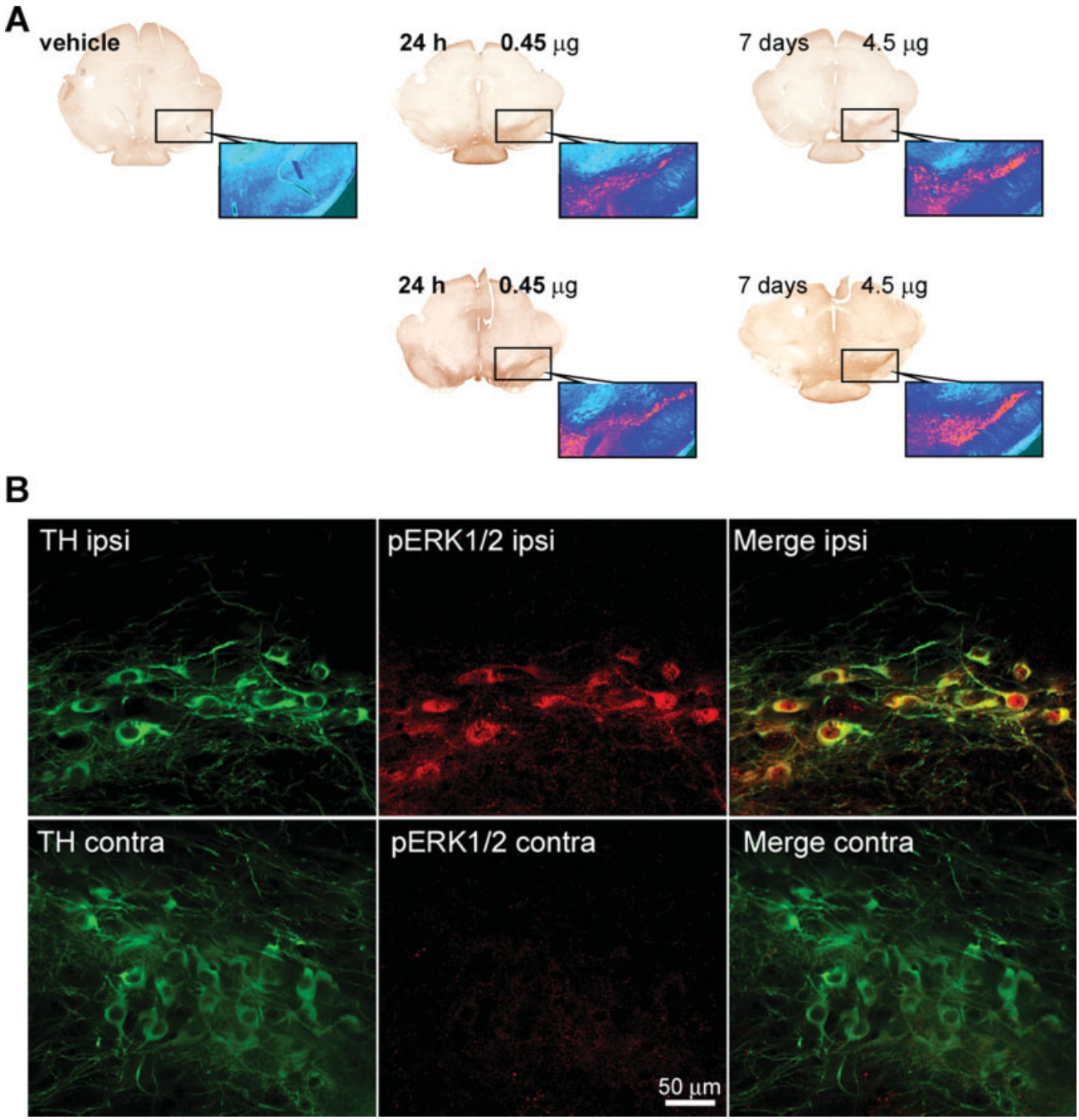

Fig. 4. Effect of intrastriatal GDNF on nigral pERK1/2. Animals received vehicle, 0.45 μg GDNF, or 4.5 μg GDNF into the striatum. After 3 hr (not shown), 24 hr, or 7 days, the animals were perfused (n = 4–8 animals). **A:** Sections were labeled with anti-pERK1/2. Representative sections are shown. The regions of magnification were modified in Metamorph software to visualize intensity differences. **B:** Nigral sections were double labeled for pERK1/2 (rabbit Ab) and TH (mouse Ab) and then incubated with Alexa Fluor 488 (goat anti-mouse) and Alexa Fluor 555 (donkey anti-rabbit) and viewed by confocal microscopy. In the ipsilateral SN, the vast majority of TH cells were dually labeled, whereas no pERK1/2 staining was observed in the contralateral SN 24 hr following an injection of 0.45 μg of GDNF into the striatum.

GFRα1-RET complex that have much lower affinity for GDNF and are involved in neuroprotection. The most likely alternative through which GDNF might exert its neuroprotective actions would be GFRα2, to which GDNF has been previously shown to bind (Baloh et al., 1997, 1998; Jing et al., 1997; Klein et al., 1997). GFRα2 as well as GFRα3 is expressed at low levels in the basal ganglia compared with GFRα1 (Trupp et al., 1998), and suboptimal ligand–receptor pairs can mediate RET signaling (Sanicola et al., 1997; Trupp et al., 1998; Eketjall

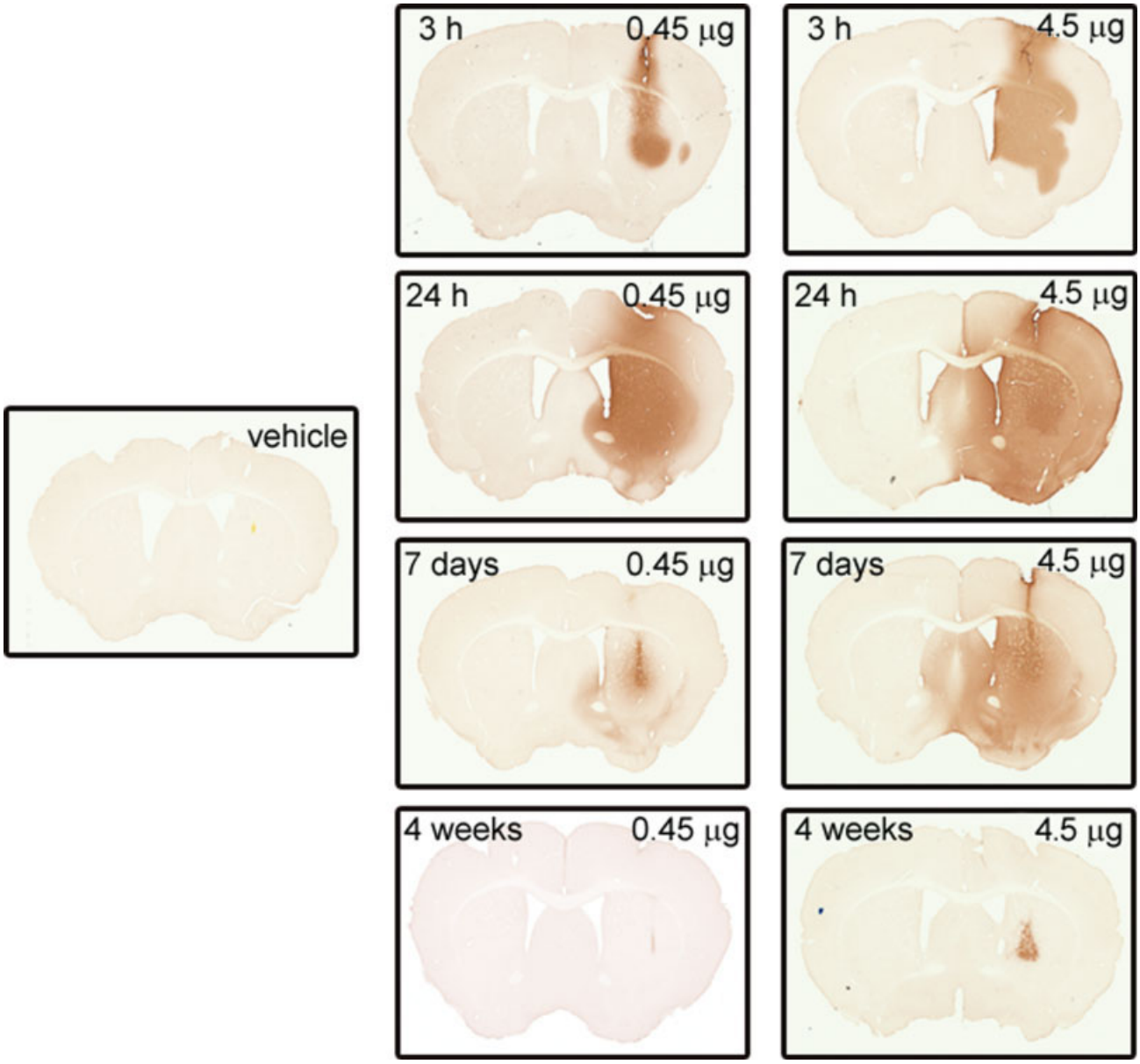

Fig. 5. Diffusion of GDNF after intrastriatal administration as a function of time. Animals were intrastriatally infused with saline or 0.45 μg or 4.5 μg of GDNF and then perfused 24 hr after injection. After 3 hr, 24 hr, 7 days, or 4 weeks, the animals were perfused, and brain sections were labeled with an antibody against GDNF. [Color figure can be viewed in the online issue, which is available at www.interscience.wiley.com.]

et al., 1999; Scott and Ibanez, 2001). Another option would be GFRα signaling without RET, which also has been reported (Poteryaev et al., 1999; Trupp et al., 1999).

ERK Phosphorylation and Its Role in Neuroprotection

A second issue raised by our results is the intracellular mechanism of the protective effects of GDNF; our findings suggest that neuroprotection by the neurotrophic factor is unlikely to be explained in terms of this increased pERK1/2 alone. This is because the level of pERK1/2 observed following a protective dose of GDNF (4.5 μg) was not higher than that observed with a nonprotective dose (0.45 μg) at any of the times examined. Furthermore, the protective 4.5-μg dose caused a sphere of down-regulated ERK1/2 phosphorylation around the injection site after 7 days, which was not present after administration of 0.45 μg GDNF. However, despite down-regulation of ERK1/2, there was still neuroprotec-

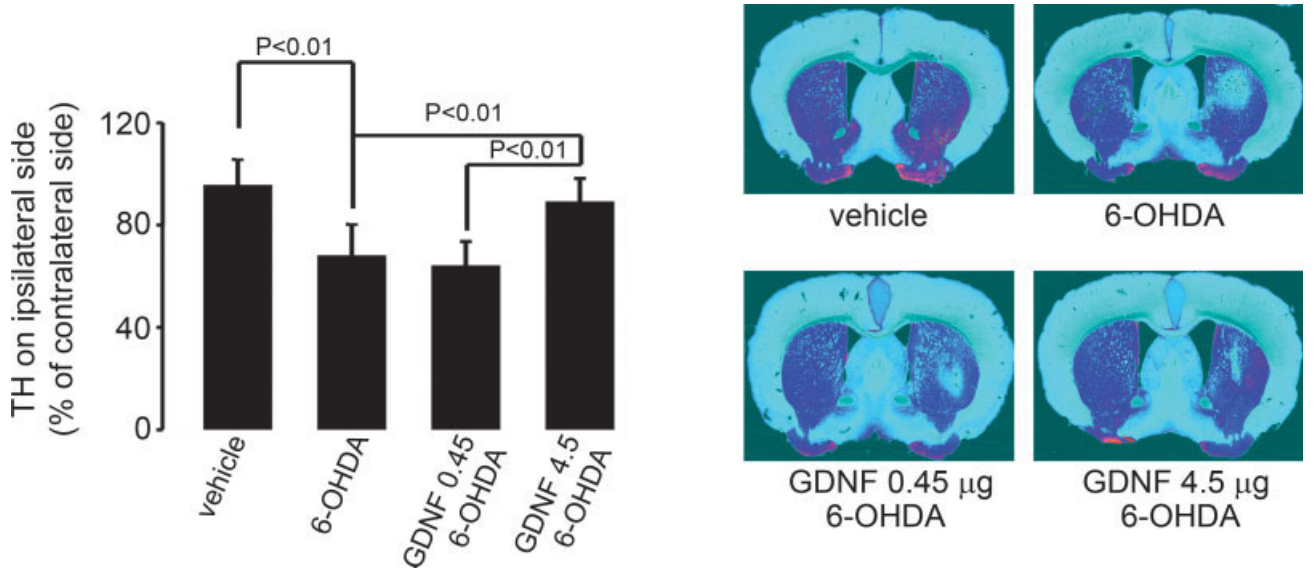

Fig. 6. Effect of GDNF on the loss of tyrosine hydroxylase induced by 6-OHDA. Animals received vehicle or 0.45 μg or 4.5 μg of GDNF into the striatum. Six hours later, 6-OHDA (0.5 μg/0.5 μl at 0.1 μl/min) or saline was infused in the striatum at the same site as the GDNF infusion. After 4 weeks, the animals were perfused and brain sections were labeled with an antibody to TH. Sections were then scanned and quantified in Metamorph software. The measured immunoreactivity in the ipsilateral striatum is expressed as a percentage of that in the noninjected contralateral striatum in all animals, including vehicle controls (n = 6 animals). Data are mean ± SEM values. $P < 0.01$ vs. vehicle, ANOVA followed by Newman-Keuls test. [Color figure can be viewed in the online issue, which is available at www.interscience.wiley.com.]

tion of DA terminals in the vicinity of the cannula track. This is further evidence supporting the hypothesis that the protection by GDNF of DA cannot be fully explained by increased pERK1/2 levels.

Some recent studies conducted in vitro support the conclusion that GDNF-induced neuroprotection involves factors other than enhanced ERK1/2 phosphorylation. Soler and colleagues (1999) showed that the neurotrophic effect exerted by GDNF on cultured motor neurons was not mediated via MEK1/2 activation and subsequent ERK1/2 phosphorylation. The same result has been obtained on cytoplasmic hybrid cells made of mitochondrial DNA from PD patients exposed to hydrogen peroxide (Onyango et al., 2005) and enteric neurons exposed to hyperglycemia (Anitha et al., 2006).

Of course, we cannot rule out the possibility that the *localization* of the pERK1/2 produced by GDNF is dose dependent. For example, 4.5 μg GDNF may result in an increase in pERK1/2 in different DA cells or a different cellular compartment of those cells from 0.45 μg GDNF. Although studies are underway to examine this possibility, we are unaware of any literature to support such an explanation. It is also possible that the temporal kinetics of the changes in pERK caused by 0.45 and 4.5 μg GDNF are different in a manner that is not reflected at the times we have selected for our analysis. For example, 4.5 μg GDNF may cause a higher maximum between 24 hr and 7 days or a longer period of elevation between 7 days and 4 weeks; if so, this would not have been observed in our study. In any event, it is also important to note that this study does not rule out the possibility that increased levels of ERK1/2 phosphorylation are still essential for neuroprotection, showing only that the increase in pERK1/2 in nigrostriatal DAergic neurons is not sufficient by itself.

Additional Insights Into the Signaling Underlying GDNF Protection

We have made two observations in preliminary studies that are consistent with the assumption that conventional cascades involving ERK1/2 are insufficient to explain GDNF-induced neuroprotection against 6-OHDA. First, whereas the MEK inhibitor SL-327 (100 mg/kg, i.p.) abolished the increase in pERK1/2 produced by the lower dose of GDNF (0.45 μg), it did not block the increased pERK1/2 produced by the higher, protective GDNF dose (4.5 μg) on pERK1/2. These results were surprising to us and might reflect a shift in the intracellular route by which GDNF activates pERK1/2. It also demonstrates that, in future projects in which the role of ERK1/2 is evaluated by inhibiting this signaling pathway, means other than pharmacological blockers of MEK1/2 will probably be needed.

The proposal that the Ras/ERK pathway is insufficient to explain GDNF-induced protection of DA neurons is further supported by a second preliminary observation. We have found that, whereas the low, nonprotective dose of GDNF (0.45 μg) does not phosphorylate Akt, the high protective dose of GDNF (4.5 μg) does cause a large increase in this phosphokinase in the striatum. This raises the new possibility of a causal connection between Akt

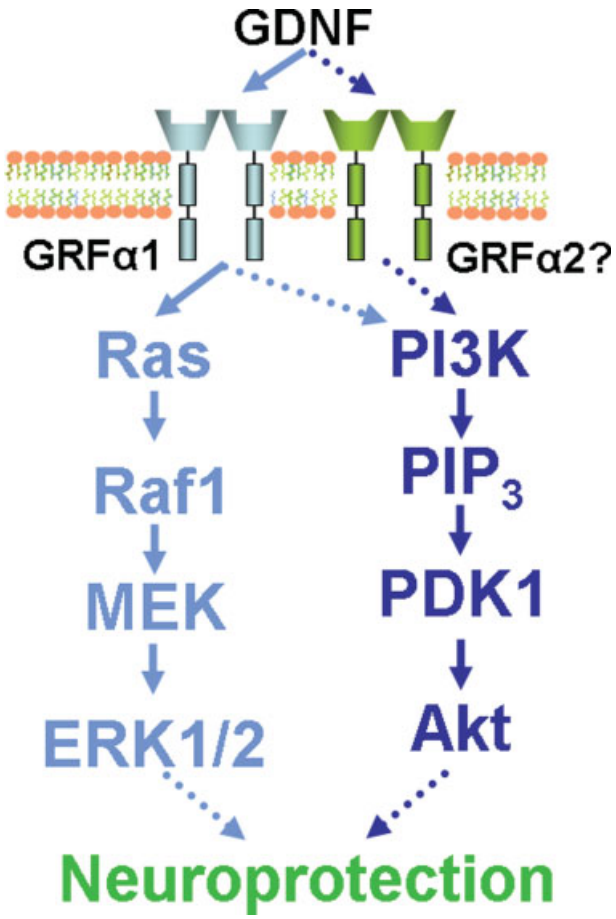

Fig. 7. A working model for the action of GDNF and its neuroprotection against oxidative stress. The solid arrows to the left represent the classical hypothesis in which GDNF protects neurons via the MAPK pathway. The dotted arrows are hypotheses presented in this paper. In particular, we are proposing that GDNF can 1) act through a mechanism that involves a receptor complex other than the conventional GRFα1/RET complex and 2) exert its neuroprotective effect at least in part via a second signaling pathway, such as the PI3K/Akt cascade. [Color figure can be viewed in the online issue, which is available at www.interscience.wiley.com.]

phosphorylation and GDNF-induced neuroprotection, which is consistent with a growing body of data from in vitro experiments proposing that the neuroprotective properties of GDNF are mediated at least in part by the PI3K/Akt pathway (Soler et al., 1999; Ugarte et al., 2003; Onyango et al., 2005; Srinivasan et al., 2005; Anitha et al., 2006; Nakamura et al., 2006) and more recent studies showing that Akt can mediate neuroprotection in animal models of PD (Ries et al., 2006; Weinreb et al., 2007). We are currently exploring these issues.

Comparison of Immunohistochemistry and Western Blotting

In this study we have shown that the increases in pERK1/2 measured via immunohistochemical analysis provides results that are comparable to those obtained via Western blotting, even though the pERK antibody used does not distinguish between the p44 and p42 isoforms in immunohistochemistry. Although Western blotting is generally considered more quantitative than is immunohistochemistry, there are methodological advantages to using histochemical analysis. First, to maintain phosphorylation levels at close to pre-mortem levels, Western blot analysis demands either the approach that we have adopted—sacrifice by microwave (O'Callaghan and Sriram, 2004)—or a rapid dissection (Svenningsson et al., 2000). However, neither microwave nor rapid dissection appears necessary for immunohistochemical analysis; perfusion with a fluid that contains a phosphatase inhibitor is adequate. Second, it is likely that histochemical analysis is often a more sensitive approach, because it permits the detection of highly localized changes in pERK1/2. For example, the down-regulation of pERK1/2 we observed near the infusion needle would have been missed with Western blotting alone. Finally, as shown by our dual-immunofluorescence analysis, the cellular resolution afforded by immunohistochemistry allows one to measure signaling changes specific to dopaminergic cells, thereby yielding superior anatomical information lost in studies on crude homogenates. Thus, our observation that immunohistochemistry can provide a quantitative result comparable to that of Western blotting should be of general interest.

CONCLUSIONS AND FUTURE DIRECTIONS

Two major conclusions can be drawn from our results, each raising important questions. The amount of GDNF that was neuroprotective in our model of PD was extremely high relative to the reported affinity of the peptide for its classical receptor complex in vitro. This raises questions about the receptor through which GDNF exerts its neuroprotective influence or the relevance of these in vitro results to the in vivo condition. Second, there was no correlation between GDNF-induced activation of ERK1/2 and protection against the loss of TH immunoreactivity in the striatum by 6-OHDA, indicating that other signaling pathways may be involved, perhaps in conjunction with ERK1/2 or on their own. One candidate is the PI3K/Akt pathway. We have provided a model that outlines these proposals and provides a conceptual framework for our ongoing studies (Fig. 7).

ACKNOWLEDGMENTS

We thank Amgen, Inc. (Thousand Oaks, CA), for their gift of GDNF. We also thank Annie D. Cohen for helpful discussions, James P. O'Callaghan for advice on the application of microwave irradiation for the sacrifice of animals prior to Western blot analyses of kinases, and Susan D. Giegel for editorial assistance.

REFERENCES

Akerud P, Canals JM, Snyder EY, Arenas E. 2001. Neuroprotection through delivery of glial cell line-derived neurotrophic factor by neural stem cells in a mouse model of Parkinson's disease. J Neurosci 21:8108–8118.

Anitha M, Gondha C, Sutliff R, Parsadanian A, Mwangi S, Sitaramen SV, Srinivasan S. 2006. GDNF rescues hyperglycemia-induced diabetic enteric neuropathy through activation of the PI3K/Akt pathway. J Clin Invest 116:344–356.

Baloh RH, Tansey MG, Golden JP, Creedon DJ, Heuckeroth RO, Keck CL, Zimonjic DB, Popescu NC, Johnson EM, Mildbrant J. 1997. TrnR2, a novel receptor that mediates neurturin and GDNF signaling through Ret. Neuron 18:793–802.

Baloh RH, Tansey MG, Lampe PA, Fahrener TA, Enomoto H, Simburger KS, Leitner ML, Araki T, Johnson EM, Mildbrant J. 1998. Artemin, a novel member of the GDNF ligand family, supports peripheral and central neurons and signals through the GFRalpha3-RET receptor complex. Neuron 21:1291–1302.

Bohn MC. 1999. A commentary on glial cell line-derived neurotrophic factor (GDNF). From a glial secreted molecule to gene therapy. Biochem Pharmacol 57:35–142.

Cacalano G, Farinas I, Wang L-C, Hagler K, Forgie A, Moore M, Armanini M, Philips H, Ryan AM, Reichardt lF, Hynes M, Davies A, Rosenthal A. 1998. GFRalpha1 is an essential receptor component for GDNF in the developing nervous system and kidney. Neuron 21:53–62.

Chen Z-Y, Chai Y-F, Cao L, Lu C-L, He C. 2001. Glial cell line-derived neurotrophic factor enhances axonal regeneration following sciatic nerve transection in adult rats. Brain Res 902:272–276.

Choi-Lundberg DL, Lin Q, Chang YN, Chiang YL, Hay CM, Mohajeri H, Davidson BL, Bohn MC. 1997. Dopaminergic neurons protected from degeneration by GDNF gene therapy. Science 275:838–841.

Ding YM, Jaumotte JD, Signore AP, Zigmond MJ. 2004. Effects of 6-hydroxydopamine on primary cultures of substantia nigra: specific damage to dopamine neurons and the impact of glial cell line-derived neurotrophic factor. J Neurochem 89:776–787.

Eketjall S, Fainzilber M, Murray-Rust J, Ibanez CF. 1999. Distinct structural elements in GDNF mediate binding to GFRalpha1 and activation of the GFRalpha1-c-Ret receptor complex. EMBO J 18:5901–5910.

Garcia-Martinez JM, Pérez-Navarro E, Gavaldà N, Alberch J. 2006. Glial cell line-derived neurotrophic factor promotes the arborization of cultured striatal neurons through the p42/p44 mitogen-activated protein kinase pathway. J Neurosci Res 83:68–79.

Gash DM, Zhang Z, Ovadia A, Cass WA, Yi A, Simmerman L, Russell D, Martin D, Lapchak PA, Collins F, Hoffer BJ, Gerhardt GA. 1996. Functional recovery in parkinsonian monkeys treated with GDNF. Nature 380:252–255.

Georgievska B, Kirik D, Björklund A. 2004. Overexpression of glial cell line-derived neurotrophic factor using a lentiviral vector induces time- and dose-dependent downregulation of tyrosine hydroxylase in the intact nigrostriatal dopamine system. J Neurosci 24:6437–6445.

Golden JP, Baloh RH, Kotzbauer PT, Lampe PA, Osborne PA, Mildbrant J, Johnson EM. 1998. Expression of neurturin, GDNF, and their receptors in the adult mouse CNS. J Comp Neurol 398:139–150.

Hoffer BJ, Hoffman A, Bowenkamp K, Huettl P, Hudson J, Martin D, Lin LF, Zhang TJ, Collins F, Armes LG. 1994. Glial cell line-derived neurotrophic factor reverses toxin-induced injury to midbrain dopaminergic neurons in vivo. Neurosci Lett 182:107–111.

Hou JG, Lin L-FH, Mytilineou C. 1996. Glial cell line-derived neurotrophic factor exerts neurotrophic effects on dopaminergic neurons in vitro and protomotes their survival and regrowth after damage by 1-methyl-4-phenylpyridinium. J Neurochem 66:74–82.

Jing S, Wen D, Yu Y, Holst PL, Luo Y, Fang M, Tamir R, Antonio L, Hu Z, Cupples R, Louis J-C, Hu S, Altrock BW, Fox GM. 1996. GDNF-induced activation of the ret protein tyrosine kinase is mediated by GDNFR-alpha, a novel receptor for GDNF. Cell 85:1113–1124.

Jing S, Yu Y, Fang M, Hu Z, Holst PL, Boone T, Delaney J, Schultz H, Zhou R, Fox GM. 1997. GFRalpha-2 and GFRalpha-3 are two new receptors for ligands of the GDNF family. J Biol Chem 272:33111–33117.

Kearns CM, Gash DM. 1995. GDNF protects nigral dopamine neurons against 6-hydroxydopamine in vivo. Brain Res 672:104–111.

Kirik D, Georgievska B, Björklund A. 2004. Localized striatal delivery of GDNF as a treatment for Parkinson disease. Nat Neurosci 7:105–110.

Klein RD, Sherman D, Ho WH, Stone D, Bennett GL, Moffat B, Vandlen R, Simmons L, Gu Q, Hongo JA, Devaux B, Poulsen K, Armanini M, Nozaki C, Asai N, Goddard A, Phillips H, Henderson CE, Takahashi M, Rosenthal A. 1997. A GPI-linked protein that interacts with Ret to form a candidate neurturin receptor. Nature 387:717–721.

Lapchak PA, Jiao S, Miller PJ, Williams LR, Cummins V, Inouye G, Matheson CR, Yan Q. 1996. Pharmacological characterization of glial cell-line derived neurotrophic factor (GDNF): implications for GDNF a a therapeutic molecule for treating neurodegenerative diseases. Cell Tissue Res 286:179–189.

Lin LF, Doherty DV, Lile JD, Bektesh S, Collins F. 1993. GDNF: a glial cell line-derived neurotrophic factor for midbrain dopaminergic neurons. Science 260:1072–1073.

Love S, Plaha P, Patel NK, Hotton GR, Brooks DJ, Gill SS. 2005. Glial cell line-derived neurotrophic factor induces neuronal sprouting in human brain. Nat Med 11:703–704.

Nakamura TY, Jeromin A, Smith G, Kurushima H, Koga H, Nakabeppu Y, Wakabayashi S, Nabekura J. 2006. Novel role of neuronal Ca^{2+} sensor-1 as a survival factor up-regulated in injured neurons. J Cell Biol 172:1081–1091.

Nicole O, Ali C, Docagne F, Plawinski L, McKenzie ET, Vivien D, Buisson A. 2001. Neuroprotection mediated by glial cell line-derived neurotrophic factor: involvement of a reduction of NMDA-induced calcium influx by the mitogen-activated protein kinase pathway. J Neurosci 21:3024–3033.

O'Callaghan JP, Sriram K. 2004. Focused microwave irradiation of the brain preserves in vivo protein phosphorylation: comparison with other methods of sacrifice and analysis of multiple phosphoproteins. J Neurosci Methods 135:159–168.

Onyango IG, Tuttle JB, Bennett JPJ. 2005. Brain-derived growth factor and glial cell line-derived growth factor use distinct intracellular signaling pathways to protect PD cybrids from H_2O_2-induced neuronal death. Neurobiol Dis 20:141–154.

Patel NK, Bunnage M, Plaha P, Svendsen CN, Heywood P, Gill SS. 2005. Intraputamenal infusion of glial cell line-derived neurotrophic factor in PD: a two-year outcome study. Ann Neurol 57:298–302.

Paxinos G, Franklin KB. 1997. The mouse brain in stereotaxic coordinates, deluxe 2nd ed. San Diego: Academic Press.

Poteryaev D, Titievsky A, Sun YF, Thomas-Crusells J, Lindahl M, Billaud M, Arumae U, Saarma M. 1999. GDNF triggers a novel ret-independent Src kinase family-coupled signaling via a GPI-linked GDNF receptor alpha1. FEBS Lett 463:63–66.

Ries V, Henchcliffe C, Kareva T, Rzhetskaya M, Bland R, During MJ, Kholodilov N, Burke RE. 2006. Oncoprotein Akt/PKB induces trophic effects in murine models of Parkinson's disease. Proc Natl Acad Sci U S A 103:18757–18762.

Salvatore MF, Zhang J-L, Large DM, Wilson PE, Gash CR, Thomas TC, Haycock JW, Bing G, Stanford JA, Gash DM, Gerhardt GA. 2004. Striatal GDNF administration increases tyrosine hydroxylase phosphorylation in the rat striatum and substantia nigra. J Neurochem 90:245–254.

Salvatore MF, Ai Y, Fischer B, Zhang AM, Grondin RC, Zhang Z, Gerhardt GA, Gash DM. 2006. Point source concentration of GDNF may explain failure of phase II clinical trial. Exp Neurol 12: 497–505.

Sanicola M, Hession C, Worley D, Carmillo P, Ehrenfels C, Walus L, Robinson S, Jaworski G, Wei H, Tizard R, Whitty A, Pepinsky RB, Cate RL. 1997. Glial cell line-derived neurotrophic factor-dependent RET activation can be mediated by two different cell-surface accessory proteins. Proc Natl Acad Sci U S A 94:6238–6243.

Scott RP, Ibanez CF. 2001. Determinants of ligand binding specificity in the glial cell line-derived neurotrophic factor family receptor alpha S. J Biol Chem 276:1450–1458.

Sherer TB, Fiske BK, Svendsen CN, Lang AE, Langston JW. 2006. Crossroads in GDNF therapy for Parkinson's disease. Move Disorders 21:136–141.

Slevin JT, Gerhardt GA, Smith CD, Gash DM, Kryscio R, Young B. 2005. Improvement of bilateral motor functions in patients with Parkinson disease through the unilateral intraputaminal infusion of glial cell line-derived neurotrophic factor. J Neurosurg 102:216–222.

Smith AD, Antion M, Zigmond MJ, Austin MC. 2003. Effect of 6-hydroxydopamine on striatal GDNF and nigral GFRα1 and RET mRNAs in the adult rat. Exp Neurol 193:420–426.

Soler RM, Dolcet X, Encinas M, Egea J, Bayascas JR, Comella JX. 1999. Receptors of the glial cell line-derived neurotrophic factor family of neurotrophic factors signal cell survival through the phosphatidylinositol 3-kinase pathway in spinal cord motoneurons. J Neurosci 19:9160–9169.

Srinivasan S, Anitha M, Mwangi S, Heuckeroth RO. 2005. Enteric neuroblasts require the phosphatidylinositol 3-kinase/Akt/Forkhead pathway for GDNF-stimulated survival. Mol Cell Neurosci 29:107–119.

Svenningsson P, Lindskog M, Ledent C, Parmentier M, Greengard P, Fredholm BB, Fisone G. 2000. Regulation of the phosphorylation of the dopamine- and cAMP-regulated phosphoprotein of 32 kDa in vivo by dopamine D1, dopamine D2, and adenosine A2A receptors. Proc Natl Acad Sci U S A 97:1856–1860.

Tomac A, Lindqvist E, Lin L-FH, Ögren SO, Young D, Hoffer BJ, Olson L. 1995. Protection and repair of the nigrostriatal dopaminergic system by GDNF in vivo. Nature 373:335–339.

Treanor JJ, Goodman L, de Sauvage F, Stone DM, Poulsen KT, Beck CD, Gray C, Armanini MP, Pollock RA, Hefti F, Phillips HS, Goddard A, Moore MW, Buj-Bello A, Davies AM, Asai N, Takahashi M, Vandlen R, Henderson CE, Rosenthal A. 1996. Characterization of a multicomponent receptor for GDNF. Nature 382:80–83.

Trupp M, Arenas E, Fainzilber M, Nilsson A-S, Sieber B-A, Grigoriou M, Kilkenny C, Salazar-Gruesco E, Pachinas V, Arumäe U, Sariola H, Saarma M, Ibanez CF. 1996. Functional receptor for GDNF encoded by the c-ret proto-oncogene. Nature 381:785–789.

Trupp M, Raynoschek C, Belluardo N, Ibanez CF. 1998. Multiple GPI-anchored receptors control GDNF-dependent and independent activation of the c-Ret receptor tyrosine kinase. Mol Cell Neurosci 11:47–63.

Trupp M, Scott R, Whittemore SR, Ibanez CF. 1999. Ret-dependent and -independent mechanisms of glial cell line-derived neurotrophic factor signaling in neuronal cells. J Biol Chem 274:20885–20894.

Ugarte SD, Lin E, Klann E, Zigmond MJ, Perez RG. 2003. Effects of GDNF on 6-OHDA-induced death in a dopaminergic cell line: modulation by inhibitors of PI3 kinase and MEK. J Neurosci Res 73:105–112.

Weinreb O, Amit T, Bar-Am O, Sagi Y, Mandel S, Yuodim MB. 2007. Involvement of multiple survival signal transduction pathways in the neuroprotective, neurorescue and APP processing activity of rasagiline and its propargyl moiety. J Neural Transm Suppl 70:457–465.

Wiklund P, Ekström PAR, Edström A. 2002. Mitogen-activated protein kinase inhibition reveals differences in signalling pathways activated by neurotrophin-3 and other growth-stimulating conditions of adult mouse dorsal root ganglia neurons. J Neurosci Res 67:62–68.

Winkler C, Sauer H, Lee CS, Björklund A. 1996. Short-term GDNF treatment provides long-term rescue of lesioned nigral dopaminergic neurons in a rat model of of Parkinson's disease. J Neurosci 16:7206–7215.

Neurochemistry

JOURNAL OF NEUROCHEMISTRY | 2008 | 106 | 860–874 doi: 10.1111/j.1471-4159.2008.05459.x

Adaptation to chronic MG132 reduces oxidative toxicity by a CuZnSOD-dependent mechanism

Rehana K. Leak,* Michael J. Zigmond*,†,‡ and Anthony K. F. Liou*

*Department of Neurology, Pittsburgh Institute of Neurodegenerative Diseases, University of Pittsburgh, Pittsburgh, Pennsylvania, USA

†Department of Neurobiology, Pittsburgh Institute of Neurodegenerative Diseases, University of Pittsburgh, Pittsburgh, Pennsylvania, USA

‡Department of Psychiatry, Pittsburgh Institute of Neurodegenerative Diseases, University of Pittsburgh, Pittsburgh, Pennsylvania, USA

Abstract

To study whether and how cells adapt to chronic cellular stress, we exposed PC12 cells to the proteasome inhibitor MG132 (0.1 μM) for 2 weeks and longer. This treatment reduced chymotrypsin-like proteasome activity by 47% and was associated with protection against both 6-hydroxydopamine (6-OHDA; 100 μM) and higher dose MG132 (40 μM). Protection developed slowly over the course of the first 2 weeks of exposure and was chronic thereafter. There was no change in total GSH levels after MG132. Buthionine sulfoximine (100 μM) reduced GSH levels by 60%, but exacerbated 6-OHDA toxicity to the same extent in both MG132-treated and control cells and failed to reduce MG132-induced protection. Chronic MG132 resulted in elevated antioxidant proteins CuZn superoxide dismutase (SOD; +55%), MnSOD (+21%), and catalase (+15%), as well as chaperone heat-shock protein 70 (+42%). Examination of SOD enzyme activity revealed higher levels of CuZnSOD (+40%), with no change in MnSOD. We further assessed the mechanism of protection by reducing CuZnSOD levels with two independent siRNA sequences, both of which successfully attenuated protection against 6-OHDA. Previous reports suggested that artificial over-expression of CuZnSOD in dopaminergic cells is protective. Our data complement such observations, revealing that dopaminergic cells are also able to use endogenous CuZnSOD in self-defensive adaptations to chronic stress, and that they can even do so in the face of extensive GSH loss.

Keywords: 6-hydroxydopamine, dopamine transporter, glutathione, Parkinson's disease, proteasome.

J. Neurochem. (2008) **106**, 860–874.

Neurodegenerative conditions such as sporadic Parkinson's disease (PD) occur only in a minority of individuals and usually do not manifest themselves until advanced age. One explanation for this phenomenon is that cells possess self-defenses against cellular stress, but that these adaptive mechanisms become less effective with age and in certain disease states. A type of cellular stress thought to be present for decades in individuals with PD is the presence of misfolded and damaged proteins, resulting in the progressive accumulation of dystrophic neurites and inclusions across many brain regions (Braak *et al.* 2003). This observation raises the possibility that in PD affected cells deal with a high burden of damaged proteins over an extended timeframe. Studying adaptive defenses to such cellular stressors may yield insight into what keeps illnesses at bay in most individuals and/or what delays neurodegeneration in individuals who do finally develop disease. Moreover, learning how to boost such endogenous defenses pharmacologically without applying stress *per se* may lead to treatments that slow the progression of neurodegeneration even further.

The proteasome is a multicatalytic complex engaging in proteolysis of misfolded, oxidized, and aggregated proteins. A reduction in its activity has been observed in Alzheimer's

Received January 6, 2008; revised manuscript received April 7, 2008; accepted April 14, 2008.

Address correspondence and reprint requests to Rehana Khan Leak, PhD, 7026 Biomedical Science Tower 3, Pittsburgh Institute for Neurodegenerative Diseases, University of Pittsburgh, Pittsburgh, PA 15260, USA. E-mail: leakrk@upmc.edu

Abbreviations used: 6-OHDA, 6-hydroxydopamine; BCA, bicinchoninic acid; BSO, buthionine sulfoximine; DA, dopamine; DMSO, dimethyl sulfoxide; Hsp, heat-shock protein; PBS, phosphate buffered saline; PD, Parkinson's disease; SOD, superoxide dismutase; TH, tyrosine hydroxylase.

disease, PD, and with advancing age (Conconi *et al.* 1996; Friguet *et al.* 2000; Keller *et al.* 2000a,b; Lopez Salon *et al.* 2000; Merker *et al.* 2001; Keck *et al.* 2003; McNaught *et al.* 2003). For example, there is an average 44% loss in chymotrypsin-like proteasome activity in postmortem PD nigra (McNaught *et al.* 2003). If and how dopaminergic cells might adapt to this burden to prolong the course of degeneration in PD has not been explored, but deserves further study, both in the human disease as a function of illness duration and in those PD models using pharmacological proteasome inhibitors (Rideout *et al.* 2001; McNaught *et al.* 2002; Ding *et al.* 2003; Fornai *et al.* 2003; Mytilineou *et al.* 2004; Inden *et al.* 2005; Miwa *et al.* 2005; Rideout *et al.* 2005; Sun *et al.* 2006). Many such reports have indicated that short-term proteasome inhibition with pharmacological compounds can indeed elicit protection against cellular stress (Bush *et al.* 1997; Lee and Goldberg 1998b; Lee *et al.* 2004; Sawada *et al.* 2004; Inden *et al.* 2005; Yamamoto *et al.* 2007). Furthermore, proteasome inhibition has been shown to activate both pro-survival and pro-apoptotic pathways, with the former response predominating at low concentrations of the inhibitor (Lin *et al.* 1998; Yew *et al.* 2005). Therefore, it seemed possible that even chronic exposure to a proteasome inhibitor at a subtoxic concentration might elicit an adaptive response that could be dissected *in vitro*. In support of our hypothesis, Ding *et al.* (2003) noted that dopaminergic SH-SY5Y cells were rendered more resilient against oxidative stress and serum withdrawal with 12 or more weeks of exposure to a proteasome inhibitor, by an unknown mechanism. Such defensive responses to stress are akin to the phenomenon of "preconditioning" or "tolerance" in studies of ischemia, where it has long been known that sublethal acute ischemic episodes protect against longer ischemic episodes (Murry *et al.* 1986; Kitagawa *et al.* 1990). Studies of preconditioning, however, have been limited to short-term exposures to sublethal stressors. The present report extends those studies to a model with a longer-term stress to better emulate the chronic conditions in human neurodegenerative diseases and aging.

One of the best characterized proteasome inhibitors is MG132, a potent inhibitor of the chymotrypsin-like activity of the proteasome that also affects cathepsins and calpains, effectively increasing the burden of misfolded proteins and concomitant cellular stress (Lee and Goldberg 1998a; Kisselev and Goldberg 2001; Fuertes *et al.* 2003; Rodgers and Dean 2003). Thus, in the present study, MG132 was applied to PC12 cells from days to weeks, and then for months onwards, to examine whether this chronic stress would alter the vulnerability of these dopaminergic cells to further injury. In this study, we report the novel observation that a chronic treatment to raise damaged protein levels actually resulted in higher resilience against oxidative stress, that the adaptive response was mediated at least in part by CuZn superoxide dismutase (SOD), and that protection was uncoupled from extensive GSH loss.

Materials and methods

Chemicals and antibodies

All chemicals were purchased from Sigma-Aldrich (St. Louis, MO, USA), unless specified otherwise. Primary and secondary antibodies were purchased and used as follows: mouse anti-tyrosine hydroxylase (TH; 1 : 1000 for immunocytochemistry and 1 : 10 000 for immunoblotting; Chemicon, Temecula, CA, USA), rabbit anti-MnSOD (1 : 5000; Upstate Inc., Charlottesville, VA, USA), rabbit anti-CuZnSOD (1 : 500, Upstate Inc.), mouse anti-catalase (1 : 5000; Sigma-Aldrich), rabbit anti-inducible heat-shock protein 70 (Hsp70, 1 : 1000; Stressgen, San Diego, CA, USA), mouse anti-ubiquitin conjugated proteins (1 : 500; Santa Cruz Biotechnology, Santa Cruz, CA, USA), mouse anti-α-tubulin (1 : 5000; Sigma-Aldrich), mouse anti-β-actin (1 : 50 000; Sigma-Aldrich), rabbit anti-β-actin (1 : 10 000; Abcam, Cambridge, MA, USA), rabbit anti-GSH (1 : 300; Chemicon), infrared anti-rabbit and anti-mouse IgG (1 : 10 000 for western blots and 1 : 1000 for In Cell Westerns; LI-COR Biotechnology, Lincoln, NA, USA), and Alexa Fluor 488 goat anti-mouse IgG (1 : 1000; Molecular Probes, Eugene, OR, USA). Omission of either primary or secondary antibodies from the assays resulted in loss of signal.

Cell maintenance

PC12 cells were left in their undifferentiated state so as to be able to continuously apply MG132 out to a maximum of 6 months as the studies proceeded. In preliminary studies, however, we found a lack of high-affinity tritiated dopamine (^{3}H-DA) uptake in undifferentiated PC12 cells. Thus, to ensure rapid uptake of 6-hydroxydopamine (6-OHDA) and specific oxidative breakdown within the intracellular milieu, we obtained PC12 cells stably transfected with the human DA transporter under control of the CMV promoter (gift of Gonzalo E. Torres, University of Pittsburgh). These cells were maintained at 37°C with 5% CO_2 in low glucose Dulbecco's modified Eagle's medium (Invitrogen, Carlsbad, CA, USA), supplemented with 5% horse serum, 5% fetal bovine serum (Invitrogen) and 50 μg/mL G418 (Cellgro, Herndon, VA, USA). Cells were plated at a density of 1061 cells per mm^2 (30 000/well in a 96-well plate) on collagen-coated plates (Becton Dickinson, Franklin Lakes, NJ, USA). Treatments or assays were typically made or initiated 24 h after plating. For siRNA treatments only, cell density was increased to 1415 cells per mm^2 (40 000/well in a 96-well plate) to achieve high confluence at the time of transfection.

Toxin treatments

To produce chronic stress, cells were maintained in 0.1 μM peptide aldehyde MG132 (Cbz-leu-leu-leucinal), purchased from EMD Bioscience (San Diego, CA, USA). MG132 was made up as a 1 mM stock solution in dimethyl sulfoxide (DMSO) and then freshly diluted only 1 μL per 10 mL media to minimize DMSO exposure. For the second, challenge treatments we chose 6-OHDA (Sigma-Aldrich Co. or Regis Technologies, Inc., Morton Grove, IL, USA) and high dose MG132. Although many *in vitro* studies of

6-OHDA use long incubation intervals, 6-OHDA oxidizes rapidly to hydrogen peroxide and other toxic by-products under typical culturing conditions (Ding *et al.* 2004; Hanrott *et al.* 2006; Saito *et al.* 2007). Thus, we prepared 6-OHDA in a vehicle composed of 0.15% ascorbic acid and 10 mM of the metal chelator diethylenetriamine pentaacetic acid, flushed with nitrogen for 10 min before use to help remove oxygen. 6-OHDA made in this vehicle was then diluted 10-fold in media added to the wells for 30 min. This procedure was designed to limit the potential confound of oxidation products within the media and increase intracellular breakdown (Clement *et al.* 2002; Ding *et al.* 2004). MG132 was left in the media during and after 6-OHDA, because we reasoned that cells in neurodegenerative conditions in aged humans would continue to suffer from cellular stress and misfolded proteins while exposed to an oxidative insult. For a challenging, test dose of MG132, 40 μM was chosen from a pilot dose–response curve, and, unlike 6-OHDA, MG132 or the same volume of DMSO were left in for another 24 h before cellular viability was assessed as described below.

Studies of chronic MG132-induced changes in vulnerability to 6-OHDA were initiated with exposure to the inhibitor ranging from 2 weeks to 6 months and averaged across time. Comparisons were always made to control, non-MG132 treated cultures maintained and assayed side-by-side with simultaneous passaging or plating at the same density. No difference in results were observed with exposure to MG132 beyond that of 2 weeks; however, slight shifts in the EC_{50} for toxins and in the degree of MG132-induced protection were observed across toxin batches and/or periods of storage of these compounds. This was especially true for 6-OHDA, as reported by us previously (Ding *et al.* 2004; Lin *et al.* 2008). Therefore, small aliquots of both toxins were rapidly flash-frozen as concentrated stocks, which helped minimize inter-experimental variability for statistical analyses.

To produce GSH depletion, buthionine sulfoximine (BSO; 100 μM) was freshly dissolved in sterile phosphate-buffered saline (PBS) as a 10 mM stock. Twenty-four hours after plating, cells were treated in media with indicated concentrations of BSO, or the same volume of PBS, for 24 h before 6-OHDA. BSO was then left in during and after 30 min 6-OHDA treatments until the indicated time of assay. Details on ensuring BSO efficacy follow, in the section below on In Cell Western infrared assays for GSH.

Tyrosine hydroxylase immunocytochemistry

For staining cells with antibodies against TH, a rate-limiting enzyme for DA biosynthesis, cells were fixed with 2% *p*-formaldehyde in PBS. Non-specific secondary binding was then minimized by blocking in 10% normal goat sera (Jackson Immunochemicals, West Grove, PA, USA) diluted in 0.3% Triton X-100 in PBS for 1 h. Cells were subsequently incubated overnight with a mouse antibody against TH diluted in 1% normal serum and 0.3% Triton X in PBS. Cells were then washed three times in PBS and subjected to secondary incubation with Alexa Fluor 488 goat anti-mouse IgG diluted in 2% normal serum and 0.3% Triton X in PBS. At the end of 1 h cells were washed again two times in PBS and stained with a 10 μg/mL solution of Hoechst 33258 (bisbenzimide) for 20 min before a final wash. Photography under brightfield, UV, or FITC illumination was then performed on a Nikon Inverted Eclipse TE 2000 microscope (Fryer Inc., Carnegie, PA, USA).

Western blotting

Cells were lysed for immunoblotting with cell lysis buffer (Cell Signaling, Danvers, MA, USA) with added protease inhibitor cocktail (Sigma-Aldrich). Lysates were sonicated for 5 s and subjected to centrifugation (15 min at 15 000 *g*) for measurements of protein content in the supernatant by the bicinchoninic acid (BCA) method (Pierce, Rockford, IL, USA). Equal amounts of protein (20 μg) from each treatment were separated on sodium dodecyl sulfate gels and transferred to Immobilon FL PVDF membranes (BioRad Laboratories, Hercules, CA, USA). Non-specific binding was reduced by incubating membranes in a fish serum blocking solution at full strength (LI-COR Biotechnology) for 1 h prior to overnight treatment at 4°C with primary antibodies diluted in the same blocking solution. Mouse or rabbit anti-β-actin antibodies were always used as a concurrent loading control. Blots were then washed three times in Tris-buffered saline with 0.1% Tween (BioRad Laboratories) and incubated 1 h with infrared secondary antibodies raised against the appropriate species, fluorescing at either 700 or 800 nm. After three washes in Tris-buffered saline–Tween, blots were visualized on an Odyssey Infrared Imager (LI-COR Biotechnology) and fluorescent signal from each protein band quantified with Odyssey software.

Proteasome activity assay

Chymotrypsin-like proteasome activity of the cytosolic 26S particle was assessed using published methods, where emitted fluorescence is in direct proportion to proteasome activity (Kisselev and Goldberg 2005). Briefly, we suspended cells in 50 mM Tris–HCl, pH 7.5, 250 mM sucrose, 5 mM $MgCl_2$, 2 mM ATP, 1 mM dithiothreitol, 0.5 mM EDTA, and 0.025% digitonin. Following 5 min of permeabilization, cytosol was separated out by centrifugation at 20 000 *g* for 15 min at 4°C. Cytosolic extract was then added to the assay buffer at a final dilution of 0.25 μg/μL, as determined by the BCA method. The buffer consisted of 50 mM Tris–HCl, pH 7.5, 40 mM KCl, 5 mM $MgCl_2$, 0.5 mM ATP, 1 mM dithiothreitol, and 0.05 mg/mL bovine serum albumin. Fluorogenic substrate for the 20S proteasome, Suc-LLVY-amc (Biomol International, Plymouth Meeting, PA, USA) was freshly prepared and then added to the assay buffer at 100 μM to specifically measure cleavage at the chymotrypsin-like site. For each group, duplicate samples were always pre-treated for 30 min at 37°C with 20 μM epoxomicin (Peptides International, Louisville, KY, USA). Epoxomicin is considered a more specific inhibitor of all three proteasome sites and was used to estimate the fraction of proteolytic activity resulting from enzymes other than the proteasome during the assay (Kisselev and Goldberg 2005). Fluorescence was recorded every 20 min over the course of 1 h (excitation 380 nm and emission 460 nm), and the raw values at each timepoint compared with the linear range of 7-amino-4-methylcoumarin standards (Bachem, Torrance, CA, USA), diluted 0.1–10 μM.

Viability assays

Cell viability was measured 24 h after treatment in two ways, by measuring ATP levels or counting viable nuclei. First ATP levels were assayed by a proprietary luciferase based reaction with Cell Titer Glo (Promega Inc., Madison, WI, USA), added according to the manufacturer's instructions and read 20 min later on a microplate reader (L-Max II; Molecular Devices, Sunnyvale, CA,

USA). Second, cells were fixed with a 2% *p*-formaldehyde solution in PBS and stained with Hoechst solution as above. Blind counts of viable cells were performed following UV-illuminated digital capture of nuclei from the center of each well, as described previously (Leak *et al.* 2006). For one set of experiments, ATP level assays were also performed 48 h after 6-OHDA removal instead of 24 h, as indicated in the Results section.

^{3}H-dopamine uptake

Cells were incubated with 200 nM ^{3}H-DA (specific activity 59.3 Ci/mmol; American Radiolabeled Chemicals, St Louis, MO, USA) in PBS for 15 min at 37°C (Leak *et al.* 2006). Negative control wells were incubated with the high-affinity DA transporter blocker nomifensine (40 μM) for 10 min prior to and during the assay. Cells were then washed three times with PBS and total tritium extracted with ethanol and perchloric acid for counts by liquid scintillation spectroscopy (Beckman LS-1800; Beckman Coulter, Inc., Fullerton, CA, USA). Counting efficiency for tritium was 0.58, and results were expressed as dpm.

Glutathione assay

For measuring total GSH in a relatively high-throughput manner, an assay was developed using the infrared In Cell Western system (LI-COR Biotechnology). A rabbit antibody raised against both oxidized and reduced GSH was applied together with a mouse antibody against α-tubulin and visualized with infrared secondary IgGs. Specificity controls for the GSH antibody included various concentrations of BSO treatments to ensure dose-dependent loss of GSH staining, as well as depletion of signal by pre-adsorption of the antibody with excess GSH tripeptide purchased in its reduced form (Sigma-Aldrich). A 100 μM concentration of BSO was then chosen for viability experiments, as it did not by itself result in any loss of α-tubulin signal or of ATP levels by Cell Titer Glo, and so was deemed non-toxic. For the remaining GSH assays, cells were fixed with *p*-formaldehyde at 3, 6, or 24 h after treatment with BSO ± 6-OHDA and stored in PBS-azide until incubation in 10% normal goat serum in 0.3% Triton X-100 in PBS for 1 h. Then cells were then exposed overnight to rabbit anti-GSH and mouse anti-α-tubulin diluted in 1% normal goat serum and 0.3% Triton X in PBS. The following day, cells were rinsed three times in PBS and incubated for 1 h in infrared goat anti-mouse (700 nm) and goat anti-rabbit (800 nm) secondary IgG, diluted in 2% normal serum and 0.3% Triton X in PBS. Plates were finally washed three times in PBS and infrared emissions from each well-bottom read on the Odyssey Imager. GSH levels as measured by this system were expressed as anti-GSH fluorescence intensity divided by anti-α-tubulin fluorescence intensity. The original images generated by this sensitive system are in a gray scale rather than color (as shown in Figures) and their bit-depth of 16 yields 2^{16} or 65 536 intensity levels.

Superoxide dismutase activity assays

Cells were harvested in PBS 24 h after plating. An aliquot of this was removed for BCA protein content assay as usual. Cells in PBS were spun at 2000 *g* for 10 min at 4°C and resuspended and homogenized in 20 mM HEPES buffer, pH 7.2, containing 1 mM EGTA, 210 mM mannitol, and 70 mM sucrose. The homogenized solution was recentrifuged at 1500 *g* for 5 min at 4°C, the supernatant collected, and 5 μg protein from each sample mixed with tetrazolium salt in each well as per manufacturer's directions for detection of superoxide radicals (Cat No.706002; Cayman Chemicals, Ann Arbor, MI, USA). A second set of duplicate samples were simultaneously treated with 2 mM potassium cyanide, an inhibitor of CuZnSOD, to permit assessment of MnSOD activity (Saggu *et al.* 1989). Absorbance was read at 450 nm and enzyme activity calculated from absorbance of SOD standards, after ensuring raw values were within their linear range.

RNA interference

For RNA interference, cells were plated at high confluency in accordance with the manufacturer's instructions for Lipofectamine 2000 (Invitrogen). siRNA concentrations were based on the manufacters's recommendations for rat cell lines (500 pmol for six-well plates with 3.5 cm diameter wells). Our pilot testing range for knockdown by immunoblotting was 25–500 pmol for each siRNA sequence. We chose to focus upon concentrations that produced a knockdown of CuZnSOD back to naïve control values within 24 h, so as to minimize adverse effects upon basal viability by long-term loss of a critical protein. From the pilot data, we chose to treat cells with 300 pmol "All Stars" negative control siRNA (Qiagen Inc., Valencia, CA, USA) or CuZnSOD siRNA (see below) in Opti-MEM/Glutamax transfection media (Invitrogen) with 5 μL Lipofectamine per 100 pmol siRNA in six-well plates (31 pmol/cm^2). The proprietary, negative control siRNA was designed to have no known homology to mammalian genes but enter the RNA-induced silencing complex. Two different CuZnSOD sequences were used, one from Qiagen Inc. (antisense sequence rUUAAUC-CUGUAAUCUGUCCdTdG) and one from Dharmacon (Lafayette, CO, USA; antisense sequence 5′-P.UUCACCGCUUGCCUUCUG-CUU). Both sequences gave similar knockdown values at 300 pmol.

For viability experiments in 96-well format (0.6 cm diameter wells), cells plated at the same number per unit surface area were treated with 8.82 pmol negative control or CuZnSOD siRNA (31 pmol/cm^2, final concentration of 88 nM). After 5 h, Opti-MEM was replaced with regular medium and cells were treated 24 h later with 6-OHDA or vehicle as usual, except that the concentration of 6-OHDA was doubled (200 μM) as the cell plating density for transfections was higher than before and affected the EC_{50}. Cells were assayed with Cell Titer Glo 24 h after 6-OHDA as usual.

Statistical analyses

Data are presented as mean ± SEM from three to seven independent experiments, each performed in triplicate wells or more and analyzed using two-tailed *t*-test when there were only two groups or otherwise by ANOVA (SPSS V10.1; SPSS Inc., Chicago, IL, USA). *Post hoc* comparisons following ANOVA were performed using the method of Bonferroni. Results were deemed significant when $p \leq 0.05$.

Results

MG132 caused no overt change in morphological appearance of PC12 cells

MG132 treated cells showed no detectable change in cellular appearance or TH enzyme expression, as assessed with

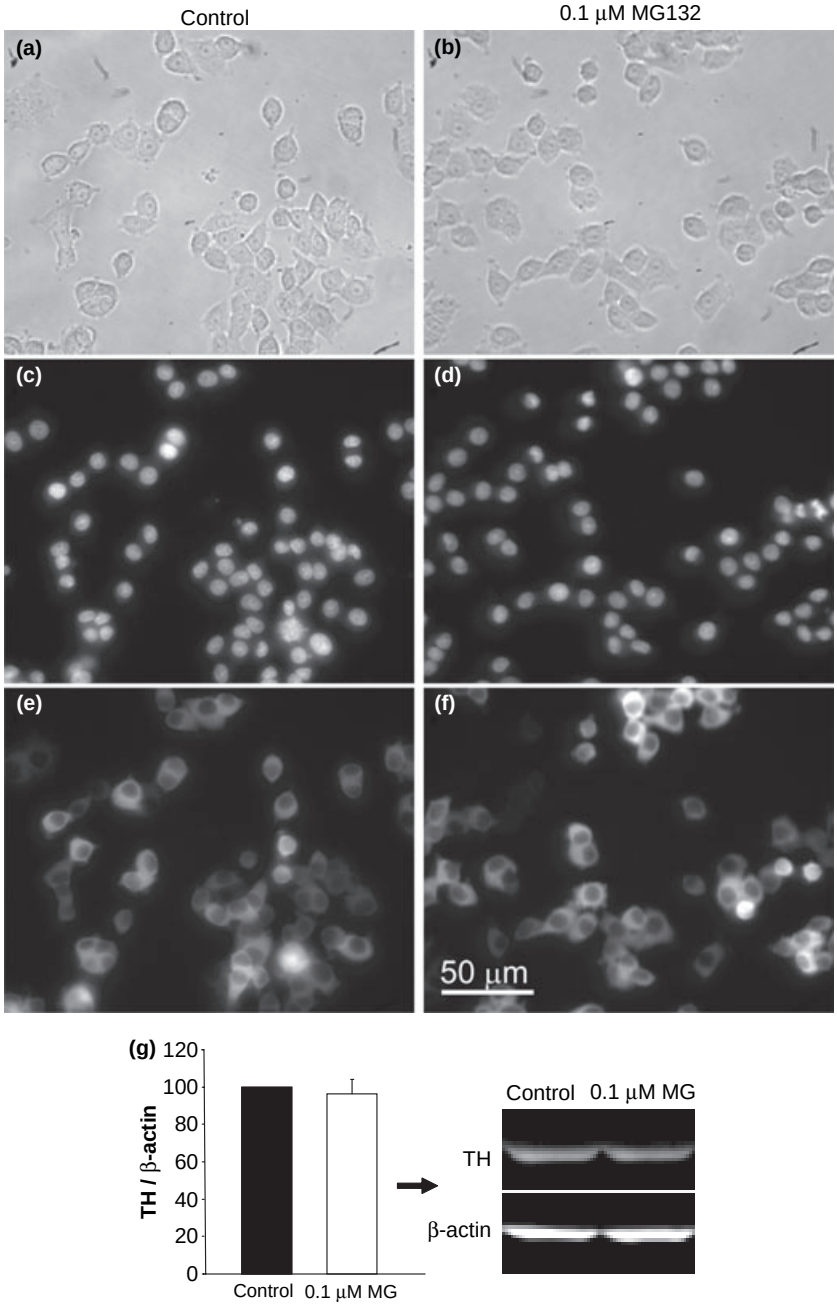

Fig. 1 Chronic MG132 treatment did not affect morphological appearance of PC12 cells. Brightfield (a and b), Hoechst staining (c and d) and TH immunolabeling (e and f) of naïve control (a, c, and e) versus chronic MG132-treated cells (b, d, and f). Cells were fixed and stained 48 h after side-by-side passaging and plating at equal densities. Images were captured at the same exposure settings for both groups. Immunoblotting verified the lack of effect upon levels of TH protein (g). Total TH levels were expressed as a fraction of β-actin label to control for variations in protein loading and presented as mean + SEM from six independent experiments. Scale bar, 50 μm (a–f).

brightfield images (Fig. 1a and b), Hoechst nuclear staining (Fig. 1c and d), and immunocytochemistry (Fig. 1e and f). Immunoblotting with anti-TH antibodies also revealed no MG132-induced change in TH protein levels (Fig. 1g), in support of the immunocytochemical results. Further, no neurite extension or signs of differentiation were observed over the course of 6 months of exposure.

MG132 decreased proteasome activity

In our model, chronic exposure to 0.1 μM MG132 reduced chymotrypsin-like activity in cytosolic extracts by 47% (Fig. 2a), indicating that our toxin was effective at this concentration. Fluorescence increased linearly over time during the assay for proteasome activity, but with no further change between groups (20 min reading shown in Fig. 2a). As a negative control, treatment of aliquots of the same extracts with epoxomicin (20 μM) before and during the assay itself dropped fluorescent emissions in both control and MG132 samples by an average of 99%.

With successful reduction of proteasome activity, one would expect substrate turnover to decrease and the levels of ubiquitin-conjugated proteins to rise. Thus, we probed

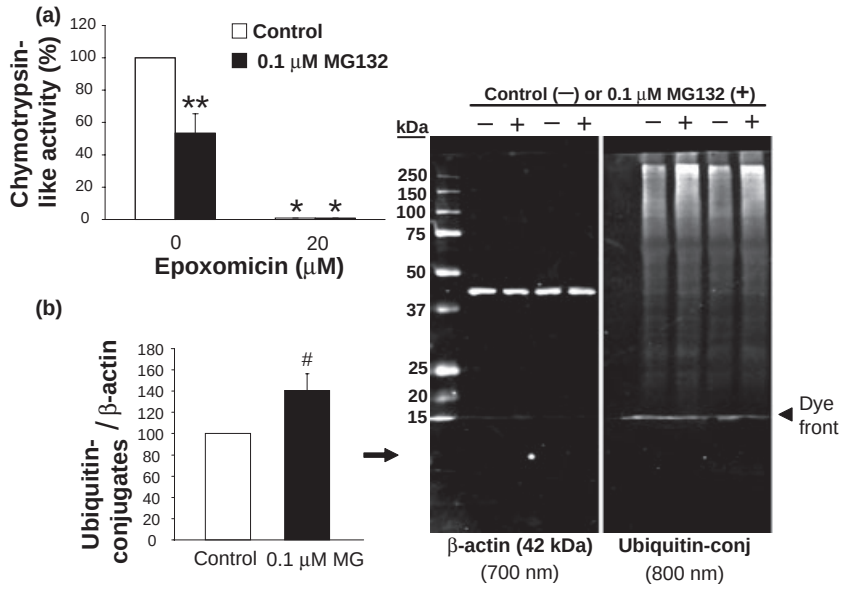

Fig. 2 Chronic MG132 decreased proteasome activity levels. (a) Fluorescent reporting of cleavage of Suc-LLVY-amc, substrate for assaying chymotrypsin-like proteasome activity, without (white bars) and with (black bars) chronic treatment of MG132. Treatment of duplicate samples with epoxomicin *during* the assay effectively dropped all fluorescence values and acted as a negative control. Bonferroni *post hoc*: $^{*}p < 0.05$ versus same group without epoxomicin and $^{**}p < 0.05$ versus adjacent white bar of naïve control cells. (b) Levels of ubiquitin-conjugated proteins in PC12 cells with and without chronic MG132 are shown with 250–15 kDa standards visible in the 700 nm channel next to the β-actin loading controls. The blue Laemmli buffer's dye front is visible in both fluorescent channels, but appears greater at 800 nm because a better signal : noise ratio of the β-actin antibody allows scanning at a lower setting. Two sets harvested maximally far apart (6 months) are illustrated. Two-tailed *t*-test: $^{\#}p = 0.076$ versus white bar of naïve control cells. Data in (a and b) are presented as mean + SEM from three to seven independent experiments.

control and MG132 treated cells for ubiquitin-conjugated proteins. In MG132 treated cells we found a trend for increased levels of such proteins by two-tailed *t*-test ($p = 0.076$, one-tailed *t*-test, p value = 0.038, six independent sets; Fig. 2b). The 42% rise in ubiquitin conjugates with proteasome inhibition was noted by quantifying the *entire* visible MW range (250–15 kDa), but the typical spread of proteins most affected were those at higher molecular weights. This pattern has been noted in figures from other authors, some of them also using MG132 (Fujimuro *et al.* 1994; Elkon *et al.* 2001; Ohtake *et al.* 2007). We show a representative immunoblot from two sets of experimental samples harvested 6 months apart, to illustrate how the response did not appear to vary over time (Fig. 2b, right panel).

MG132 protected against oxidative stress and higher concentrations of MG132

Chronic MG132 exposure attenuated the toxic effects of 6-OHDA as well as a high concentration of MG132, as measured by both ATP level assay (Cell Titer Glo) and the Hoechst nuclear stain (Fig. 3a–d). The MG132-induced rise in viability following 6-OHDA treatment typically ranged from 25% to 30% with these assays (Fig. 3a and b). A similar pattern was observed for high dose MG132 post-treatment, with ~30% rise in viability apparent with both assays (Fig. 3c and d). Subsequent experiments focused solely upon 6-OHDA, as it is considered to be a classic model of oxidative stress for catecholaminergic cells (Zigmond and Keefe 1997). Furthermore, as ATP levels are likely to be more indicative of functionally protected cells than the appearance of Hoechst-stained intact nuclei, the Cell Titer Glo assay was chosen for subsequent viability assays.

The PC12 cells used here were stably transfected with the human DA transporter to achieve rapid, high-affinity transport of 6-OHDA within a short interval and prevent its extracellular breakdown in media [see *Materials and methods*; discussed at length by Clement *et al.* (2002)]. To gauge whether MG132 by itself might reduce intracellular entry of 6-OHDA, we examined the uptake of ^{3}H-DA across the plasma membrane. We found that chronic MG132 treatment did not reduce ^{3}H-DA uptake, instead, a 36% increase was observed (Fig. 3e). In contrast, the DA transport blocker nomifensine applied during the assay effectively reduced ^{3}H-DA uptake, supporting the specificity of our measure. We inferred from these data that any MG132-induced protection against 6-OHDA could not be attributed to reductions in toxin entry.

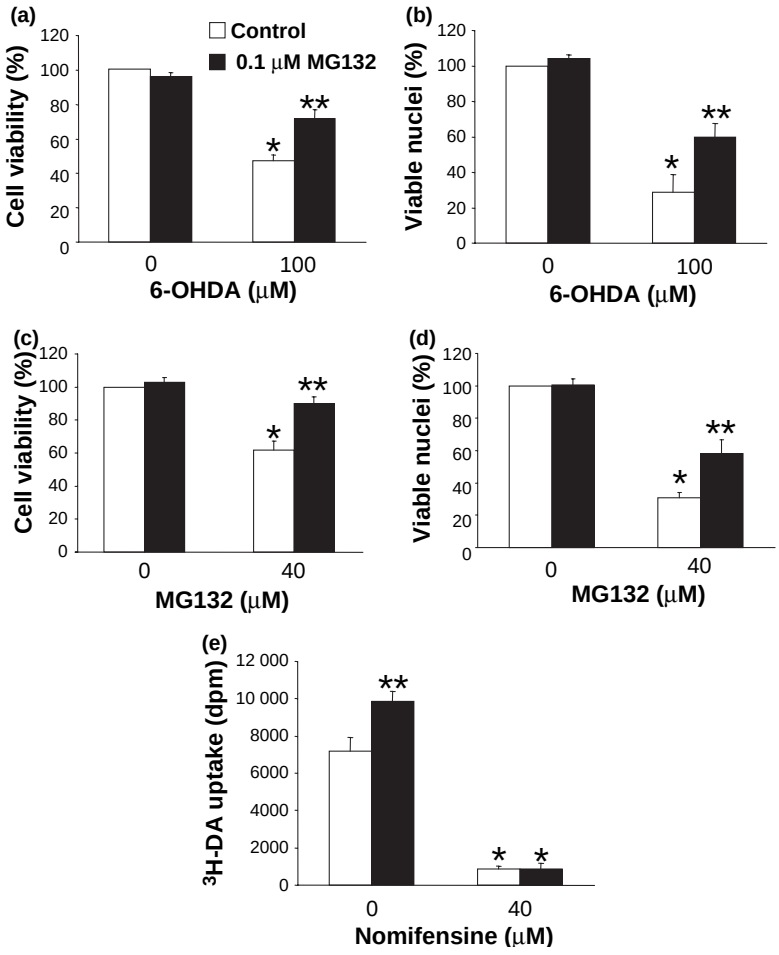

Fig. 3 Chronic MG132 protected against two different types of cellular injury and increased transport of tritiated dopamine (^{3}H-DA) across the membrane. (a-d) MG132 treatment protected against both 6-OHDA and a high concentration of MG132. Viability was assessed by measuring ATP levels with Cell Titer Glo (a and c) or by counting Hoechst-positive viable nuclei (b and d). Cells were treated with vehicle or 6-OHDA (a and b) and DMSO or MG132 (c and d) at indicated concentrations, and assayed 24 h thereafter. (e) ^{3}H-DA uptake in control and MG132 treated cells, with and without high-affinity DA transport blocker nomifensine (negative control applied *during* assay). Bonferroni *post hoc* following ANOVA: $^*p < 0.05$ versus same group without 6-OHDA or without high dose MG132 treatment in A-D: $^*p < 0.05$ versus same group without nomifensine in E and $^{**}p < 0.05$ versus white bar of naïve control cells in A-E. Data are presented as mean + SEM from three to five independent experiments.

Protection against 6-OHDA was not elicited or submaximal with short-term MG132 treatment, and was lost upon MG132 removal

To examine whether protection could be elicited with a short interval of exposure to MG132, naïve PC12 cells were exposed to 0.1 μM MG132 for 24 h prior to 6-OHDA treatment. MG132 was then left in during and after 6-OHDA (24 h), as this was also the protocol for all the chronic stress experiments (see *Materials and methods*). Thus, the previously naïve cells had experienced a total interval of 48.5 h of 0.1 μM MG132 at the time of viability assay (Fig. 4a). Such short-term treatment failed to confer any protection, cause significant cell loss, or hyperproliferation by itself, suggesting that a longer period of exposure was required for protection and supporting the hypothesis that growth rates remained constant. Then we examined closely the interval between lack of protection (1 day exposure before application of 6-OHDA) and the ≥14-day period. For this, naïve control cells were treated with 0.1 μM MG132 for 4, 8, or ≥14 days at time of 6-OHDA. Thus, the 4 and 8 days groups were plated at days 3 and 7 for 6-OHDA treatment the next day, and assayed at days 5 and 9, 1 day after 6-OHDA, respectively. In these experiments, we found a smaller degree of protection at 4 days (20% rise in viability from controls) and 8 days (14% rise) relative to exposure for 14 days or longer (32% rise; Fig. 4b).

We then proceeded to characterize basal viability in cells grown for 0, 3, 7, or > 14 days in MG132, and plated for Cell Titer Glo assay after an additional 24 h (0, 4, 8, or > 14 days at assay) or 48 h (0, 5, 9, or > 14 days when assayed). No differences in cell density were observed across time between any groups (Fig. 4c). Next, we asked whether the MG132 treatment simply delayed cell death for 24 h or could effect longer-lasting protection (48 h after removal of 6-OHDA). We found robust MG132-induced protection even 2 days after 6-OHDA removal (Fig. 4d). Finally, we examined if the protection would linger in the long-term absence of MG132. However, we found that a removal of the stimulus for 2 weeks resulted in loss of protection and a complete reversal back to the original state of vulnerability to 6-OHDA (Fig. 4e).

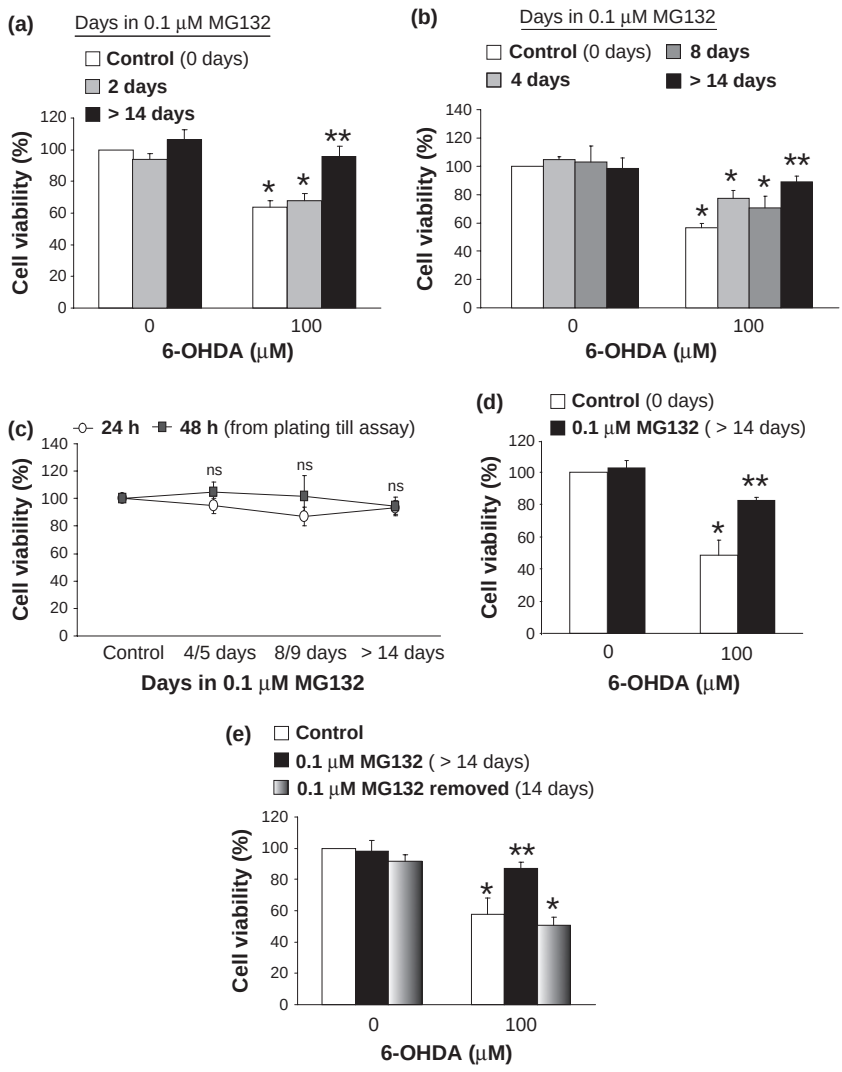

Fig. 4 MG132 needed to be chronic and maintained to elicit maximal protection. (a) Naïve control cells were pre-treated for 24 h with 0.1 μM MG132, and then MG132 was also present during and after 6-OHDA (additional 24.5 h). Cells were assayed for cellular viability 24 h after 6-OHDA removal (48.5 total hours of MG132 for gray bars). Side-by-side experiments on control (white bars) and chronic MG132-treated (> 14 days, black bars) cells serve as negative and positive controls to verify long-term MG132-induced protection against 6-OHDA toxicity. (b) Growing PC12 cells for 4 days (light gray) and 8 days (dark gray) in MG132 prior to 6-OHDA exposure elicited sub-maximal protection relative to > 14 days exposure (black bars). Cells were assayed 24 h after 6-OHDA removal. (c) Basal viability was not affected by the 0.1 μM dose of MG132, as measured at multiple timepoints. Cells grown for 4/5, 8/9, or > 14 days in MG132 did not exhibit differences in cell density over the course of 24 or 48 h from time of plating (at 3, 7, and 14+ days) until assay 24 or 48 h later. ns = not significant. See text for details. (d) Assaying 48 h after removal of 6-OHDA challenge revealed continued, robust protection against 6-OHDA toxicity. (e) Removing MG132 for 2 weeks (bars with gray gradient) caused a reversal back to the original 6-OHDA vulnerability. Experiments on control and chronic MG132-treated cells verified protection against 6-OHDA toxicity in the same experiments. All viability measures in (a and e) were performed with Cell Titer Glo. Data are presented as mean + SEM from three to four independent experiments. Bonferroni *post hoc* following ANOVA: $*p < 0.05$ versus same group without 6-OHDA and $**p < 0.05$ versus white bar denoting naïve control cells.

MG132-induced protection against 6-OHDA was not mediated by an increase in GSH

Previous studies suggested that short-term treatment with proteasome inhibitors increased GSH synthesis in PC12 cells and may have conferred protection against 6-OHDA and hydrogen peroxide (Yamamoto *et al.* 2007). We therefore investigated whether long-term treatment with MG132 protected PC12 cells against 6-OHDA by a GSH-dependent mechanism. To accomplish this, we first developed the assay for total GSH described in the Materials and methods section

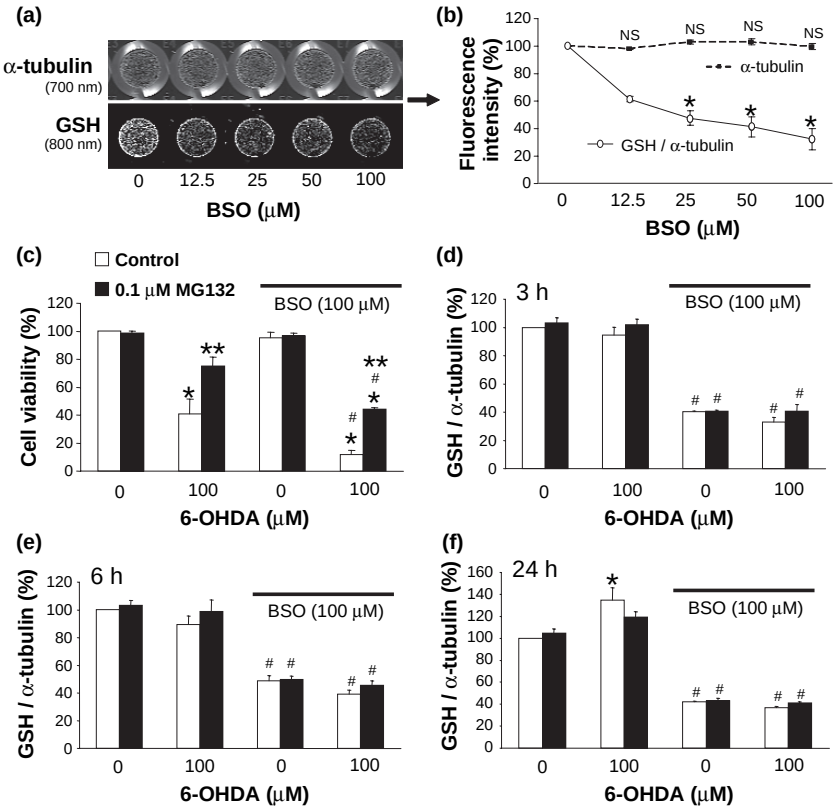

Fig. 5 Glutathione (GSH) depletion did not attenuate protection conferred by chronic MG132. (a) Development of infrared In Cell Western assay for total GSH levels, showing same plate wells dual-stained for mouse anti-α-tubulin primary (labeled with 700 nm goat anti-mouse secondary) and rabbit anti-total GSH primary (800 nm goat anti-rabbit secondary). Note that measurements are of the interior of each well, which excludes the background fluorescence of the walls in the 700 nm channel. GSH levels dropped with increasing concentrations of buthionine sulfoximine (BSO; 24 h) without similar effect upon α-tubulin levels at these doses. Quantification of GSH (solid line, white circles) and α-tubulin levels (dashed line, black squares) is depicted in (b). GSH is expressed as a percentage of α-tubulin levels within the same wells across three independent experiments. (c) BSO exacerbated 6-OHDA toxicity but did not affect the degree of protection conferred by MG132. Cells were treated with BSO (all bars under solid black line) or an equal volume of PBS (remaining bars) for 24 h before 6-OHDA or vehicle (30 min). 6-OHDA was removed and cells then left in BSO for an additional 24 h before viability assay with Cell Titer Glo. (D-F) show In Cell Western data for GSH levels at 3, 6, and 24 h after 6-OHDA removal. Cells were treated precisely in the same format as in (c). MG132 did not increase GSH levels and BSO depleted GSH to the same extent in both naïve control and MG132 treated cells at every timepoint. Data are mean + SEM from three to four independent experiments. Bonferroni *post hoc* following ANOVA: $^{*}p < 0.05$ versus no BSO in (b) and versus same group without 6-OHDA in (c–f), $^{**}p < 0.05$ versus adjacent white bar of naïve control cells, and $^{\#}p < 0.05$ versus same group without BSO in (c–f).

and illustrated in Fig. 5a and b. An immunocytochemical method such as this will not discriminate free GSH from GSH-protein adducts, but one would expect both measures to rise and fall in parallel under most circumstances. First we verified in naïve controls that BSO treatment for 24 h reduced the GSH signal in a concentration-dependent manner without affecting cell density (12.5–100 μM). Higher concentrations of BSO resulted in loss of α-tubulin signal (data not shown), thus, we chose the 100 μM concentration for our following experiments.

Naïve and MG132 treated cells were then exposed to BSO ± 6-OHDA or their respective vehicles to examine whether GSH depletion would attenuate protection (Fig. 5c). However, BSO significantly exacerbated the toxicity of 6-OHDA in both control and MG132 treated cells to the same extent (29% BSO-induced drop in naïve cells and 31% drop in MG132 treated cells), failing to reduce the extent of MG132-induced protection against 6-OHDA (34% rise in viability in the absence of BSO and 32% rise in viability in the presence of BSO). BSO had no effect upon basal viability by itself in either group, as expected from the lack of effect upon α-tubulin signal noted above.

To ensure that BSO actually reduced GSH to the same extent in both control and MG132 treated cells, both groups were assayed for GSH after BSO ± 6-OHDA or their respective vehicles, 3, 6, and 24 h later (Fig. 5d–f). How-

ever, we found that the difference in GSH between naïve and MG132 pre-treated cells was not statistically significant under any treatment condition. Indeed, BSO resulted in ~60% loss of GSH at each time irrespective of treatment group. At 24 h, there was a significant 6-OHDA induced rise in GSH levels in control cells not treated with BSO, an effect of 6-OHDA which did not quite reach significance in cells treated with MG132 (Bonferroni *post hoc*: $p = 0.08$) (Fig. 5f).

CuZnSOD, MnSOD, catalase, and Hsp70 were higher in MG132 treated cells

6-Hydroxydopamine has been shown to generate the superoxide radical (Heikkila and Cohen 1973) and is commonly used to model intracellular toxicity caused by oxidative stress. Therefore, protection against 6-OHDA might be expected to be provided by antioxidant enzymes, prominent among which are cytosolic CuZnSOD (Asanuma *et al.* 1998; Pong *et al.* 2000; Barkats *et al.* 2002), mitochondrial MnSOD (Callio *et al.* 2005), and catalase (Tiffany-Castiglioni *et al.* 1982; Hanrott *et al.* 2006; Saito *et al.* 2007). We thus began to determine whether these protective enzymes were higher in MG132 chronically treated cells with immunoblotting, and found significantly higher levels of MnSOD (21%), CuZnSOD (55%), and catalase (15%) following MG132 treatment (Fig. 6). Hsp70 is known to rise upon cellular exposure to misfolded proteins, such as would be expected to occur after treatment with MG132 (Bush *et al.* 1997; Lee and Goldberg 1998b). Therefore, we also measured inducible Hsp70 levels by immunoblotting, and found that levels of Hsp70 were 42% higher in MG132 treated cells (Fig. 6). In contrast, no significant change in another chaperone, Hsp25, was observed (data not shown).

CuZnSOD down-regulation by RNA interference attenuated MG132 induced protection against 6-OHDA

CuZnSOD has a high level of endogenous expression in nigral DA neurons (Zhang *et al.* 1993; Kunikowska and Jenner 2001, 2003), and has been shown to be protective against 6-OHDA (Asanuma *et al.* 1998; Pong *et al.* 2000; Barkats *et al.* 2002). We thus focused our attention on the next hypothesis that CuZnSOD played a key role in the protection afforded by MG132. First we examined SOD activity to determine whether it increased in parallel to the MG132-induced increase observed in SOD proteins. We observed that CuZnSOD activity was increased by 40% (Fig. 7a). This was not accompanied by a detectable change in MnSOD activity, suggesting that the modest rise in MnSOD apparent by immunoblotting was beyond the sensitivity of the activity assay or that it did not represent an increase of active protein. Cells harvested over the course of the initial 2 weeks in MG132 were also probed for CuZnSOD levels. A slow incremental rise was found – 100% for controls, 123% ± 10 at 4 days, 128% ± 9 at 8 days, and 147% ± 4 at > 14 days spent in 0.1 μM MG132 (four independent observations, $p < 0.05$, Bonferroni *post hoc*). Ubiquitin-conjugated protein levels also rose progressively, but with the higher variability also apparent in Fig. 2 – 100% for controls, 111% ± 9 at 4 days, 121% ± 16 at 8 days, and 140% ± 25% for 14+ days (four independent observations).

Finally, to test whether there was indeed a causal relationship between protection and CuZnSOD levels, we

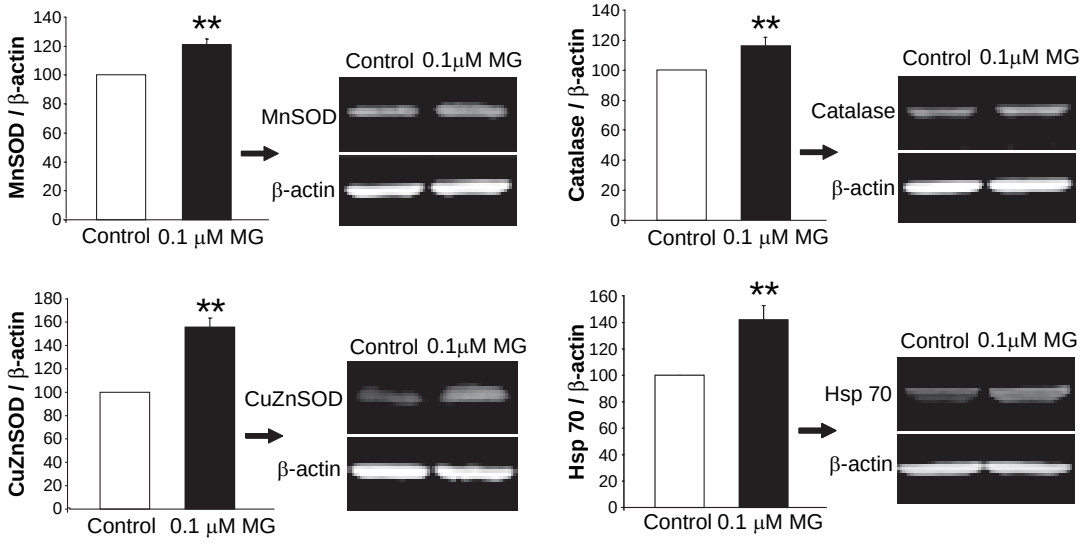

Fig. 6 Chronic MG132 was associated with higher protein levels of three antioxidant enzymes and a stress-responsive chaperone. (a) Protein levels of SODs, catalase, and inducible Hsp70 were assessed by western immunoblotting with infrared secondary probes. β-Actin served as a loading control. Data are presented as mean + SEM from three to seven independent experiments. Two-tailed *t*-test: $^{**}p < 0.05$ versus control naïve cells.

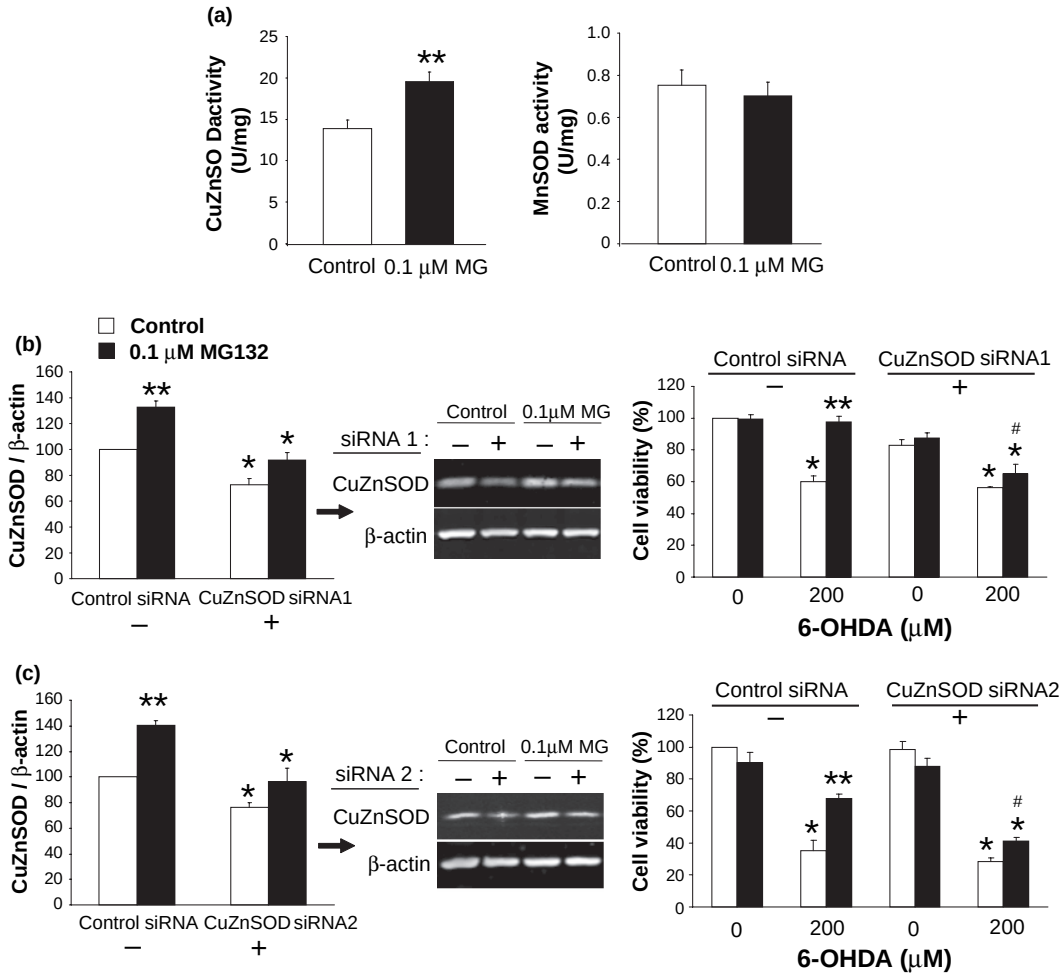

Fig. 7 CuZnSOD activity levels are increased with MG132 and CuZnSOD knockdown attenuated protection against oxidative stress. (a) SOD enzyme activity assays for CuZn and MnSOD showed an increase in the activity of the former. For SOD activity, 1 U is the amount of enzyme needed to exhibit 53% dismutation of the superoxide radical. Two-tailed *t*-test: $^{**}p < 0.05$ versus control naïve cells. (b and c) On the left are shown quantification of western immunoblots with negative control siRNA (–) or CuZnSOD siRNA (+) in naïve control (white bars) and chronic MG132-treated cells (black bars). A dose of siRNA that knocked down CuZnSOD levels back to near control values 24 h later was purposely chosen for these experiments (31 pmol/cm^2 for both sequences). (b) Illustrates data with sequence 1 from Qiagen Inc. and (c) illustrates sequence 2 from Dharmacon. On the right are Cell Titer Glo viability data 24 h after 6-OHDA treatment. 6-OHDA was applied 24 h following either CuZnSOD siRNA or the same dose of control siRNA (31 pmol/cm^2, 88 nM). CuZnSOD siRNA treatment successfully attenuated the MG132-induced rise in viability relative to side-by-side controls. Data are presented as mean + SEM from three independent experiments. Bonferroni *post hoc* following ANOVA: $^{*}p < 0.05$ versus same group with control siRNA in immunoblots on left, and versus same group without 6-OHDA in viability data on right in (b and c), $^{**}p < 0.05$ versus adjacent white bar of naïve control cells in (a–c), and $^{\#}p < 0.05$ versus same group with control siRNA in viability data on the right in (b and c).

used RNA interference with two independent sequences. So as to minimize adverse effects upon basal viability by loss of a protective molecule, we strove to achieve knockdown only to the basal values of naïve control cells. For this, a small pilot immunoblotting study was undertaken to yield information on siRNA dose and knockdown temporal profile. Using these preliminary data it was determined with both sequences that 31 pmol/cm^2 of siRNA reduced CuZnSOD levels in MG132 treated cells to near-control values at 24 h (Fig. 7b and c, left panels), the chosen time of 6-OHDA treatment for the viability experiments presented below.

For each sequence, we repeated the siRNA knockdown for 6-OHDA toxicity studies with the same concentration (31 pmol/cm^2 or 88 nM siRNA). 6-OHDA was administered at 200 μM because of increased confluence expected of the Lipofectamine protocol, 24 h after siRNA treatment and cell viability was measured as usual 24 h thereafter. Knockdown with either sequence resulted in significant loss of MG132-induced protection against 6-OHDA, in that we observed a

32% drop with siRNA sequence 1 and a 27% drop with siRNA sequence 2 (Fig. 7b and c, right panels). CuZnSOD knockdown thus rendered MG132 treated cells comparable with controls in their sensitivity to oxidative stress. Slight differences in viability between the two siRNA sequences may be attributable both to differences in siRNA transfection efficiency and in the toxicity of 6-OHDA and MG132 batches (see Materials and methods). In contrast to findings with BSO where basal GSH levels were dropped by 60% (see Fig. 5), the slight CuZnSOD knockdown in naïve controls with either sequence failed to significantly affect their response to 6-OHDA.

Discussion

Characterization of model and effect of MG132 on cellular resilience

We began by characterizing our new model of chronic stress. First the MG132 treatment did not produce overt changes in cellular morphology or TH expression, nor were signs of neurite extension or differentiation observed over the course of 6 months. Second, we showed that MG132 in this paradigm inhibited chymotrypsin-like proteasome activity by 47%, as measured by a highly specific assay for the cytosolic 26S particle (Kisselev and Goldberg 2005). A statistical trend towards an average 42% rise in levels of ubiquitin-conjugated proteins was observed (two-tailed p value of 0.076 and one-tailed p value of 0.038). Exposure to MG132 was then found to protect against 6-OHDA, with the protection developing over the course of 2 weeks. Protection was verified by two independent assays – cell counts (Hoechst-stained live nuclei) and an index of ATP levels (Cell Titer Glo). We also observed that chronic MG132 exposure decreased the toxic effects of a much higher concentration of MG132, a treatment which would not rely upon the DA transporter for inducing toxicity and was suggestive of non-specific "cross-tolerance" (see below). Finally, nomifensine-sensitive uptake through the high-affinity DA transporter was slightly increased by MG132 (36%). This latter finding suggested that any MG132-induced protection against 6-OHDA could not be readily explained by reductions in DA transporter function. In sum, the reduction in the toxic effects of both 6-OHDA and high-dose MG132 as measured by two independent assays is suggestive of a non-specific cross-tolerance against multiple types of injury. Interestingly, a previous preconditioning study of ours showed that acute sublethal 6-OHDA also induced cross-tolerance against normally toxic levels of MG132 (Leak *et al.* 2006).

The possible involvement of cathepsins and calpains, in addition to the proteasome, in our MG132 model system would be expected to increase damaged proteins and cellular stress as well, and was not viewed as undesirable for our particular questions. Nevertheless, in preliminary studies we also found that epoxomicin, still believed to be more specific than MG132, elicited protection against 6-OHDA, but within a narrow range of concentration (~1.25 nM). This is consistent with previous work showing that epoxomicin and lactacystin are protective against oxidative insults in other models (Lee *et al.* 2004; van Leyen *et al.* 2005), although these other models did not involve chronic pre-treatments. At higher doses (> 2.5 nM) epoxomicin led to cell death of the entire population over the course of 2 or more weeks. We emphasize here that in our model, high enough stress levels are expected to cause an *exacerbation* of toxicity instead of protection, in an inverted U-shaped dose–response curve. For example, one study on SH-SY5Y cells noted that 200 μM MG132 potentiated 50 μM 6-OHDA toxicity (Elkon *et al.* 2001). In PC12 cells, we similarly found that higher concentrations of MG132 (4 μM) actually exacerbated 6-OHDA toxicity, doubling the drop in viability after 50 μM 6-OHDA (19% loss in ATP in control cells and 40% loss with high dose MG132).

In our PC12 model, in contrast to long-term exposures to MG132 of 14 days or longer, short-term, 24 h exposure was insufficient to elicit any protection, and protection was submaximal with exposure to 4 and 8 days of MG132. Protection was still apparent 48 h after removal of the 6-OHDA challenge. In contrast, removal of the MG132 stimulus for 14 days resulted in a complete loss of acquired adaptive defenses and a reversal to the original state of vulnerability to 6-OHDA. These data suggest that the effect does not appear to represent delay of inevitable 6-OHDA-induced cell death but that the stimulus must be prolonged and maintained for this adaptive response.

Mechanism of protection against 6-OHDA

In an effort to determine the mechanism underlying the protection against reactive oxygen species conferred by chronic MG132, we first examined GSH antioxidant defenses. We observed that 100 μM BSO, which reduced overall GSH levels by 60%, did not affect the degree of MG132-induced protection against 6-OHDA at all. Instead, it successfully enhanced the toxicity of 6-OHDA in both control and MG132 treated cells by almost precisely the same extent, showing that the overall levels of GSH were not simply in excess of cellular requirements in this paradigm. 6-OHDA treatment caused a slight increase in GSH levels in naïve cells 24 h following removal, perhaps as an adaptive response to oxidative injury. In contrast, MG132 did not cause a significant change in GSH levels from that of control cells under any treatment condition. Therefore, we conclude that GSH was equally important for defense against oxidative stress in both control and MG132 treated groups, and that protection arising from MG132 exposure *per se* was unrelated to GSH. These findings are important in light of the well-known drop in GSH levels in the substantia nigra in

early PD (Dexter *et al.* 1994), and illustrate that cells, at least initially, are able to rely upon alternate pathways for adaptive defenses in the face of extensive GSH loss.

Next, we examined four well-known defensive proteins – catalase, MnSOD, CuZnSOD and Hsp70 – and found levels of each to be significantly higher in MG132 treated cells. No significant changes in Hsp25 or TH levels argue against global, non-specific changes. In our study, we have no evidence regarding whether the above changes represent an increase in protein synthesis, a decrease in protein degradation, or both. However, microarray studies have shown transcriptional changes with proteasome inhibitors (Yew *et al.* 2005), and previous studies reported an increase in Hsp mRNA with MG132 (Bush *et al.* 1997; Lee and Goldberg 1998b). Furthermore, a recent *Arabidopsis* study revealed that microRNA suppression of CuZnSOD gene expression is released by oxidative stress and plays a critical role in the subsequent induction of stress-induced tolerance (Sunkar *et al.* 2006).

As blotting revealed a trend towards a rise in ubiquitinated proteins, which could have included CuZnSOD (Kabuta *et al.* 2006), one might wonder whether the defensive proteins assayed were actually functional. This hypothesis was inconsistent with our observations that functional enzyme activity levels of CuZnSOD were higher with MG132 and that knockdown of CuZnSOD with each of two independent siRNA sequences attenuated protection. We reasoned that knockdown of CuZnSOD levels to approximate that of naïve controls would minimize adverse effects upon basal viability and allow some CuZnSOD to be present for normal homeostatic function. This strategy also allowed us to test whether similar 6-OHDA induced toxicity values would then arise as in controls. Overall, the data support the hypothesis that CuZnSOD, but not GSH, mediated chronic MG132-induced protection. Whether catalase and Hsp70 similarly contribute to chronic stress-induced protection remains to be determined.

Prior studies have used virally mediated or transgenic over-expression of CuZnSOD to examine whether this protein can be protective in models of PD (Przedborski *et al.* 1992; Asanuma *et al.* 1998; Barkats *et al.* 2002, 2006; Choi *et al.* 2006; Wang *et al.* 2006). One *in vivo* study of CuZnSOD knockouts showed increased DA terminal degeneration in a PD model (Zhang *et al.* 2000). Our present study extends such observations by indicating that dopaminergic cells faced with long-term stress also use this enzyme for *endogenous* self-defense. There is a prominent loss of CuZnSOD mRNA from the ventral midbrain in 6-OHDA-treated rats, MPTP-treated monkeys, and human PD (Kunikowska and Jenner 2001, 2003), as well as anatomical observations of high endogenous expression of CuZnSOD within melanized human DA neurons (Zhang *et al.* 1993). Thus, it can be speculated that endogenous CuZnSOD plays a critical role in self-protecting DA neurons. Whether this enzyme is higher in DA cells experiencing high levels of damaged proteins *in vivo* is not clear, but with our novel findings we suggest that CuZnSOD is worthy of detailed characterization across all the brain regions exhibiting synuclein-positive inclusions, preferably as a function of the Braak staging of PD (Braak *et al.* 2003).

Implications for *in vivo* studies of proteasome inhibition

Studies involving the intracerebral administration of proteasome inhibitors typically find dopaminergic cell death rather than protection (Fornai *et al.* 2003; McNaught *et al.* 2003; McNaught 2004; Miwa *et al.* 2005; Schapira *et al.* 2006; Sun *et al.* 2006), although a large number of studies with systemic treatments failed to find toxicity (Beal and Lang 2006). In contrast, a few studies actually show protection of DA neurons with intracerebral proteasome inhibitors (Sawada *et al.* 2004; Inden *et al.* 2005). Such varying effects of proteasome inhibitors have been discussed as concentration dependent, with low doses eliciting adaptive responses (Lin *et al.* 1998; Sawada *et al.* 2004; Setsuie *et al.* 2005) as seen in the present study. Our findings also carry some implications for the use of proteasome inhibitors in cancer treatment (Zavrski *et al.* 2007), for they suggest that there may be a "paradoxical" resilience in those tumor cells that fail to experience high enough concentrations of the drug.

Conclusions

The motor symptoms of PD progress slowly despite a reduction in nigral proteasome activity (McNaught *et al.* 2003). The present report examined whether PC12 cells might adapt to chronic MG132, a treatment that dropped chymotrypsin activity by 47% and was expected to increase levels of cellular stress. MG132 at a sublethal dose of 0.1 μM did not appear to affect cell growth rates and rendered PC12 cells resistant to both the oxidative toxicity of 6-OHDA (100 and 200 μM) and to normally lethal concentrations of MG132 (40 μM). The decrease in 6-OHDA vulnerability was independent of GSH but was associated with higher levels of several defensive proteins. Evidence was then obtained suggesting that enzymatically active CuZnSOD played a key role in MG132-induced resilience to oxidative stress. When considered together with similar reports in the literature, these data indicate that the ability to mount defensive responses to injury is a fundamental and intrinsic cellular property. Whether similar adaptations serve to reduce the incidence of neurodegenerative diseases and delay its appearance in those that develop such conditions in their older years deserves further examination. Our results also raise the possibility that increasing endogenous defenses through drug treatment or gene therapy will delay the progression of such illnesses even further.

Acknowledgements

The research described herein was supported by Grants from the National Institute of Neurological Disorders and Stroke (NS19608) and the US Army (ERMS#03281022) to MJZ. We thank Donald B. DeFranco, Juliann D. Jaumotte, and Ruth G. Perez for helpful discussions and Gonzalo E. Torres for providing stably transfected PC12 cells.

References

Asanuma M., Hirata H. and Cadet J. L. (1998) Attenuation of 6-hydroxydopamine-induced dopaminergic nigrostriatal lesions in superoxide dismutase transgenic mice. *Neuroscience* **85**, 907–917.

Barkats M., Millecamps S., Bilang-Bleuel A. and Mallet J. (2002) Neuronal transfer of the human Cu/Zn superoxide dismutase gene increases the resistance of dopaminergic neurons to 6-hydroxydopamine. *J. Neurochem.* **82**, 101–109.

Barkats M., Horellou P., Colin P., Millecamps S., Faucon-Biguet N. and Mallet J. (2006) 1-Methyl-4-phenylpyridinium neurotoxicity is attenuated by adenoviral gene transfer of human Cu/Zn superoxide dismutase. *J. Neurosci. Res.* **83**, 233–242.

Beal F. and Lang A. (2006) The proteasomal inhibition model of Parkinson's disease: ''boon or bust''? *Ann. Neurol.* **60**, 158–161.

Braak H., Del Tredici K., Rub U., de Vos R. A., Jansen Steur E. N. and Braak E. (2003) Staging of brain pathology related to sporadic Parkinson's disease. *Neurobiol. Aging* **24**, 197–211.

Bush K. T., Goldberg A. L. and Nigam S. K. (1997) Proteasome inhibition leads to a heat-shock response, induction of endoplasmic reticulum chaperones, and thermotolerance. *J. Biol. Chem.* **272**, 9086–9092.

Callio J., Oury T. D. and Chu C. T. (2005) Manganese superoxide dismutase protects against 6-hydroxydopamine injury in mouse brains. *J. Biol. Chem.* **280**, 18536–18542.

Choi H. S., An J. J., Kim S. Y. *et al.* (2006) PEP-1-SOD fusion protein efficiently protects against paraquat-induced dopaminergic neuron damage in a Parkinson disease mouse model. *Free Radic. Biol. Med.* **41**, 1058–1068.

Clement M. V., Long L. H., Ramalingam J. and Halliwell B. (2002) The cytotoxicity of dopamine may be an artefact of cell culture. *J. Neurochem.* **81**, 414–421.

Conconi M., Szweda L. I., Levine R. L., Stadtman E. R. and Friguet B. (1996) Age-related decline of rat liver multicatalytic proteinase activity and protection from oxidative inactivation by heat-shock protein 90. *Arch. Biochem. Biophys.* **331**, 232–240.

Dexter D. T., Sian J., Rose S. *et al.* (1994) Indices of oxidative stress and mitochondrial function in individuals with incidental Lewy body disease. *Ann. Neurol.* **35**, 38–44.

Ding Q., Dimayuga E., Martin S., Bruce-Keller A. J., Nukala V., Cuervo A. M. and Keller J. N. (2003) Characterization of chronic low-level proteasome inhibition on neural homeostasis. *J. Neurochem.* **86**, 489–497.

Ding Y. M., Jaumotte J. D., Signore A. P. and Zigmond M. J. (2004) Effects of 6-hydroxydopamine on primary cultures of substantia nigra: specific damage to dopamine neurons and the impact of glial cell line-derived neurotrophic factor. *J. Neurochem.* **89**, 776–787.

Elkon H., Melamed E. and Offen D. (2001) 6-Hydroxydopamine increases ubiquitin-conjugates and protein degradation: implications for the pathogenesis of Parkinson's disease. *Cell. Mol. Neurobiol.* **21**, 771–781.

Fornai F., Lenzi P., Gesi M. *et al.* (2003) Fine structure and biochemical mechanisms underlying nigrostriatal inclusions and cell death after proteasome inhibition. *J. Neurosci.* **23**, 8955–8966.

Friguet B., Bulteau A. L., Chondrogianni N., Conconi M. and Petropoulos I. (2000) Protein degradation by the proteasome and its implications in aging. *Ann. NY Acad. Sci.* **908**, 143–154.

Fuertes G., Martin De Llano J. J., Villarroya A., Rivett A. J. and Knecht E. (2003) Changes in the proteolytic activities of proteasomes and lysosomes in human fibroblasts produced by serum withdrawal, amino-acid deprivation and confluent conditions. *Biochem. J.* **375**, 75–86.

Fujimuro M., Sawada H. and Yokosawa H. (1994) Production and characterization of monoclonal antibodies specific to multi-ubiquitin chains of polyubiquitinated proteins. *FEBS Lett.* **349**, 173–180.

Hanrott K., Gudmunsen L., O'Neill M. J. and Wonnacott S. (2006) 6-Hydroxydopamine-induced apoptosis is mediated via extracellular auto-oxidation and caspase 3-dependent activation of protein kinase Cdelta. *J. Biol. Chem.* **281**, 5373–5382.

Heikkila R. E. and Cohen G. (1973) 6-Hydroxydopamine: evidence for superoxide radical as an oxidative intermediate. *Science* **181**, 456–457.

Inden M., Kondo J., Kitamura Y., Takata K., Nishimura K., Taniguchi T., Sawada H. and Shimohama S. (2005) Proteasome inhibitors protect against degeneration of nigral dopaminergic neurons in hemiparkinsonian rats. *J. Pharmacol. Sci.* **97**, 203–211.

Kabuta T., Suzuki Y. and Wada K. (2006) Degradation of amyotrophic lateral sclerosis-linked mutant Cu,Zn-superoxide dismutase proteins by macroautophagy and the proteasome. *J. Biol. Chem.* **281**, 30524–30533.

Keck S., Nitsch R., Grune T. and Ullrich O. (2003) Proteasome inhibition by paired helical filament-tau in brains of patients with Alzheimer's disease. *J. Neurochem.* **85**, 115–122.

Keller J. N., Hanni K. B. and Markesbery W. R. (2000a) Impaired proteasome function in Alzheimer's disease. *J. Neurochem.* **75**, 436–439.

Keller J. N., Huang F. F. and Markesbery W. R. (2000b) Decreased levels of proteasome activity and proteasome expression in aging spinal cord. *Neuroscience* **98**, 149–156.

Kisselev A. F. and Goldberg A. L. (2001) Proteasome inhibitors: from research tools to drug candidates. *Chem. Biol.* **8**, 739–758.

Kisselev A. F. and Goldberg A. L. (2005) Monitoring activity and inhibition of 26S proteasomes with fluorogenic peptide substrates. *Methods Enzymol.* **398**, 364–378.

Kitagawa K., Matsumoto M., Tagaya M. *et al.* (1990) 'Ischemic tolerance' phenomenon found in the brain. *Brain Res.* **528**, 21–24.

Kunikowska G. and Jenner P. (2001) 6-Hydroxydopamine-lesioning of the nigrostriatal pathway in rats alters basal ganglia mRNA for copper, zinc- and manganese-superoxide dismutase, but not glutathione peroxidase. *Brain Res.* **922**, 51–64.

Kunikowska G. and Jenner P. (2003) Alterations in m-RNA expression for Cu,Zn-superoxide dismutase and glutathione peroxidase in the basal ganglia of MPTP-treated marmosets and patients with Parkinson's disease. *Brain Res.* **968**, 206–218.

Leak R. K., Liou A. K. and Zigmond M. J. (2006) Effect of sublethal 6-hydroxydopamine on the response to subsequent oxidative stress in dopaminergic cells: evidence for preconditioning. *J. Neurochem.* **99**, 1151–1163.

Lee D. H. and Goldberg A. L. (1998a) Proteasome inhibitors: valuable new tools for cell biologists. *Trends Cell Biol.* **8**, 397–403.

Lee D. H. and Goldberg A. L. (1998b) Proteasome inhibitors cause induction of heat shock proteins and trehalose, which together confer thermotolerance in *Saccharomyces cerevisiae*. *Mol. Cell. Biol.* **18**, 30–38.

Lee C. S., Tee L. Y., Warmke T., Vinjamoori A., Cai A., Fagan A. M. and Snider B. J. (2004) A proteasomal stress response: pre-treatment with proteasome inhibitors increases proteasome activity and

reduces neuronal vulnerability to oxidative injury. *J. Neurochem.* **91**, 996–1006.

van Leyen K., Siddiq A., Ratan R. R. and Lo E. H. (2005) Proteasome inhibition protects HT22 neuronal cells from oxidative glutamate toxicity. *J. Neurochem.* **92**, 824–830.

Lin K. I., Baraban J. M. and Ratan R. R. (1998) Inhibition versus induction of apoptosis by proteasome inhibitors depends on concentration. *Cell Death Differ.* **5**, 577–583.

Lin E., Cavanaugh J. E., Leak R. K., Perez R. G. and Zigmond M. J. (2008) Rapid activation of ERK by 6-hydroxydopamine promotes survival of dopaminergic cells. *J. Neurosci. Res.* **86**, 108–117.

Lopez Salon M., Morelli L., Castano E. M., Soto E. F. and Pasquini J. M. (2000) Defective ubiquitination of cerebral proteins in Alzheimer's disease. *J. Neurosci. Res.* **62**, 302–310.

McNaught K. S. (2004) Proteolytic dysfunction in neurodegenerative disorders. *Int. Rev. Neurobiol.* **62**, 95–119.

McNaught K. S., Belizaire R., Isacson O., Jenner P. and Olanow C. W. (2003) Altered proteasomal function in sporadic Parkinson's disease. *Exp. Neurol.* **179**, 38–46.

McNaught K. S., Bjorklund L. M., Belizaire R., Isacson O., Jenner P. and Olanow C. W. (2002) Proteasome inhibition causes nigral degeneration with inclusion bodies in rats. *Neuroreport* **13**, 1437–1441.

Merker K., Stolzing A. and Grune T. (2001) Proteolysis, caloric restriction and aging. *Mech. Ageing Dev.* **122**, 595–615.

Miwa H., Kubo T., Suzuki A., Nishi K. and Kondo T. (2005) Retrograde dopaminergic neuron degeneration following intrastriatal proteasome inhibition. *Neurosci. Lett.* **380**, 93–98.

Murry C. E., Jennings R. B. and Reimer K. A. (1986) Preconditioning with ischemia: a delay of lethal cell injury in ischemic myocardium. *Circulation* **74**, 1124–1136.

Mytilineou C., McNaught K. S., Shashidharan P., Yabut J., Baptiste R. J., Parnandi A. and Olanow C. W. (2004) Inhibition of proteasome activity sensitizes dopamine neurons to protein alterations and oxidative stress. *J. Neurol. Transm.* **111**, 1237–1251.

Ohtake F., Baba A., Takada I. *et al.* (2007) Dioxin receptor is a ligand-dependent E3 ubiquitin ligase. *Nature* **446**, 562–566.

Pong K., Doctrow S. R. and Baudry M. (2000) Prevention of 1-methyl-4-phenylpyridinium- and 6-hydroxydopamine-induced nitration of tyrosine hydroxylase and neurotoxicity by EUK-134, a superoxide dismutase and catalase mimetic, in cultured dopaminergic neurons. *Brain Res.* **881**, 182–189.

Przedborski S., Kostic V., Jackson-Lewis V., Naini A. B., Simonetti S., Fahn S., Carlson E., Epstein C. J. and Cadet J. L. (1992) Transgenic mice with increased Cu/Zn-superoxide dismutase activity are resistant to N-methyl-4-phenyl-1,2,3,6-tetrahydropyridine-induced neurotoxicity. *J. Neurosci.* **12**, 1658–1667.

Rideout H. J., Larsen K. E., Sulzer D. and Stefanis L. (2001) Proteasomal inhibition leads to formation of ubiquitin/alpha-synuclein-immunoreactive inclusions in PC12 cells. *J. Neurochem.* **78**, 899–908.

Rideout H. J., Lang-Rollin I. C., Savalle M. and Stefanis L. (2005) Dopaminergic neurons in rat ventral midbrain cultures undergo selective apoptosis and form inclusions, but do not up-regulate iHSP70, following proteasomal inhibition. *J. Neurochem.* **93**, 1304–1313.

Rodgers K. J. and Dean R. T. (2003) Assessment of proteasome activity in cell lysates and tissue homogenates using peptide substrates. *Int. J. Biochem. Cell Biol.* **35**, 716–727.

Saggu H., Cooksey J., Dexter D., Wells F. R., Lees A., Jenner P. and Marsden C. D. (1989) A selective increase in particulate superoxide dismutase activity in parkinsonian substantia nigra. *J. Neurochem.* **53**, 692–697.

Saito Y., Nishio K., Ogawa Y., Kinumi T., Yoshida Y., Masuo Y. and Niki E. (2007) Molecular mechanisms of 6-hydroxydopamine-induced cytotoxicity in PC12 cells: involvement of hydrogen peroxide-dependent and -independent action. *Free Radic. Biol. Med.* **42**, 675–685.

Sawada H., Kohno R., Kihara T. *et al.* (2004) Proteasome mediates dopaminergic neuronal degeneration, and its inhibition causes alpha-synuclein inclusions. *J. Biol. Chem.* **279**, 10710–10719.

Schapira A. H., Cleeter M. W., Muddle J. R., Workman J. M., Cooper J. M. and King R. H. (2006) Proteasomal inhibition causes loss of nigral tyrosine hydroxylase neurons. *Ann. Neurol.* **60**, 253–255.

Setsuie R., Kabuta T. and Wada K. (2005) Does proteasome [corrected] inhibition decrease or accelerate toxin-induced dopaminergic neurodegeneration? *J. Pharmacol. Sci.* **97**, 457–460.

Sun F., Anantharam V., Zhang D., Latchoumycandane C., Kanthasamy A. and Kanthasamy A. G. (2006) Proteasome inhibitor MG-132 induces dopaminergic degeneration in cell culture and animal models. *Neurotoxicology* **27**, 807–815.

Sunkar R., Kapoor A. and Zhu J. K. (2006) Posttranscriptional induction of two Cu/Zn superoxide dismutase genes in *Arabidopsis* is mediated by downregulation of miR398 and important for oxidative stress tolerance. *Plant Cell* **18**, 2051–2065.

Tiffany-Castiglioni E., Saneto R. P., Proctor P. H. and Perez-Polo J. R. (1982) Participation of active oxygen species in 6-hydroxydopamine toxicity to a human neuroblastoma cell line. *Biochem. Pharmacol.* **31**, 181–188.

Wang D., Qian L., Xiong H., Liu J., Neckameyer W. S., Oldham S., Xia K., Wang J., Bodmer R. and Zhang Z. (2006) Antioxidants protect PINK1-dependent dopaminergic neurons in Drosophila. *Proc. Natl Acad. Sci. USA* **103**, 13520–13525.

Yamamoto N., Sawada H., Izumi Y., Kume T., Katsuki H., Shimohama S. and Akaike A. (2007) Proteasome inhibition induces glutathione synthesis and protects cells from oxidative stress: relevance to Parkinson disease. *J. Biol. Chem.* **282**, 4364–4372.

Yew E. H., Cheung N. S., Choy M. S. *et al.* (2005) Proteasome inhibition by lactacystin in primary neuronal cells induces both potentially neuroprotective and pro-apoptotic transcriptional responses: a microarray analysis. *J. Neurochem.* **94**, 943–956.

Zavrski I., Jakob C., Kaiser M., Fleissner C., Heider U. and Sezer O. (2007) Molecular and clinical aspects of proteasome inhibition in the treatment of cancer. *Recent Results Cancer Res.* **176**, 165–176.

Zhang P., Damier P., Hirsch E. C., Agid Y., Ceballos-Picot I., Sinet P. M., Nicole A., Laurent M. and Javoy-Agid F. (1993) Preferential expression of superoxide dismutase messenger RNA in melanized neurons in human mesencephalon. *Neuroscience* **55**, 167–175.

Zhang J., Graham D. G., Montine T. J. and Ho Y. S. (2000) Enhanced N-methyl-4-phenyl-1,2,3,6-tetrahydropyridine toxicity in mice deficient in CuZn-superoxide dismutase or glutathione peroxidase. *J. Neuropathol. Exp. Neurol.* **59**, 53–61.

Zigmond M. J. and Keefe K. (1997) *6-Hydroxydopamine as a Tool for Studying Catecholamines in Adult Animals: Lessons From the Neostriatum*, pp 75–108. Humana Press, Totowa, NJ.

Neurobiology of Disease 32 (2008) 116–124

Contents lists available at ScienceDirect

Neurobiology of Disease

journal homepage: www.elsevier.com/locate/ynbdi

Wild-type LRRK2 but not its mutant attenuates stress-induced cell death via ERK pathway

Anthony K.F. Liou *, Rehana K. Leak, Lihua Li, Michael J. Zigmond

Pittsburgh Institute for Neurodegenerative Diseases, Department of Neurology, University of Pittsburgh School of Medicine, 3501 Fifth Avenue, BST3-7026, Pittsburgh, PA 15260, USA

ARTICLE INFO

Article history:
Received 16 August 2007
Revised 27 May 2008
Accepted 24 June 2008
Available online 8 July 2008

ABSTRACT

Leucine-rich repeat kinase 2 (LRRK2) is a recently identified gene that, when mutated at specific locations, results in the onset of parkinsonian symptoms with clinical features indistinguishable from idiopathic Parkinson's disease. Based on structural and domain analysis, LRRK2 is predicted to function as a stress-responsive protein scaffold mediating the regulation of mitogen activating protein kinase (MAPK) pathways. Consistent with this notion, our results supported the notion that expression of wild-type LRRK2 but not Y1699C or G2019S mutants enhanced the tolerance of HEK293 and SH-SY5Y cells towards H_2O_2-induced oxidative stress. This increase in stress tolerance was dependent on the presence of the kinase domain of the LRRK2 gene and manifested through the activation of the ERK pathway. Collectively, our results indicated that cells expressing LRRK2 mutants suffer a loss of protection normally derived from wild-type LRRK2, making them more vulnerable to oxidative stress.

Published by Elsevier Inc.

Introduction

Leucine-rich repeat kinase 2 (LRRK2), a member of the ROCO protein family, is a recently identified gene whose mutants have been linked to the onset of parkinsonian symptoms (Haugarvoll and Wszolek, 2006; Klein and Schlossmacher, 2006; Olanow, 2007; Whaley et al., 2006). Sequence domain analysis of this gene has revealed that the 285 kDa protein for which it encodes comprises ROC, COR, kinase, and WD40 domains, in that order, with the ROC domain beginning after the first 1000 amino acids (Jain et al., 2005; West et al., 2005). The ROC domain, with its GDP/GTP binding motif has been shown to be capable of altering the kinase activity of LRRK1, a paralog of LRRK2 (Korr et al., 2006). To date, the impact of these mutations on wild-type LRRK2 is yet unclear.

Expressions of LRRK2 mutant genes, such as Y1699C and R1441C, result in a loss of basal cell viability in SHSY5Y cells (Greggio et al., 2006; West et al., 2005) demonstrating their innate toxicity. Since G2019S and I2020T mutants show higher kinase activities than wild-type LRRK2, it has been speculated that alteration of kinase activity is involved in the manifestation of parkinsonian symptoms caused by LRRK2 mutations (Bialecka et al., 2005; Tomiyama et al., 2006; West et al., 2005). However, further investigation showed that different LRRK2 mutants have different inherent kinase activity based on an auto-phosphorylation assay. Indeed, some mutants have lower kinase activity than the wild-type counterpart. For example, it has been shown that the Y1699C mutant has lower kinase activity than wild-type LRRK2 and yet has the highest propensity to elicit the formation of protein aggregates (Greggio et al., 2006). Therefore, it is uncertain whether changes in kinase activities among the LRRK2 mutants contribute to the cause of pathology.

Phylogenetic analysis of the LRRK2 kinase domain has revealed sequence similarity to the receptor interaction protein (RIP) protein family as well as mixed lineage kinases (Meylan and Tschopp, 2005; Xu et al., 2001), raising the possibility of parallel functions among these kinases. In fact, Meylan and Tschopp (2005) have termed LRRK1 and LRRK2 as RIP6 and RIP7 respectively. Both of these kinase families participate in the signaling events in response to cellular stresses caused by various stimuli (Gloeckner et al., 2006). Therefore, it is likely that LRRK2 wild-type gene product is also involved in stress-induced signaling events leading to cell death.

In this study, our main objective was to investigate whether LRRK2 is involved in a stress-induced signaling cascade mediating cell death and, if so, to identify differential responses derived from LRRK2 wild-type, Y1699C and G2019S mutant genes in these events. Our results suggest that expression of LRRK2 wild-type or Y1699C mutant genes in HEK293 cells suppressed basal levels of activated ERK but not JNK, independent of its kinase domain. Moreover, the presence of LRRK2 wild-type gene product but not Y1699C or G2019S mutant gene product conferred protection against H_2O_2-induced cell death through activation of the ERK pathway mediated by its kinase domain in HEK293 and SH-SY5Y cells. Therefore, based on our results, this multi-functional domain LRRK2 gene is able to affect the activation of the ERK pathway.

* Corresponding author. Fax: +1 412 624 7327.
E-mail address: lioukf@upmc.edu (A.K.F. Liou).
Available online on ScienceDirect (www.sciencedirect.com).

0969-9961/$ – see front matter. Published by Elsevier Inc.
doi:10.1016/j.nbd.2008.06.016

Materials and methods

Materials

The LRRK2 wild-type, Y1699C, and G2019S mutant genes fused with GFP on their C-terminal in pCDNA3.1 expression vector were a kind gift from Dr. Matthew Farrer of the Neurogenetics Laboratories, Mayo Clinic Jacksonville. All the chemicals were obtained from Fisher Scientific (Pittsburgh, PA, USA) and all the inhibitors were obtained from BIOMOL (Plymouth Meeting, PA, USA) unless otherwise stated.

Cell culture

HEK293 cells (ATCC, Manassas, VA, USA) were maintained in DMEM media supplemented with 10% fetal bovine serum (Hyclone, Logan, UT, USA). SH-SY5Y cells, a kind gift from Dr. James P. Bennett Jr, University of Virginia were maintained in DMEM media supplemented with 10% fetal bovine serum (Hyclone, Logan, UT, USA). The cells were plated in various configurations at 80% confluence before undergoing transfection. The transfection process was performed before treatments with either inhibitors or H_2O_2.

Transfections

Transfection of various constructs into HEK293 cells were performed using Lipofectamine 2000 (Invitrogen, Carlsbad, CA, USA) in accordance with the manufacturer's instructions. In brief, cells were seeded in various configurations to yield 80% confluency. In the case of HEK293 cells, cell densities were 20,000 cells per well of a 96-well plate and 1×10^6 cells per well of a 6 cm plate. As for SH-SY5Y cells, cell densities were 100,000 cells per well of a 96-well plate and 5×10^6 cells per well of a 6 cm plates. After optimization, we found that the optimal DNA/lipofectamine ratio for HEK293 cells and SH-SY5Y cells were 1:3 and 1:2 respectively. To instigate transfection, conditioned medium was first replaced with Opti-I media (Invitrogen, Carlsbad, CA, USA). Then, the correct amounts of DNA and Lipofectamine 2000 reagent were added to Opti-I medium and incubated at room temperature for 5 min. After a further incubation at room temperature for 15 min, the DNA–lipofectamine complex was added drop-wise evenly throughout the area with cells. Then, the cells were incubated at 37 °C for 4 h before the medium was changed completely back into growth medium. The transfection efficiency was estimated by eye under fluorescence illumination to visualize GFP and compared to the total number of cells under bright field illumination for HEK293 cells typically showing at least 70% transfection efficiency. On the other hand, the transfection efficiency for SH-SY5Y cells was determined by counting GFP^+ cells over total cell number indicating that the efficiency was on average about 13%.

H_2O_2 and inhibitor treatment

Chronic treatments of H_2O_2, U0126 (BIOMOL, Plymouth Meeting, PA), were carried out after transfection when Opti-I medium was replaced with growth media. Cells were pre-treated with MEK1 inhibitor (U0126) for 1 h before H_2O_2 was introduced into the medium. Typically, total cell death was quantified by WST-1 assay and necrotic cell death as described below.

Assessment of cell survival by WST-1 assay

Cell viability of HEK293 cells was determined using the WST-1 assay kit (Roche, Penzberg, Germany) in accordance with the manufacturer's recommended protocol. In brief, after the respective treatments, the spent medium was removed, replaced with fresh growth medium, and incubated at 37 °C for 3 h. The medium was then replaced again with fresh growth medium supplemented with 10% WST-1 reagent. This was followed by an additional incubation at 37 °C for 30–60 min. Changes in cell viability were reflected by changes in optical density detected at 420 nm, which was measured using a spectrophotometer microplate reader (SpectraMax 340, Molecular Devices, Sunnyvale, CA, USA). All values in the figures were calculated from at least 2–3 independent experiments with each experiment containing at least 6–8 replicates in each experimental condition.

Assessment of necrosis by LDH assay

Necrosis is characterized by early loss of cell membrane integrity and the release of cytosolic lactate dehydrogenase (LDH). Hence, LDH release was measured in the present study to quantify necrotic cell death using the LDH assay kit developed by Pointe Scientific, Inc. (Fisher Scientific, Pittsburgh, PA, USA). In brief, 30 µl of the spent medium was collected from each treatment condition and mixed with 150 µl of reagent comprised of Reagent A and Reagent B pre-mixed in a ratio of 1:6. Changes in optical density at 340 nm were measured using a spectrophotometric microplate reader and the maximum reaction rate was calculated to reflect the LDH level in the spent medium. The percentage of LDH release under each experimental condition was then calculated against the total cellular contents of LDH in control wells. Total LDH contents were assessed by subtracting the amount of LDH in untreated cell culture medium (total viable cells) from that in cultures lysed with 1% Triton X-100 for 10 min (total release).

Assessment of cell survival by cell count post-stained with Hoechst stain

Cell density of SH-SY5Ycells expressing LRRK2 wild-type, Y1699C or G2019S mutant was determined by direct cell count due to the presence of GFP fusion to each of the genes. Twenty-four hours after treatment with H_2O_2, the cells were fixed with 4% para-formaldehyde and 4% sucrose in PBS for 20 min at room temperature. Then, the cells were permeablized with 0.1% Triton X-100 in PBS for another 20 min at room temperature. Afterwards, the cells were stained with Hoechst stain for 1 h before it was replaced with PBS. Then, the cells were observed via fluorescent microscopy. For each treatment conditions, three independent frames of the cells were captured showing cells expressing LRRK2–GFP fusion. The same frames of the cells stained with Hoechst stain to reveal total number of cells was captured too. In this way, the number of cells expressing LRRK2 (wild-type and mutants) and the total of cells were determined by direct cell count. In this manner, the percentage survival of SH-SY5Y cells expressing each of the LRRK2 genes was determined. In addition, the change in percentage survival of SH-SY5Y cells in response to H_2O_2 insult was also determined.

Deletion mutant construction in mammalian expression vector

The deletion mutants for wild-type LRRK2 and Y1699C mutant genes were created using the same approach. In each case, the gene was cut with endonucleases Cla I (New England Biolabs, Ipswich, MA, USA) and Pac I (New England Biolabs, Ipswich, MA, USA), respectively, to remove the kinase domain. Meanwhile, two oligomers of sequences "CGAGCGGCCGC-GAT" and "CGCGGCCGCT" were synthesized and annealed to form a linker with ends compatible to Cla I and Pac I sites respectively. Then, the linker was used to connect the open ends of the deleted genes giving rise to the pair of deletion mutants corresponding to LRRK2 wild-type gene and Y1699C mutant gene. The excision sites of the deletion mutants were sequenced. In addition, we retained the parental vector pCDNA3.1 and the GFP fusion at the C-terminal for the deletion mutants.

PAGE and Western blotting

Standard PAGE and Western blotting protocols recommended by Cell Signaling Technology (Danvers, MA, USA) were used in this study.

Statistical analysis

Results are reported as mean value±SEM. The significance of difference between means was assessed by ANOVA and *post hoc* Fisher's protected least significant difference (PLSD) tests, with $p<0.05$ considered statistically significant.

Results

In this study, we characterized functional differences between wild-type LRRK2 and its mutants (Y1699C and G2019S) in response to oxidative stress. We had selected HEK293 cells as host for expressing these genes as we consistently attained at least 70% transfection efficiency. In

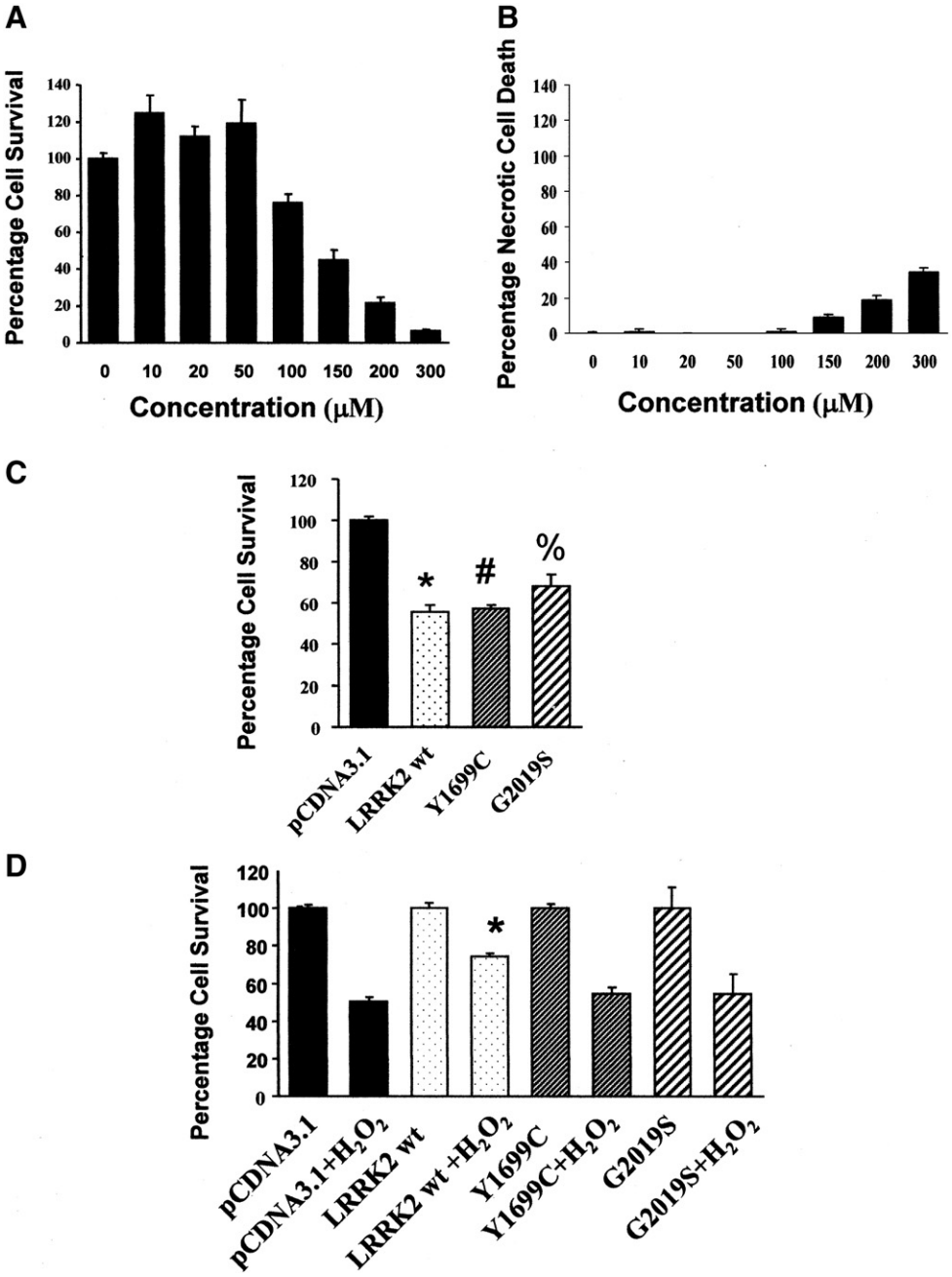

Fig. 1. Impact of wild-type LRRK2 and its mutants Y1699C and G2019S on basal cell viability and under the insult of H_2O_2 in HEK293 cells. (A) Cell survival profile in response to 0–300 μM of treatment of H_2O_2 for 18 h in HEK293 cells; (B) Changes in percentage cell death due to necrosis as estimated by LDH assay in response to 0–300 μM of treatment of H_2O_2 for 18 h in HEK293 cells; (C) Decrease in basal cell viability in HEK293 cells expressing wild-type LRRK2 and its mutants Y1699C and G2019S. Data are means±SEM, at least 24 readings per data point, from six independent experiments. *$p<0.01$, #$p<0.01$, %$p<0.01$ versus viability of cells transfected with pCDNA3.1. Statistics were derived from ANOVA and *post hoc* Fisher's protected least significant difference (PLSD) tests; (D) Attenuation of H_2O_2-induced cell death for cells expressing wild-type LRRK2 but not in cells expressing mutant Y1699C or G2019S. Percentage cell survival after H_2O_2 insult among cells transfected with pCDNA3.1, expressing wild-type LRRK2 or its mutants Y1699C and G2019S is normalized against untreated cells transfected with the same vector or expressing the same proteins. Data are means±SEM, at least 24 readings per data point, from six independent experiments. *$p<0.01$ versus viability of cells transfected with pCDNA3.1 after 150 μM of H_2O_2 treatment for 18 h. Statistics were derived from ANOVA and *post hoc* Fisher's protected least significant difference (PLSD) tests.

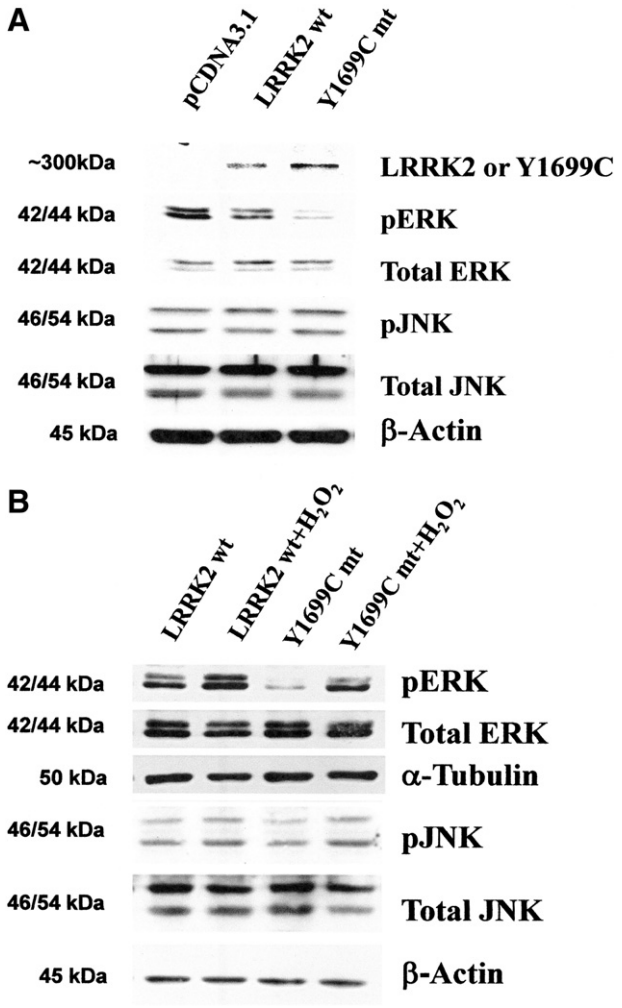

Fig. 2. Impact of expressing wild-type LRRK2 and Y1699C mutant on basal level of phospho-ERK (pERK) and phospho-JNK (pJNK). (A) Changes in basal level of pERK and pJNK in HEK293 cells expressing wild-type LRRK2 and Y1699C mutant as compared to those transfected with pCDNA3.1. In the top panel, an anti-GFP antibody was used to examine expression of wild-type LRRK2 and Y1699C mutant gene in HEK293 cells via immunoblotting. The corresponding changes in basal level of pERK, total ERK, pJNK, and total JNK are also shown and β-actin was used as a loading control; (B) Corresponding changes in pERK, total ERK, pJNK, and total JNK in HEK293 cells expressing wild-type LRRK2 or Y1699C mutant with and without chronic treatment with 150 μM of H_2O_2 for 18 h. β-Actin was used as loading control.

addition, we have also verified the consistency of the key results in neuronal SH-SY5Y cells. Since it has been reported that 6-OHDA and H_2O_2 toxicities utilized similar pathways to achieve cell death (Mazzio et al., 2004; Saito et al., 2007) and in view of its stability over 6-OHDA, we chose H_2O_2 as the source of oxidative stress to induce degeneration in our study.

Changes in basal cell viability and H_2O_2-induced cell death due to expression of wild-type LRRK2 and its mutants Y1699C and G2019S

First, we have to determine the concentration of H_2O_2 that will elicit 50% cell death (EC_{50}). When we treated HEK293 cells with H_2O_2 between 1 and 300 μM for 18 h, we obtained a dose response curve indicating that 150 μM H_2O_2 consistently elicited 50% cell death (Fig. 1A). To ascertain the mode of cell death at this condition, we then measured the corresponding percentage necrotic cell death using the LDH assay (Fig. 1B). We observed that chronic treatment with 150 μM of H_2O_2 resulted in 10% of necrotic cell death, indicating that the predominant mode of cell death at these conditions is apoptosis. Therefore, the paradigm adopted in this study was the treatment of HEK293 cells with H_2O_2 at 150 μM for 18 h.

The delivery of wild-type LRRK2, Y1699C and G2019S genes into HEK293 cells was mediated via transfection with lipofectamine 2000. After optimization, the typical transfection efficiency was at least 70% (data not shown). Comparable transfection efficiency was ensured by monitoring the expression of each LRRK2 gene with fluorescence microscopy since a GFP moiety is fused to each of their C-terminal. Twenty-four hours after transfection, we observed a consistent 30–45% drop in basal viability among cells expressing wild-type and its mutants Y1699C and G2019S with no significant difference between them (Fig. 1C). However, when the cells expressing wild-type and mutant LRRK2 genes were exposed to H_2O_2 at 150 μM for 18 h, we observed that cells expressing wild-type LRRK2 were more tolerant to H_2O_2 toxicity than were those expressing each of the mutants (Fig. 1D). In comparison, cells expressing wild-type LRRK2 experienced 50% attenuation in H_2O_2-induced cell death relative to those cells expressing Y1699C or G2019S mutants. On the other hand, there was no significant difference in the percentage cell death among cells expressing either of the mutants as well as those transfected with the parental vector pCDNA3.1. Therefore, the results suggest that Y1699C and G2019S mutants did not further exacerbate cell death in response to H_2O_2 toxicity. Since the impact on basal cell viability and in response to H_2O_2 toxicity are the same in cells expressing Y1699C and G2019S mutants, we performed more detailed investigation on the mechanistic difference between wild-type LRRK2 and Y1699C mutants in subsequent experiments.

The impact of wild-type LRRK2 and Y1699C mutants on ERK1/2

Based on structural and domain analysis, the physiological role of wild-type of LRRK2 is predicted to be a stress-responsive protein scaffold mediating the regulation of mitogen activated protein kinase (MAPK) pathways (Mata et al., 2006). Under this notion, LRRK2 must crosstalk with the proteins involving the MAP kinase cascade. Hence, we first examined changes in basal levels of phospho-ERK1/2 (pERK) and phospho-JNK (pJNK) due to expression of wild-type LRRK2 or Y1699C mutant in HEK293 cells which may suggest crosstalk between LRRK2 and the MAP kinase pathways. The lysate from cells expressing wild-type LRRK2 or Y1699C mutant as well as those transfected with parental vector pCDNA3.1 were prepared and the changes in basal levels of pERK and pJNK were determined by immunoblot analysis (Fig. 2A). The presence of wild-type LRRK2 and Y1699C mutant in HEK293 cells was also visualized by probing immunoblots with an antibody recognizing GFP (Fig. 2A, top panel).

No band was detected in lysate derived from cells transfected with pCDNA3.1 vector. We also failed to detect endogenous wild-type LRRK2 in HEK293 cells with several commercially available antibodies (data not shown). By comparison, the endogenous wild-type LRRK2 was significantly lower than those being over-expressed and hence functional changes attributed to the over-expressed LRRK2 (wild-type and mutant) would receive minimal interference from endogenous wild-type LRRK2. In comparison, the basal level of pERK was decreased in cells expressing wild-type LRRK2 and Y1699C mutant with no change to the level of total ERK1/2 (tERK) (Fig. 2A). Moreover, the decrease in the basal level of pERK in cells expressing Y1699C mutant was higher in cells expressing wild-type LRRK2. In contrast, there was no significant change in the basal level of pJNK or total JNK (tJNK) in cells expressing wild-type LRRK2 and Y1699C mutant to those transfected with pCDNA3.1. On the other hand, after 18 h of treatment with H_2O_2 at EC_{50} (150 μM), cells expressing wild-type LRRK2 consistently elicited a higher level of pERK than those expressing Y1699C mutant with no significant change in the level of tERK (Fig. 2B). As to pJNK and tJNK, there was no significant difference in their level changes in response to H_2O_2 toxicity between cells

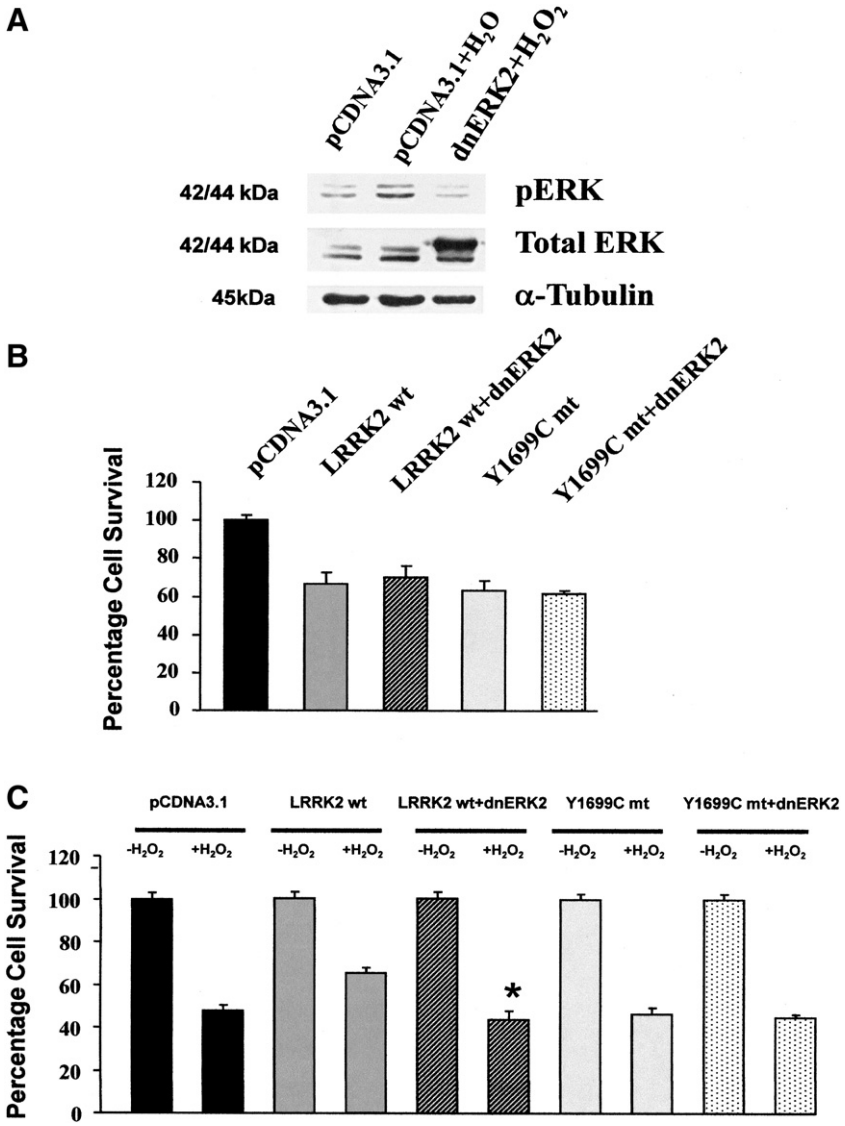

Fig. 3. Effect of co-expression of wild-type LRRK2, Y1699C mutant with dnERK2 respectively on basal cell viability and cell death in response to H_2O_2 toxicity. (A) Demonstration of the efficacy of using dnERK2 to silence ERK activation. In the top panel, cells expressing pCDNA3.1 showed activation in response to H_2O_2 (middle lane); on the other hand, cells expressing dnERK2 gene showed suppression of ERK activation under the same stimulus (right lane). The second panel indicates expression of the dnERK2 gene. α-Tubulin was used as loading control. (B) Co-expression of dnERK2 with LRRK2 wild-type gene or Y1699C mutant gene did not significantly alter the decrease in basal cell viability due to the expression of LRRK2 genes or its mutants. (C) Co-expression of dnERK2 with wild-type LRRK2 abrogated the protection conferred by the latter gene against cell death induced by H_2O_2 in HEK293 cells. No significant changes in cell death induced by H_2O_2 toxicity were detected when dnERK2 was co-expressed with Y1699C mutant in HEK293 cells. Percentage cell death induced by H_2O_2 among cells transfected with pCDNA3.1, expressing LRRK2 wt or Y1699C mt gene in the absence or presence of dnERK2 are normalized against untreated cells transfected with the same vector or expressing the same proteins. Data are means ± SEM, at least 12 readings per data point, from three independent experiments. *$p < 0.05$ versus cell viability of cells expressing LRRK2 wt without dnERK2 after chronic treatment with H_2O_2 for 18 h. Statistics were derived from ANOVA and *post hoc* Fisher's protected least significant difference (PLSD) tests.

expressing wild-type LRRK2 and Y1699C mutant. Collectively, these results suggest the potential crosstalk between LRRK2 and the ERK1/2 pathway.

Wild-type LRRK2 activated the ERK1/2 pathway to protect against H_2O_2 toxicity

In view of the higher pERK level in cells expressing wild-type LRRK2 and the corresponded decrease in H_2O_2-induced cell death, we speculated the possibility that the activation of ERK1/2 pathway had been employed by wild-type LRRK2 to confer protection against cell death induced by H_2O_2 toxicity. To test this hypothesis, we cloned a dominant negative version of the ERK2 gene (dnERK2) into the same parental vector pcDNA3.1. The dominant negative version of the ERK2 gene is one with its Thr202 and Tyr204 replaced with Alanine. Over-expression of dnERK2 will saturate the activated MEK1 inhibiting the proper phosphorylation/activation of ERK1/2. As expected, upon expression of dnERK2, the activation of ERK1/2 in response to H_2O_2 was significantly suppressed (Fig. 3A). In addition, the successful expression of the dnERK2 was confirmed indicated by the stronger upper band of the rightmost column of the second panel in Fig. 3A.

Using the dnERK2 construct to suppress the activation of ERK1/2, we could examine the impact of ERK1/2 activation on basal viability and cell death induced by H_2O_2 toxicity. Co-expression of dnERK2 and wild-type LRRK2 and Y1699C mutant did not alter the decrease in basal viability of HEK293 cells elicited by expressing wild-type LRRK2 and Y1699C mutant alone (Fig. 3B), suggesting that the decrease in basal pERK was not the cause of this drop in basal viability. On the other hand, under the persistent insult of H_2O_2 at 150 μM, cells co-expressing wild-type LRRK2 and dnERK2 abolished the protection against H_2O_2-

induced cell death conferred by wild-type LRRK2 (Fig. 3C). This loss of protection has brought the percentage cell death to a level comparable to cells transfected with pCDNA3.1 or expressing Y1699C mutant. Furthermore, co-expression of Y1699C mutant and dnERK2 did not elicit any further decrease in H_2O_2-induced cell death. Similarly, pre-treatment with the MEK inhibitor U0126 (10 μM) suppressed the activation of the ERK1/2 pathway and also abrogated the protection conferred by wild-type LRRK2, without any significant impact on the H_2O_2-induced cell death in cells expressing Y1699C mutant (data not shown). Collectively, these results suggest the notion that wild-type LRRK2 but not Y1699C mutant activated the ERK1/2 pathway and thereby protected against H_2O_2-induced cell death.

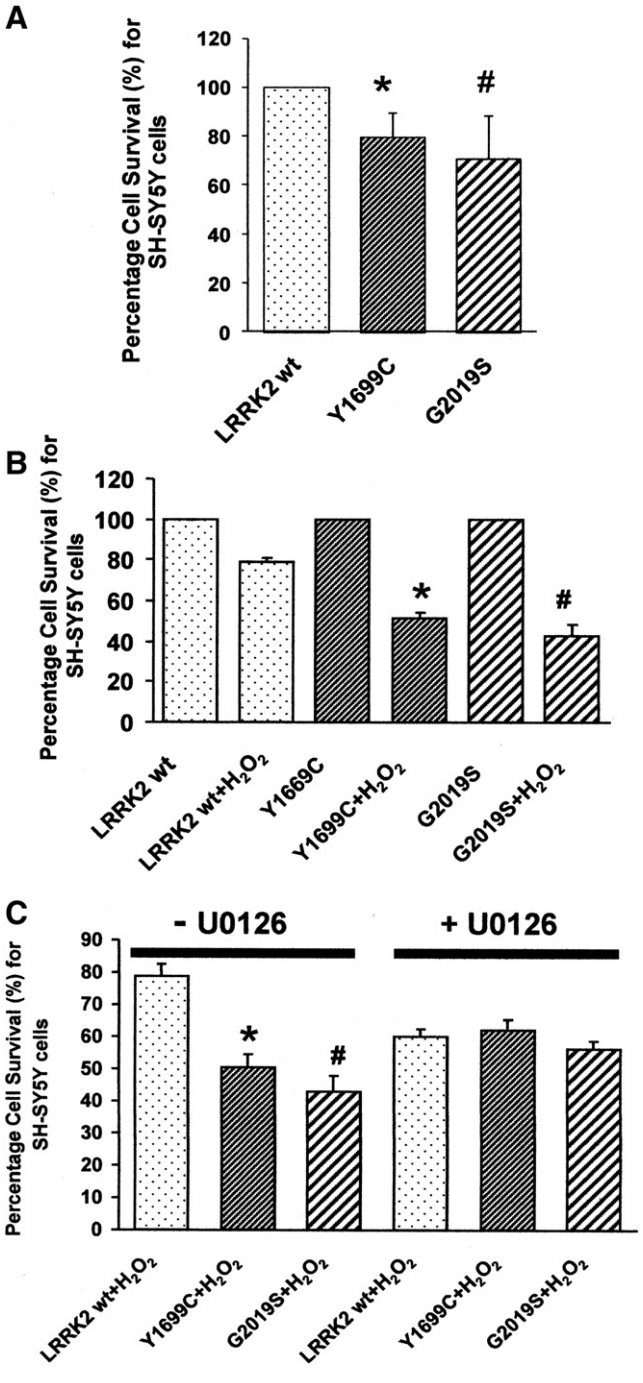

Differential cell death in neuronal cells expressing LRRK2 wild-type and mutants (Y1699C or G2019S) in response to H_2O_2 toxicity

Thus far, we have observed that HEK293 cells expressing LRRK2 wild-type are more resistant to H_2O_2 toxicity as compared to cells expressing mutants (Y1699C or G2019S) and this difference can be attributed to the capacity of LRRK2 wild-type to activate the ERK1/2 pathway. At this juncture, we are interested to determine whether this differential functional impact from LRRK2 wild-type and mutants (Y1699C or G2019S) against oxidative stress can be extended to neuronal cells. To address this, we transfected the same set of LRRK2 wild-type and mutant genes into human dopaminergic neuronal SH-SY5Y cells via lipofectamine 2000, followed by determining their influence on cell viability in response to H_2O_2 toxicity (60 μM, 18 h). Due to the low transfection efficiency (~13%), the percentage cell survival was determined by direct cell count of cells exhibiting GFP fluorescence against total cell number visualized by Hoechst stain.

First, the impact from these LRRK2 gene products on basal cell viability of SH-SY5Y cells was determined (Fig. 4A). In comparison, we observed a decrease in basal viability of 20% in cells expressing Y1699C and nearly 30% in cells G2019S than those cells expressing LRRK2 wild-type. Consistent with reported studies, both of the LRRK2 mutants exhibited higher innate toxicity than LRRK2 wild-type (Gloeckner et al., 2006; Smith et al., 2006).

Then, we investigated the differential change in percentage cell survival among cells expressing LRRK2 wild-type and mutants in response to H_2O_2 toxicity in SH-SY5Y cells. Similar to that observed in HEK293 cells, cells expressing LRRK2 wild-type experienced a 27–36% lowering in cell death as compared to cells expressing Y1699C or G2019S respectively (Fig. 4B). Moreover, in the presence of 10 μM U0126 pre-treated 1 h before the treatment of H_2O_2, the difference in percentage cell survival between cells expressing LRRK2 wild-type and its mutants was abolished (Fig. 4C) suggesting that the difference is mostly likely due to the activation of the ERK1/2 pathway mirroring that observed in HEK293 cells.

The protection conferred by wild-type LRRK2 is dependent on its kinase domain

To date, the limited biochemical characterization of LRRK2 has indicated a change in the kinase activity due to the identified mutations based on in vitro cell free kinase assay (Greggio et al., 2006; Ito et al., 2007; West et al., 2005). However, it is yet uncertain which protein along the ERK signaling cascade can interact with wild-type LRRK2 protein

Fig. 4. Impact of LRRK2 wild-type and mutants on basal viability and cell viability in response to H_2O_2 insult in SH-SY5Y cells. (A) Change in basal viability due to expression of LRRK2 wild-type and mutants (Y1699C and G2019S). Data are means ± SEM, 3 readings per data point, from at least three independent experiments. $^*p<0.05$ versus basal cell viability of cells expressing LRRK2 wild-type; $^{\#}p<0.05$ versus basal cell viability of cells expressing LRRK2 wild-type. Statistics were derived from ANOVA and *post hoc* Fisher's protected least significant difference (PLSD) tests. (B) Change in percentage cell survival between cells expressing LRRK2 wild-type and mutants (Y1699C or G2019S) in response to H_2O_2 insult. Data are means ± SEM, 3 readings per data point, from at least three independent experiments. $^*p<0.01$ versus percentage cell viability of cells expressing LRRK2 wild-type after H_2O_2 insult; $^{\#}p<0.01$ versus basal cell viability of cells expressing LRRK2 wild-type after H_2O_2 insult. Statistics were derived from ANOVA and *post hoc* Fisher's protected least significant difference (PLSD) tests. (C) Change in percentage cell survival between cells expressing LRRK2 wild-type and mutants (Y1699C or G2019S) in the absence and presence of 10 μM U0126 in response to H_2O_2 insult. Each of the percentage cell survival of cells expressing LRRK2 wild-type and mutants (Y1699C or G2019S) after H_2O_2 insult was normalized from corresponding cells expressing the same LRRK2 gene without H_2O_2 insult. Data are means ± SEM, 3 readings per data point, from at least three independent experiments. $^*p<0.01$ versus percentage cell viability of cells expressing LRRK2 wild-type after H_2O_2 insult; $^{\#}p<0.01$ versus basal cell viability of cells expressing LRRK2 wild-type after H_2O_2 insult. Statistics were derived from ANOVA and *post hoc* Fisher's protected least significant difference tests.

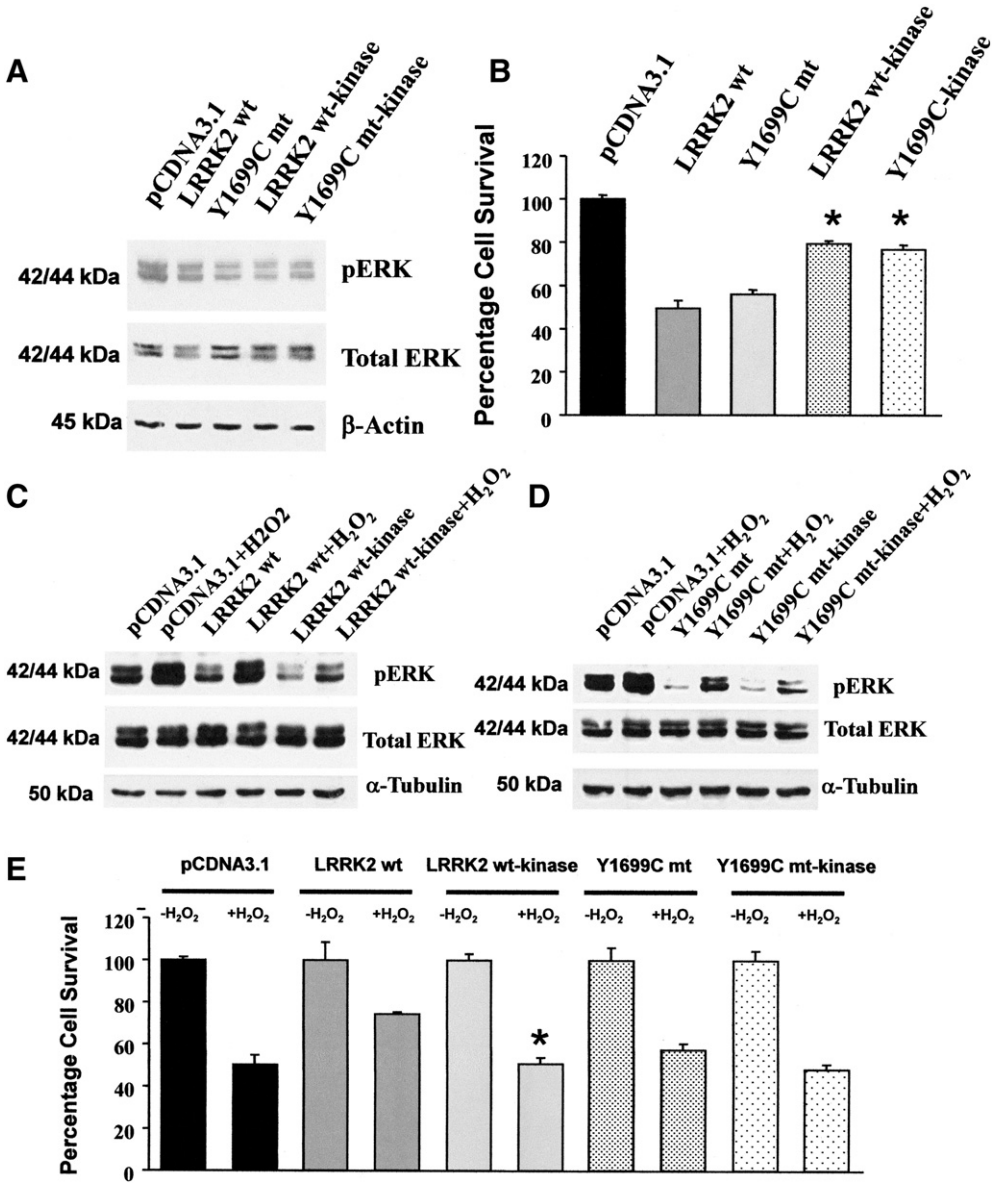

Fig. 5. Characterization of the deletion mutants. (A) Change in basal pERK in HEK293 cells expressing wild-type LRRK2, Y1699C mutant, and their respective deletion mutants. (B) Expression of deletion mutants resulted in significantly less decrease in basal cell viability as compared to their complete gene counterpart. Data are means±SEM, at least 12 readings per data point, from three independent experiments. *$p<0.05$ versus basal cell viability of cells expressing the corresponding complete gene. Statistics were derived from ANOVA and *post hoc* Fisher's protected least significant difference (PLSD) tests. (C) Impact of expressing LRRK2 wild-type-kinase (deletion mutant) on ERK response in HEK293 cells towards H_2O_2 toxicity. The changes in pERK and total ERK with and without H_2O_2 treatment in cells transfected with pCDNA3.1, expressing wild-type LRRK2 (LRRK2 wt), and LRRK2 wild-type-kinase (LRRK2 wt-kinase) were visualized by immunoblotting probed with antibodies recognizing pERK, total ERK and β-actin respectively. β-actin was used as loading control. (D) Impact of expressing Y1699C mutant-kinase (deletion mutant) on ERK response in HEK293 cells towards H_2O_2 toxicity. The changes in pERK and total ERK with and without H_2O_2 treatment in cells transfected with pCDNA3.1, expressing Y1699C mutant (Y1699C mt) and Y1699C mutant-kinase (Y1699C mt-kinase) were visualized by immunoblotting probed with antibodies recognizing pERK, total ERK and β-actin respectively. β-actin was used as loading control. (E) Comparative impact on cell death induced by treatment with 150 μM of H_2O_2 in cells expressing pCDNA3.1, wild-type LRRK2, LRRK2 wt-kinase, Y1699C mutant, and Y1699C mt-kinase. Percentage cell death induced by H_2O_2 among cells transfected with pCDNA3.1, expressing wild-type LRRK2, Y1699C mutant, or their corresponding deletion mutant are normalized against untreated cells transfected with the same vector or expressing the same proteins. Data are means±SEM, at least 12 readings per data point, from three independent experiments. *$p<0.05$ versus cell viability of cells expressing LRRK2 wt after chronic treatment with H_2O_2 for 18 h. Statistics were derived from ANOVA and *post hoc* Fisher's protected least significant difference (PLSD) tests.

directly. Thus, it is the common belief that the kinase activity of LRRK2 will dictate its physiological function. Therefore, we were interested to determine whether the kinase domain is involved in the protective phenotype of wild-type LRRK2 observed in our paradigm. Since all the reported studies related to the change in kinase activity of LRRK2 due to specific mutations (Greggio et al., 2006; Ito et al., 2007; West et al., 2005) or the development of kinase dead mutations (Burke, 2007; Greggio et al., 2006; Lu and Tan, 2008) were based on cell free in vitro kinase assay using auto-phosphorylation or myelin basic protein (MBP) as substrates, it is uncertain the same specific change in kinase activity for Y1699C and G2019S can be extended to the protein that activates the ERK1/2 pathway in view of the unique protein–protein interaction between the kinase and each of its substrates. The same mutations would elicit unique impact on the activity of the kinase towards each of its substrates. Hence, under these circumstances, we decided to delete the kinase domain in lieu of mutating specific residues to create a kinase-dead

version of wild-type LRRK2 and Y1699C mutant. In constructing the deletion mutants, we utilized unique endonuclease cut-sites of Cla I and Pac I flanking the kinase domain of the LRRK2 gene. Using these sites, the kinase domain was excised from the LRRK2 wild-type and Y1699C mutant gene. After the excision, the ends were joined by an in-frame short DNA linker created by annealing two complementary primers. The sequences are shown in Materials and methods section.

Using the deletion mutants in conjunction with their corresponding complete gene, we could determine whether their differential response towards oxidative stress mandates the presence of the kinase domain. With this strategy, we observed that removal of the kinase domain from the wild-type LRRK2 further decreased the basal level of pERK to a comparable level elicited by full length Y1699C mutant (Fig. 5A). On the other hand, removal of the kinase domain from Y1699C mutant did not further decrease the basal level of pERK, suggesting that the kinase domain was not involved in the suppression of basal level of pERK. Nevertheless, these results supported the notion that wild-type LRRK2 but not Y1699C mutant has the capacity to activate the ERK pathway. However, the removal of the kinase domain from full length wild-type LRRK2 and Y1699C mutant mitigated the drop in basal viability by 20% when expressed in HEK293 cells, which was 20% less than the cells expressing their full length counterpart (Fig. 5B).

Under the chronic insult of H_2O_2, we found that cells expressing the deletion mutant of wild-type LRRK2 cannot elicit an increase in pERK level as observed in cells expressing full length wild-type LRRK2 (Fig. 5C). In the case of Y1699C mutant, cells expressing the full length or deletion mutant version of the gene do not exhibit significant difference in their capacity to increase pERK level (Fig. 5D). Correspondingly, cells expressing the deletion mutant of wild-type LRRK2 lost the protective phenotype conferred by full length wild-type LRRK2 against H_2O_2-induced cell death (Fig. 5E), suggesting that the protective phenotype of wild-type LRRK2 is dependent on the kinase domain and hence kinase activity. Moreover, deletion of the kinase domain from Y1699C mutant did not increase the H_2O_2-induced cell death and was comparable to cells transfected with pCDNA3.1. Collectively, the results suggest that wild-type LRRK2 but not Y1699C mutant is capable of activating the ERK pathway to confer protection against H_2O_2-induced cell death.

Discussion

Studies on the biochemical characterization of functional differences between wild-type LRRK2 and its mutants are limited. The few reported biochemical studies have focused on the impact of the LRRK2 mutant-kinase activity on intracellular physiological functions, including the formation of inclusion bodies and cell death (Gloeckner et al., 2006; Greggio et al., 2006; Smith et al., 2006; West et al., 2005). Overall, it has been speculated that LRRK2 mutant could elicit a "toxic gain of function" that leads to degenerative consequences within the cell. The objective of the present study was to identify functional differences between wild-type LRRK2 and the mutants Y1699C and G2019S in response to oxidative stress. Collectively, our results indicated that wild-type LRRK2 but not Y1699C or G2019S mutants attenuated H_2O_2-induced cell death in HEK293 cells and SH-SY5Y cells. Further mechanistic determination indicated that the mutation such as Y1699C lost the inherent protective capacity of wild-type LRRK2 against oxidative stress in its inability to activate the ERK1/2 pathway. Nevertheless, the results from this study cannot rule out the possibility that specific mutations in the LRRK2 gene abolished protective capacity of LRRK2 against oxidative stress in conjunction with a gain of toxic function as suggested in other reported studies.

Impact of wild-type LRRK2 and its mutants on basal viability

In non-neuronal HEK293 cells, expressing wild-type LRRK2, Y1699C or G2019S mutants experienced a 30–40% decrease in basal cell viability showing no significant difference in their individual toxic impact. In contrast, expression of Y1699C or G2019S mutants in neuronal SH-SY5Y cells resulted in at least 20% higher drop in basal viability than its wild-type counterpart suggesting greater toxicity for the mutants consistent with reported studies (Greggio et al., 2006; Smith et al., 2006). This discrepancy may be due to the differential endogenous protein profiles in HEK293 cells and SH-SY5Y cells. It is speculated that the LRRK2 mutants interact with neuronal specific proteins which are absence in HEK293 cells, actualizing their inherent higher toxicity than LRRK2 wild-type. On the other hand, the activation of the ERK pathway by LRRK2 wild-type in response to H_2O_2 toxicity was via protein/s present in HEK293 and SH-SY5Y cells and hence account for the consistent observation in both cell lines. Therefore, despite the high transfection efficiency for HEK293 cells, one must be careful in data interpretation as it is not always possible to generalize results obtained in non-neuronal cells to neuronal cells.

To date, several reported studies have suggested that the toxicity of LRRK2 mutants resides solely on their change in kinase activity from LRRK2 wild-type (Greggio et al., 2006; Smith et al., 2006; West et al., 2005, 2007). If this is the case, expression of the deletion mutants should not decrease the basal viability by 20% higher than cells that have undergone transfection with pCDNA3.1 or expressing GFP alone (data not shown), albeit their corresponding impacts on basal viability were 15–20% lower than cells expressing full length LRRK2 wild-type or mutants (Fig. 5B). This result suggested two components for the inherent toxicity of LRRK2 wild-type and mutants. First, cells expressing the kinase deletion mutants experienced a 15–20% increase in basal viability when compared to cells expressing their full length counterpart suggesting a kinase dependent inherent toxic component of LRRK2. However, the 20% drop in basal viability in cells expressing the kinase deletion mutants when compared to cells transfected with pCDNA3.1 or expressing GFP also suggests a component of the inherent toxicity for LRRK2 that is independent of its kinase activity.

Can a kinase independent component of the inherent toxicity for LRRK2 possible? Sequence and functional domain analysis of LRRK2 led to the prediction of its function to be a protein scaffold that enables the formation of a multi-protein signaling complex similar to that of the protein kinase suppressor of Ras (Ksr) (Gloeckner et al., 2006; Kolch, 2005; Mata et al., 2006). Potential crosstalk between LRRK2 and the ERK pathway was first suggested by the decrease in basal level of pERK in cells expressing LRRK2 wild-type, its mutant and their corresponding deletion mutants which were consistent with its predicted role as a protein scaffold facilitating the activation of the ERK1/2 pathway. This is because as a protein scaffold facilitating the activation of the ERK1/2 pathway, over-expressing LRRK2 wild-type or mutants would inevitably suppress the activation of the ERK1/2 pathway which may come with detrimental consequences to cell growth and maintenance of cell viability. In parallel, it has been reported that over-expressing the scaffolding protein, JIP1, results in the suppression of JNK activation through sequestration of MEK or JNK despite the fact that physiological function of JIP1 is to *facilitate* JNK activation (Dickens et al., 1997; Harding et al., 2001; Li et al., 2005; Mooney and Whitmarsh, 2004). This may account for the kinase independent component of the inherent toxicity of this protein.

Impact of LRRK2 wild-type and mutants on the cell death in response to oxidative stress

Collectively, our results indicated that LRRK2 wild-type but not its mutants has the capacity to attenuate H_2O_2-induced cell death via activation of the ERK1/2 pathway in both HEK293 and SH-SY5Y cells. This change in tolerance towards oxidative stress is likely to be attributed to their differential capacity to activate the ERK1/2 pathway. Our evidence further indicates that the activation of the ERK1/2 pathway by wild-type LRRK2 is kinase domain dependent.

However, it is yet uncertain which protein along the ERK signaling cascade can interact with wild-type LRRK2 protein directly.

Although our study suggests a cellular function for wild-type LRRK2 in attenuating oxidative stress, it is likely that this protein has other physiological functions yet to be identified. In summary, our results suggested that mutations on LRRK2 can alter its capacity to activate the ERK1/2 signaling cascade, which significantly affect cell death in response to oxidative stress. This observation is consistent with the observation that the G2019S mutation decreases the phosphorylation of MAP kinase (White et al., 2007). However whether LRRK2 functions as an intracellular scaffold facilitating the activation of other MAP kinase signaling cascade merits further investigation.

Acknowledgments

We thank Mr. Leonard Kotveski for his technical assistance towards the completion of this project. This work is supported by NINDS (NS019608) and the U.S. Army (ERMS#03281022).

References

Bialecka, M., et al., 2005. Analysis of LRRK 2 G 2019 S and I 2020 T mutations in Parkinson's disease. Neurosci. Lett. 390, 1–3.
Burke, R.E., 2007. Inhibition of mitogen-activated protein kinase and stimulation of Akt kinase signaling pathways: two approaches with therapeutic potential in the treatment of neurodegenerative disease. Pharmacol. Ther. 114, 261–277.
Dickens, M., et al., 1997. A cytoplasmic inhibitor of the JNK signal transduction pathway. Science 277, 693–696.
Gloeckner, C.J., et al., 2006. The Parkinson disease causing LRRK2 mutation I2020T is associated with increased kinase activity. Hum. Mol. Genet. 15, 223–232.
Greggio, E., et al., 2006. Kinase activity is required for the toxic effects of mutant LRRK2/dardarin. Neurobiol. Dis. 23, 329–341.
Harding, T.C., et al., 2001. Inhibition of JNK by overexpression of the JNL binding domain of JIP-1 prevents apoptosis in sympathetic neurons. J. Biol. Chem. 276, 4531–4534.
Haugarvoll, K., Wszolek, Z.K., 2006. PARK8 LRRK2 parkinsonism. Curr. Neurol. Neurosci. Rep. 6, 287–294.
Ito, G., et al., 2007. GTP binding is essential to the protein kinase activity of LRRK2, a causative gene product for familial Parkinson's disease. Biochemistry 46, 1380–1388.
Jain, S., et al., 2005. Molecular genetic pathways in Parkinson's disease: a review. Clin. Sci. (Lond). 109, 355–364.
Klein, C., Schlossmacher, M.G., 2006. The genetics of Parkinson disease: implications for neurological care. Nat. Clin. Pract. Neurol. 2, 136–146.
Kolch, W., 2005. Coordinating ERK/MAPK signalling through scaffolds and inhibitors. Nat. Rev. Mol. Cell Biol. 6, 827–837.
Korr, D., et al., 2006. LRRK1 protein kinase activity is stimulated upon binding of GTP to its Roc domain. Cell Signal. 18, 910–920.
Li, C.H., et al., 2005. Activated mitogen-activated protein kinase kinase 7 redistributes to the cytosol and binds to Jun N-terminal kinase-interacting protein 1 involving oxidative stress during early reperfusion in rat hippocampal CA1 region. J. Neurochem. 93, 290–298.
Lu, Y.W., Tan, E.K., 2008. Molecular biology changes associated with LRRK2 mutations in Parkinson's disease. J. Neurosci. Res.
Mata, I.F., et al., 2006. LRRK2 in Parkinson's disease: protein domains and functional insights. Trends Neurosci. 29, 286–293.
Mazzio, E.A., et al., 2004. The role of oxidative stress, impaired glycolysis and mitochondrial respiratory redox failure in the cytotoxic effects of 6-hydroxydopamine in vitro. Brain Res. 1004, 29–44.
Meylan, E., Tschopp, J., 2005. The RIP kinases: crucial integrators of cellular stress. Trends Biochem. Sci. 30, 151–159.
Mooney, L.M., Whitmarsh, A.J., 2004. Docking interactions in the c-Jun N-terminal kinase pathway. J. Biol. Chem. 279, 11843–11852.
Olanow, C.W., 2007. The pathogenesis of cell death in Parkinson's disease—2007. Mov Disord. 22 Suppl. 17, S335–S342.
Saito, Y., et al., 2007. Molecular mechanisms of 6-hydroxydopamine-induced cytotoxicity in PC12 cells: involvement of hydrogen peroxide-dependent and -independent action. Free Radic. Biol. Med. 42, 675–685.
Smith, W.W., et al., 2006. Kinase activity of mutant LRRK2 mediates neuronal toxicity. Nat. Neurosci. 9, 1231–1233.
Tomiyama, H., et al., 2006. Clinicogenetic study of mutations in LRRK2 exon 41 in Parkinson's disease patients from 18 countries. Mov. Disord. 21, 1102–1108.
West, A.B., et al., 2005. Parkinson's disease-associated mutations in leucine-rich repeat kinase 2 augment kinase activity. Proc. Natl. Acad. Sci. U. S. A. 102, 16842–16847.
West, A.B., et al., 2007. Parkinson's disease-associated mutations in LRRK2 link enhanced GTP-binding and kinase activities to neuronal toxicity. Hum. Mol. Genet. 16, 223–232.
Whaley, N.R., et al., 2006. Clinical and pathologic features of families with LRRK2-associated Parkinson's disease. J. Neural Transm. Suppl. 221–229.
White, L.R., et al., 2007. MAPK-pathway activity, Lrrk2 G2019S, and Parkinson's disease. J. Neurosci. Res.
Xu, Z., et al., 2001. The MLK family mediates c-Jun N-terminal kinase activation in neuronal apoptosis. Mol. Cell Biol. 21, 4713–4724.